

UNIVERSITY OF CALIFORNIA
Los Angeles

Molecular differences between human small intestine and colon stem
and progenitor cells

A dissertation submitted in partial satisfaction of the
requirements for the degree Doctor of Philosophy
in Molecular Biology

by

Sophia Yenchuan Kuo Lewis

2018

© Copyright by

Sophia Yenchuan Kuo Lewis

2018

ABSTRACT OF THE DISSERTATION

Molecular differences between human small intestine and colon stem
and progenitor cells

by

Sophia Yenchuan Kuo Lewis

Doctor of Philosophy in Molecular Biology

University of California, Los Angeles, 2018

Professor Dana Leanne Jones, Chair

Maintenance of the mammalian intestine throughout life relies on rapidly dividing stem cells located at the base of invaginating crypts in both the small intestine and the colon. These crypts constitute a protective niche to provide signals conducive to stem cell proliferation and maintenance, while preventing exposure to harmful toxins that may be present in the gut lumen. During homeostasis, gut stem cells respond to signals from the niche to either self-renew or differentiate to generate specialized epithelial cells. Intestinal and colonic stem cells are both specifically marked by the Wnt target gene *Lgr5*. While much has been learned about intestinal stem cell biology through the use of *Lgr5*-labeled transgenic mouse models, relatively little is known about how stem cell behavior differs between small intestine and colon, particularly in human. Colon cancer is far more common than small intestinal cancers and is thought to arise from malignant transformation of gut stem cells during aging. Yet how the stem cells of small intestine and colon differ molecularly under homeostatic conditions and during aging remains unclear. Three-dimensional organoids, which permit long-term self-renewal of mammalian gut stem cells *in vitro*, provide a convenient and accessible system for investigating regional differences in stem cell behavior. Additionally, the epigenetic clock – a measure of age based

on age-dependent DNA methylation changes – provides a quantitative tool for analyzing aging of different tissues and cell types.

Here, we show that colon stem cells grown in culture proliferate slower than small intestinal stem cells, have decreased stem cell function, and have a greater tendency to differentiate. In addition to stem cell behavioral differences in culture, we find that human small intestine and colon exhibit different aging profiles as measured by the epigenetic clock. We demonstrate that small intestine crypt cells have decreased epigenetic clock aging rates compared to colon crypts and to surrounding small intestine mucosal cells, and these regional differences in epigenetic aging appear to be maintained *in vitro*.

The dissertation of Sophia Yenchuan Kuo Lewis is approved.

Amander Therese Clark

Brigitte N. Gomperts

William Edward Lowry

Martin G. Martin

Dana Leanne Jones, Committee Chair

University of California, Los Angeles

2018

Acknowledgements

I would first and foremost like to thank my mentor, Dr. Leanne Jones, for her guidance and support throughout my predoctoral training. I am grateful for the invaluable learning experiences in her laboratory and for the independence I was given to pursue a new system for the lab.

I want to also thank my thesis committee members, Professors Martin G. Martin, Bill Lowry, Brigitte Gomperts and Amander Clark, for their helpful feedback during our meetings.

Infinite thanks to all the members of the Jones lab, past and present, for their comments and guidance throughout the past four years. While their focus and expertise lies mainly in *Drosophila* stem cell biology and aging, they provided both technical support and thought-provoking feedback on my projects.

I am also grateful for the UCLA Medical Scientist Training Program and the Broad Stem Cell Research Center for their funding and support throughout graduate school.

Lastly, I would like to thank my family for supporting my academic endeavors, and my husband, Arick, for always being my cheerleader when research proved challenging. Arick, thank you for the 24/7 support and molecular biology expertise.

Table of Contents

List of Figures	viii
List of Tables	x
Vita	xi
Chapter 1: Introduction	
Structure-function relationship in mammalian small intestine and colon epithelia	1
Intestinal stem cell identity	2
Intestinal stem cell homeostasis	3
<i>In vitro</i> intestinal organoids	4
Intestinal stem cells in aging and cancer	6
References	14
Chapter 2: Regional differences in gut stem cell behavior <i>in vitro</i>	21
References	51
Chapter 3: DNA methylation analysis reveals differences in aging between human small intestine and colon	56
References	91
Chapter 4: Conclusions and Future Directions	97
References	102
Appendix	105
A: Spheroid forming efficiency for human small intestine and colon samples	106

B: Proliferation rate of paired jejunum and transverse colon from the same donor	107
C: BMP inhibition prevents differentiation during starvation	108
D: Regional expression of Gata4 is maintained in spheroids derived from human duodenum and colon	109
E: Spheroid forming efficiency of adult human small intestine crypts by age	110
F: Response to irradiation-induced DNA damage for human small intestine and colon spheroids	111

List of Figures

Chapter 1

- Figure 1-1: Epithelial cell composition in mammalian small intestine and colon 9
- Figure 1-2: Niche factors that regulate intestinal stem cell homeostasis 10
- Figure 1-3: Schematic of mouse and human-derived intestinal organoids 11

Chapter 2

- Figure 2-1: Stem and differentiated cell markers in human small intestine-derived spheroids and enteroids 43
- Figure 2-2: Human CoSCs are slow cycling compared to ISC under *in vitro* stem cell-promoting conditions 45
- Figure 2-3: BMP inhibition increases proliferation and inhibits differentiation on CoSCs *in vitro* 47
- Figure S2-1: Human colon derived spheroids and differentiated colonoids 49
- Figure S2-2: BMP inhibition increases proliferation of ISCs in vitro 50

Chapter 3

- Figure 3-1: Differential methylation analysis of human intestinal and colonic mucosa, crypts and organoids 77
- Figure 3-2: Epigenetic clock analysis of human small intestine and colon reveals decreased ticking rate in crypt cells 79
- Figure 3-3: Epigenetic clock analysis of paired jejunum and colon crypts isolated from four individuals 80
- Figure 3-4: Epigenetic clock analysis of *in vitro* human intestinal stem-like and differentiated cultures 81

Figure S3-1: Batch effect and differential methylation analysis at CpG islands and gene bodies	82
Figure S3-2: Differential methylation analysis at gene bodies and CpG islands for human intestinal and colonic crypts and organoids	84
Figure S3-3: Epigenetic clock analysis of paired small intestine and colon mucosa and crypts	85
Figure S3-4: Gender distribution among samples used for DNAm analysis	86
Figure S3-5: Gene expression analysis of small intestine and colon crypt preparations	87

List of Tables

Chapter 1

Table 1-1:	Mouse intestinal and colonic organoid culture conditions	12
Table 1-2:	Human small intestine and colon organoid culture conditions	13

Chapter 3

Supplemental Table 3-1:	Summary of human samples used	89
-------------------------	-------------------------------	----

Vita

Doctor of Medicine (in progress), 2012-2014

David Geffen School of Medicine at UCLA, Los Angeles, California

Bachelor of Arts, 2007-2011

University of California Berkeley, Berkeley, California

Major in Molecular and Cell Biology

Concentration in Genetics, Genomics and Development

Minor in Chinese Language

Funding Awards

2017-2018 Broad Stem Cell Research Center at UCLA: Predoctoral Training Grant

2016-2017 Broad Stem Cell Research Center at UCLA: Predoctoral Training Grant

Publications

Resnik-Docampo M, Koehler C, Clark RI, Schinaman J, Sauer V, Wong DM, **Lewis S**, D'Alterio C, Walker D, Jones L. Tricellular junctions regulate intestinal stem cell behaviour to maintain homeostasis. *Nat Cell Biol.* 2017;19(1):52-59.

Nan X, Tamgüney TM, Collisson EA, Lin LJ, Pitt C, Galeas J, **Lewis S**, Gray JW, McCormick F, Chu S. Ras-GTP dimers activate the Mitogen-Activated Protein Kinase (MAPK) pathway. *Proc Natl Acad Sci USA.* 2015;112(26):7996-8001.

Sherwood RI*, Hashimoto T*, O'Donnell CW*, **Lewis S**, Barkal AA, van Hoff JP, Karun V, Jaakkola T, Gifford DK. Discovery of directional and nondirectional pioneer transcription factors by modeling DNase profile magnitude and shape. *Nat Biotechnol.* 2014;32(2):171-8. (*These authors contributed equally).

Nan X, Collisson EA, **Lewis S**, Huang, J; Meyer, TM; Liphardt, J; McCormick, F; Gray, JW; Chu, S. Single molecule super resolution imaging allows quantitative analysis of RAF multimer formation and signaling. *Proc Natl Acad Sci USA*. 2013;110(46):18519-24.

Heiser LM, Sadanandam A, Kuo WL, Benz SC, Goldstein TC, Ng S, Gibb WJ, Wang NJ, Ziyad S, Tong F, Bayani N, Hu Z, Billig JI, Dueregger A, **Lewis S**, Jakkula L, Korkola JE, Durinck S, Pepin F, Guan Y, Purdom E, Neuvial P, Bengtsson H, Wood KW, Smith PG, Vassilev LT, Hennessy BT, Greshock J, Bachman KE, Hardwicke MA, Park JW, Marton LJ, Wolf DM, Collisson EA, Neve RM, Mills GB, Speed TP, Feiler HS, Wooster RF, Haussler D, Stuart JM, Gray JW, Spellman PT. Subtype and pathway specific responses to anticancer compounds in breast cancer. *Proc Natl Acad Sci USA*. 2012;109(8):2724-9.

Chapter 1: Introduction

Structure-function relationship in mammalian small intestine and colon epithelia

Extending from the stomach to the anus, the mammalian intestine consists of two continuous but physiologically and anatomically distinct regions – the small intestine proximally, and the large intestine, or colon, distally. The small intestine can be further segmented into three regions based on physiology and anatomy: the duodenum, jejunum, and ileum. Within the small intestine, the duodenum and jejunum are the primary sites of nutrient digestion and absorption, while the ileum is responsible for Vitamin B12 and bile salt reabsorption. Differences in organ size, anatomical structure, and epithelial composition along the proximal-distal axis of the gastrointestinal tract help support the region-specific physiology of the small intestine and colon. In addition to comprising the majority (up to 75%) of the length of the gut, the small intestine epithelial lining is organized with villus finger-like projections, which increase surface area to accommodate the high absorptive activity of this region[1]. At the base of each villus, the epithelium invaginates to form crypts of Lieberkühn. The colon, on the other hand, is largely responsible for water absorption, elimination of waste, and housing the majority of commensal bacteria. In contrast to the small intestine, the colon exhibits a flat surface epithelium devoid of villi, along with invaginating crypts [2] (Figure 1-1).

In both organs, the inner mucosal lining of the gut tube consists of a single layer of columnar epithelial cells over an underlying a connective tissue known as the lamina propria and the thin muscularis mucosae. Along the length of the gut, the mature epithelial layer is composed of several major lineages (Figure 1-1). Enterocytes and colonocytes make up the differentiated absorptive cells in the small intestine and colon, respectively. In both regions, secretory cells include mucin-secreting Goblet cells and hormone-secreting enteroendocrine cells, while antimicrobial-secreting Paneth cells reside in the small intestine alone [3]. Less

abundant mature cell types include microfold (M) cells at lymphatic Peyer's patches in the ileum and chemosensory tuft cells [4].

The gut epithelium is one of the most rapidly regenerating tissues in the body. To maintain homeostasis throughout life, short-lived specialized epithelial cells are regularly turned over and replaced through the differentiation of stem cells that reside in protective niches at the base of the invaginating crypts [3,5] (Figure 1-1). These stem cells give rise to transit-amplifying progenitors that subsequently differentiate into the specialized cells. Most differentiated lineages migrate up toward the luminal surface during maturation and subsequently die, shedding into the lumen within a few days. Paneth cells, conversely, migrate down to their position at the crypt bottom, turning over after 6-8 weeks [6].

Intestinal stem cell identity

Early studies on intestinal epithelial homeostasis proposed two parallel stem cell populations – rapidly proliferative crypt-based columnar cells (CBCs) at the crypt bottom, and label-retaining cells (LRCs) in the +4 position from the crypt base [3,7]. Subsequent experiments have confirmed the CBC hypothesis; seminal lineage tracing studies in mouse small intestine and colon demonstrated that actively cycling CBCs in both organs are specifically marked by the Wnt target gene *Lgr5* and exhibit classic stem cell function, including self-renewal and multi-lineage differentiation [8]. These stem cells can be referred to as intestinal stem cells (ISCs) and colonic stem cells (CoSCs) in the small intestine and colon, respectively.

The identity and function of the second stem cell pool, the LRC, has remained more unclear. Contrary to initial studies that proposed +4 cells were radiation-sensitive proliferative populations [7], many recent studies have concluded that these LRCs are likely a radiation-resistant, quiescent reserve population that proliferates after injury. Through lineage tracing analysis, numerous markers of the +4 LRC have been proposed, including *Bmi1*, *Hopx*, *mTert*,

and Lrig [9-12]. However, these proposed markers were subsequently found to have broader expression, including in Lgr5+ ISCs and transit-amplifying progenitors, complicating the interpretation of lineage tracing experiments[6,13].

In contrast to approaches that focused on identifying the +4 cell by unique genetic markers, Buczacki et al. confirmed the presence of quiescent cells that have the characteristic feature of label retention and identified secretory precursor LRCs predominantly in the +3 position. These LRCs co-express Lgr5+ and secretory gene programs, exhibit multi-lineage stem cell potential *in vitro*, and are able to reconstitute proliferative clonogenic stem cells after injury [14]. Together, these experiments suggest there is a subpopulation of ISCs that function as a quiescent reserve population, likely committing to secretory lineages under homeostasis but proliferating to restore the ISC compartment after injury [14] (Figure 1-1). Unlike small intestine, however, little is known about the presence of reserve cells in the mammalian colon.

Intestinal stem cell homeostasis

The balance between stem cell self-renewal and differentiation is regulated by evolutionarily conserved signaling pathways (Figure 1-2). Wnt signaling is necessary for the initiation of the crypt compartment during development, and transgenic deletion of Tcf4 or β -catenin results in loss of crypt cell proliferation in adult mice [15-17]. Notch signaling at the base of crypts maintains stem cells in their undifferentiated state, while Notch lateral inhibition in the transit-amplifying progenitor zone regulates the balance between absorptive and secretory lineages, with Notch inhibition leading to secretory cell commitment [4]. Unlike EGF signaling, which supports crypt proliferation [18,19], BMP signaling is thought to be a negative regulator of crypt cell division. Overexpression of Noggin, a BMP inhibitor, leads to ectopic crypt formation [20]. Yet, it remains unclear whether the primary source of BMP signaling is epithelial-intrinsic or derived from underlying mesenchyme, such as myofibroblasts[20-22].

The stem cell niche has been investigated primarily using murine small intestine, where ISCs have long been observed intercalated between Paneth cells at the crypt bottom [3]. In addition to producing antimicrobials such as defensins and lysozyme, Paneth cells are thought to be the source of several of the key niche factors including EGF, Notch ligands, and Wnt3[23,24]. Incomplete ablation of murine Paneth cells led to partial loss of ISCs, initially suggesting that these cells do constitute an essential niche for ISCs and may be an irreplaceable source of the pro-proliferative and stemness signal Wnt3[23]. By contrast, further examination demonstrated intact function of Lgr5+ ISCs in a complete Paneth cell ablation model [25], suggesting that there may in fact be redundant sources of ISC-supportive Wnt signals, such as those derived from subepithelial myofibroblasts and subepithelial telocytes [26,27].

The colon, however, lacks Paneth cells, and supportive niche cells in the distal gut have remained less well characterized. Sasaki et al. recently demonstrated the existence of a Paneth cell-like deep crypt secretory cell marked by Reg4 in the colon [28] (Figure 1-1). Ablation of Reg4+ cells leads to loss of Lgr5+ CoSCs through a combination of cell death and differentiation [28]. In contrast to Paneth cells, Reg4+ cells express Delta and EGF but not Wnts, so the precise sources of Wnt signaling within the colon crypt remains less clear [23,28].

In vitro intestinal organoids

The development of 3D intestinal organoids or “mini-guts” that recapitulate intestinal crypt-villus architecture has transformed the field of intestinal epithelial biology [29]. Until the generation of these 3D culture techniques, *in vitro* experimentation on gut epithelium relied primarily on the use of 2D colon cancer cell lines, but these models are genetically transformed and do not faithfully recapitulate epithelial architecture or stem cell homeostatic behavior. With organoid methods, isolated murine intestinal crypts or single sorted Lgr5+ stem cells can form self-organizing 3D structures when embedded in 3D matrix with a refined cocktail of growth

factors, even in the absence of mesenchymal support cells [5,30]. Together, supplementation with EGF, BMP inhibition via Noggin, and Wnt augmentation with R-spondin allow for formation and long-term propagation of murine intestinal organoids that maintain proliferative crypt domains containing Lgr5⁺ stem cells and differentiated villus domains containing secretory and absorptive lineages [5] (Figure 1-3A). Organoids can be readily established for mouse small intestine with this limited set of niche factors; in contrast, mouse colon organoids require addition of Wnt3A, a requirement attributed to the colon crypt's lack of epithelial intrinsic Wnt signaling in the absence of the Paneth cell lineage [31] (Table 1-1).

Human intestinal and colon organoids require a more complex set of growth factors to support derivation and long-term propagation [31,32]. Unlike mouse, human organoids require Wnt3 for survival regardless of region, and in addition to EGF, Noggin and R-spondin, human cultures are generally supplemented with Nicotinamide, Gastrin, a p38 inhibitor, and a TGF- β inhibitor [31]. These human organoids tend to be stem cell-enriched, and differentiation can be obtained with the withdrawal of stem cell maintenance factors, such as Wnt [31,32] (Figure 1-3B). Yet, there is little consensus on human organoid culture methods, with variable cocktails of small molecules being employed by different research groups [31-34] (Table 1-2). Furthermore, in contrast to mouse cultures, human culture conditions to date are not region-specific, with the same niche factors generally used to support small intestine and colon organoids [31]. Whether there are optimal region-specific niche requirements for human gut organoids *in vitro* is unclear, and will be examined, in part, in Chapter 2.

While Lgr5⁺ stem cells maintain epithelial homeostasis in both small intestine and colon, ISCs and CoSCs have several differences: they give rise to different populations/distributions of differentiated progeny (ie., Paneth cells exclusively in the small intestine, greater proportion of Goblet cells in the colon, etc); their differentiated progeny cells carry out unique digestive functions; they experience segment-specific environmental exposure (including regional differences in microbiome composition); and ISCs and CoSCs reside in distinct niches (colonic

crypts are longer than small intestine crypts and lack Paneth cells). Yet, there has been limited direct comparison of stem cell behavior for human ISCs and CoSCs, and little is known about how ISCs and CoSCs may differ molecularly and behaviorally to support their distinct physiological functions. *In vitro* organoid techniques provide an accessible model to begin to assess segment-specific differences in human stem cell behavior. This topic is addressed in Chapter 2 of this thesis.

Moreover, while regional identity is thought to be maintained in gut organoids [35], this evidence relies on the expression of a handful of region-specific markers and analysis was restricted to small intestine segments. It is less clear whether additional regional differences between small intestine and colon are maintained *in vitro* – a question investigated, in part, in Chapter 3 of this thesis.

Intestinal stem cells in aging and cancer

Aging of many organs is associated with impaired regenerative capacity due to altered activity of tissue-specific stem cells or the surrounding niche [36-38]. In the human gastrointestinal tract, aging is associated with altered motility, chronic inflammation, changes to the microbiome, barrier dysfunction, and increased risk of colorectal cancer [39,40]. The relationship between age-related changes in intestinal physiology and alterations in stem cell behavior are not fully understood.

Age-associated alterations in ISC/CoSC behavior that impact the balance between turnover and regeneration could lead to impaired epithelial repair after injury or a tendency toward overproliferation and intestinal dysplasia. In such a rapidly proliferating tissue, mechanisms that guard against accumulation of damage over time are critically important, yet how gut stem cells accomplish this is not completely understood. While some stem cells asymmetrically segregate newly synthesized DNA to daughter cells to defend against DNA replication-induced mutations, mammalian ISCs do not demonstrate this “immortal strand”

protective mechanism, indicating that they may require other methods to resist accumulation of damage throughout life [41]. To this end, murine ISCs are thought to display enhanced telomerase activity, compared to differentiated cells, which could lead to enhanced chromosomal stability [41]. Furthermore, mammalian intestinal crypts exhibit “neutral drift” and become clonal over time due to symmetric ISC division [42,43]. The process of neutral drift involves stochastic stem cell loss and replacement in the crypt, which could be a protective mechanism to limit stem cells harboring mutations from reaching clonal dominance [43].

Despite these potential safeguards, a number of studies have suggested that crypt cells undergo age-related functional decline. Aging has been linked to impaired crypt repair after high dose irradiation in mice [44]. Additionally, decreased Wnt signaling with age impairs the ability of mouse ISCs to maintain tissue homeostasis [45], while calorie restriction, a lifespan extending intervention, enhances stem cell numbers and regenerative capacity [46,47]. These data suggest gut stem cells are likely susceptible to degenerative changes with age.

Moreover, Lgr5+ stem cells have been proposed to play a role in the pathogenesis of colorectal cancer, a disease with age-associated increased incidence. Specifically, ISC gene expression patterns are recapitulated in stem-like cancer cells capable of colon tumor initiation in mice, and ISC gene signatures are correlated with colon cancer relapse in patients [48]. Additionally, ISCs are thought to be the cell-of-origin of intestinal cancer, as oncogenic mutations in murine stem cells give rise to intestinal tumor formation at higher rates than mutations in transit amplifying cells [49].

Given that colon cancer is common in older individuals and is the third leading cause of cancer-related deaths in the United States[43], the precise role(s) the tissue stem cell plays in age-related pathology warrants further investigation. In striking contrast to colon, however, small bowel cancers are rare throughout life, indicating that these ISCs may be less susceptible than CoSCs to age-related changes that contribute to loss of homeostasis. Yet, whether this

discrepancy could be due to segmental differences in susceptibility to molecular cellular changes during aging is unclear, especially in human.

Several groups have recently adapted the use of 3D organoid cultures to study small intestine and colon stem cell aging in mouse [45,50], but to do so in human, it is important to first confirm whether these mesenchyme-free cultures maintain hallmarks of biological age in the absence of an aging intestinal microenvironment. Aging hallmark analysis of small intestine and colon, and their respective *in vitro* organoids, is the focus of Chapter 3 of this thesis.

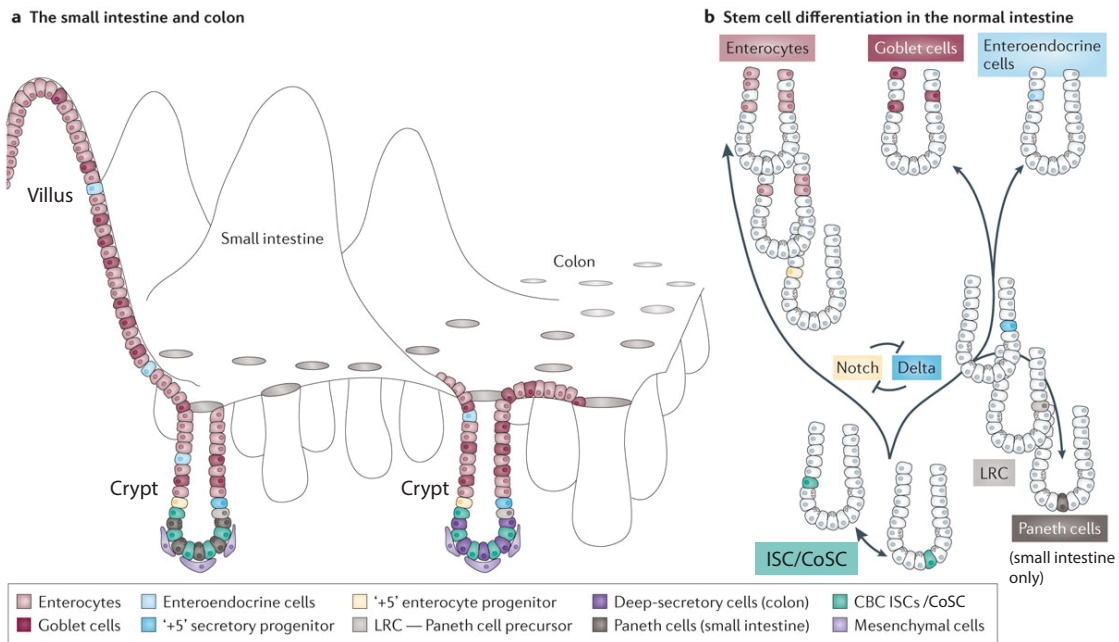


Figure 1-1: Epithelial cell composition in mammalian small intestine and colon. (A) The small intestine epithelium is composed of invaginating crypts and finger-like villi, while the colon epithelium is made of invaginating crypts and flat surface epithelial cells. (B) The surface epithelium is maintained by Lgr5+ crypt-based columnar stem cells, which can self-renew or differentiate to give rise to major secretory lineages (Goblet, enteroendocrine, and Paneth cells) or to absorptive lineages (enterocytes).

(Adapted from Vermeulen and Snippert, *Nature Reviews Cancer*, 2014[43])

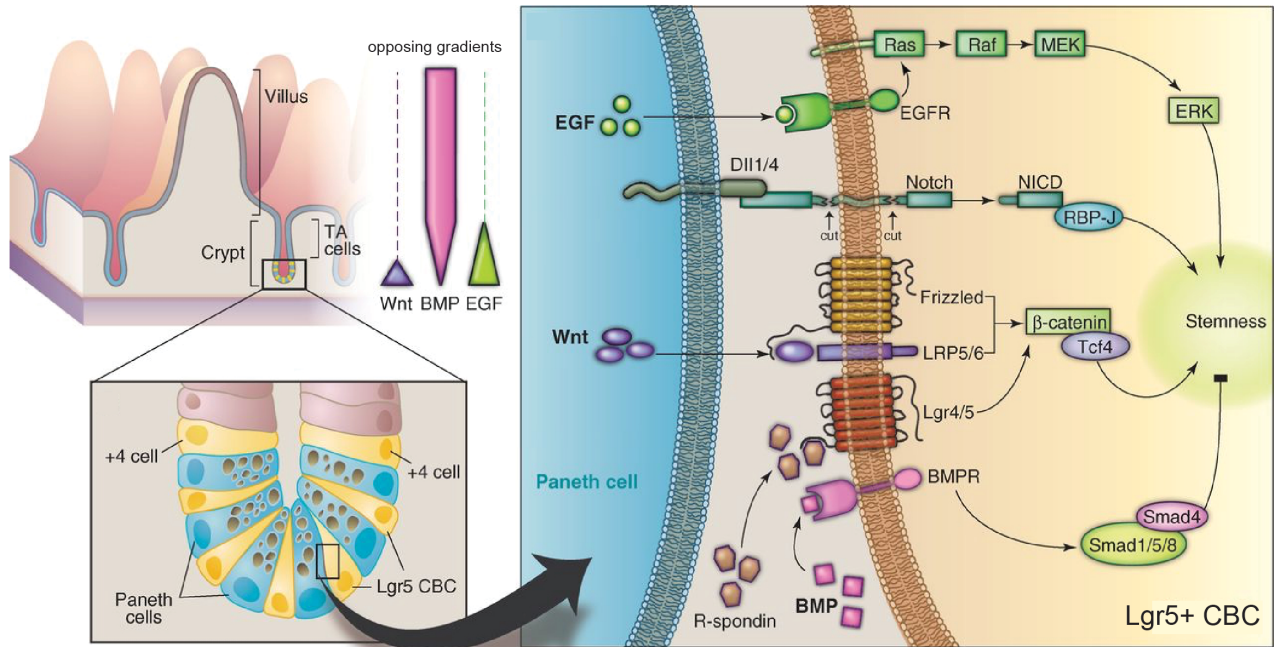


Figure 1-2: Niche factors that regulate intestinal stem cell homeostasis. Opposing gradients of stem cell promoting signals (Wnt and EGF) and negative regulators of stemness (BMP) help maintain homeostatic balance between proliferation and differentiation in the intestinal epithelium.

(Adapted from Sato and Clevers, *Science*, 2013[29])

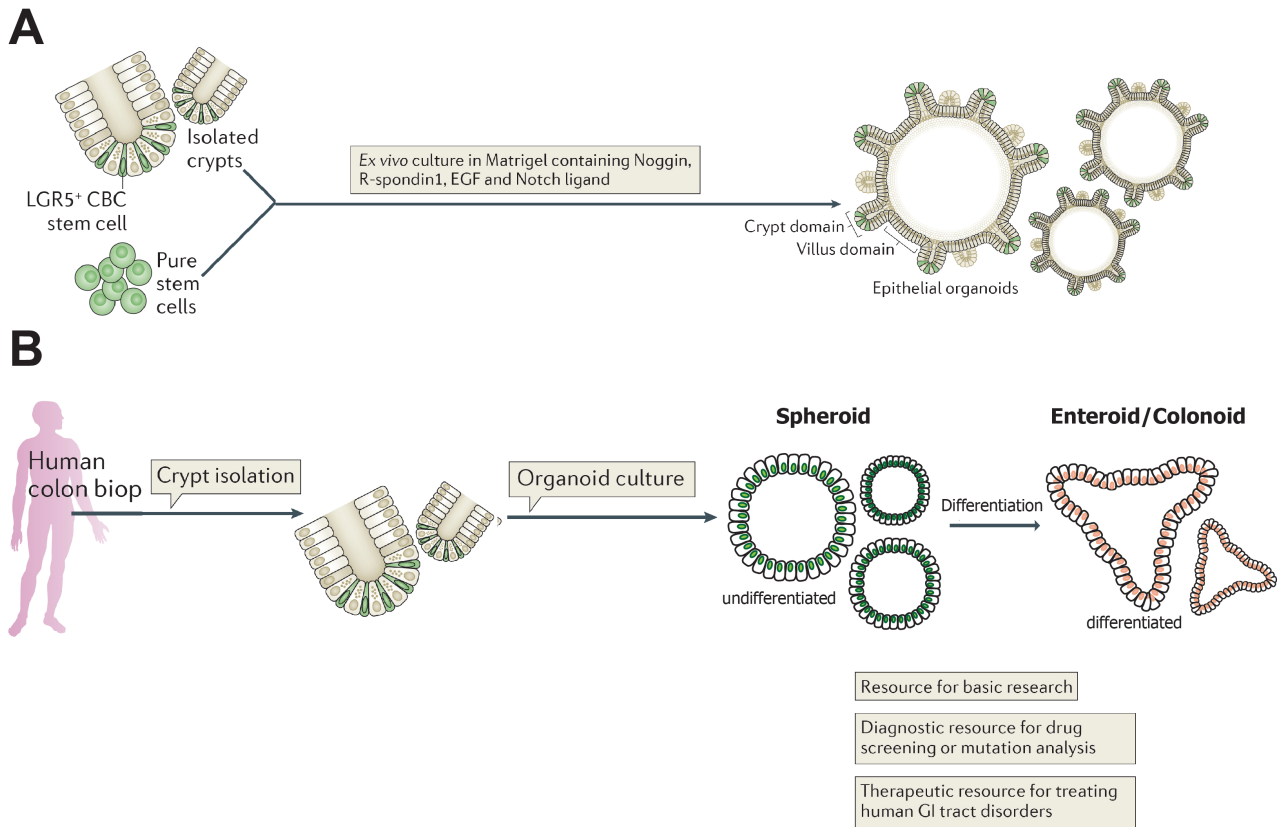


Figure 1-3: Schematic of mouse and human-derived intestinal organoids. (A) Mouse organoids can be derived from isolated intestinal crypts or purified stem cells, sorted from transgenic mice with fluorescently marked Lgr5⁺ stem cells. Mouse organoids maintain crypt and villus domains. (B) Human organoids can be derived from isolated intestinal or colonic crypts. Three-dimensional cultures can be established as stem cell-enriched spheroids, which can subsequently be differentiated to form enteroids, from small intestine, or colonoids, from colon. Organoids provide an *in vitro* resource for regenerative medicine, drug screening, and basic research into epithelial cell biology.

(Adapted from Barker, *Nat Rev Mol Cell Biol*, 2014[51])

Species	Organ	Wnt3A	EGF	Noggin	R-spondin	Cell types supported	Citation
Mouse	Small intestine	-	+	+	+	stem + differentiated	Sato, 2009
	colon	+	+	+	+	stem (withdraw Wnt for differentiation)	Sato, 2011

Table 1-1: Mouse intestinal and colonic organoid culture conditions. Mouse small intestine organoids are grown in media containing EGF, Noggin and R-spondin and recapitulate crypt-villus architecture. Mouse colon organoids require supplemental Wnt3A, which promotes stem cell-enriched cultures capable of differentiation upon Wnt withdrawal. Listed are the core growth factors for growing organoids for different regions of the gut and what cell types are supported under these conditions.

Organ	Wnt3A, EGF, Noggin, R-spondin	Nicotinamide	Gastrin	SB202190 (p38 inh)	A8301 (TGF- β inh)	LY2157299 (TGF- β inh)	PGE2	Cell types supported	Citation
Small intestine	+	+	+	+	+	-	-	Stem cell (Differentiation: remove Wnt, SB202190, A8301)	Sato, 2011
Colon	+	+	+	+	+	-	-	Stem cell (Differentiation: remove Wnt, SB202190, A8301)	Sato, 2011
Small intestine	+	-	+	+	+	-	-	Stem cell	Sugimoto 2017
Colon	+	-	+	+	+	-	-	Stem cell	Sugimoto 2017
Colon	+	+	+	+	-	+	+	Stem cell (Differentiation: remove Wnt, Nicotinamide, SB202190, PGE2, add DAPT)	Jung, 2011
Colon	+	+	+	+	+	-	+	Stem cell (Differentiation: remove Wnt, R-spondin, Nicotinamide, SB202190, A8301, PGE2)	Jung, 2015

Table 1-2: Human small intestine and colon organoid culture conditions. Contrary to mouse small intestine and colon organoid conditions, human small intestine and colon cultures do not have region-specific media requirements to date, nor is there a uniform consensus of culture conditions. Listed are published organoid culture conditions for human, including the core growth factors and what cell types are supported under these conditions.

References

1. Delaunoy T, Neczyporenko F, Limburg PJ, Erlichman C. Pathogenesis and risk factors of small bowel adenocarcinoma: a colorectal cancer sibling? *Am J Gastroenterol*. 2005 Mar;100(3):703–10.
2. Mowat AM, Agace WW. Regional specialization within the intestinal immune system. *Nat Rev Immunol*. 2014 Oct;14(10):667–85.
3. Cheng H, Leblond CP. Origin, differentiation and renewal of the four main epithelial cell types in the mouse small intestine. III. Entero-endocrine cells. *Am J Anat*. 1974 Dec;141(4):503–19.
4. Clevers H. The Intestinal Crypt, A Prototype Stem Cell Compartment. *Cell*. 2013 Jul;154(2):274–84.
5. Sato T, Vries RG, Snippert HJ, van de Wetering M, Barker N, Stange DE, van Es JH, Abo A, Kujala P, Peters PJ, Clevers H. Single Lgr5 stem cells build crypt–villus structures in vitro without a mesenchymal niche. *Nature*. Nature Publishing Group; 2009 Mar 29;459(7244):262–5.
6. Barker N, van Oudenaarden A, Clevers H. Identifying the stem cell of the intestinal crypt: strategies and pitfalls. *Cell Stem Cell*. 2012 Oct 5;11(4):452–60.
7. Potten CS. Extreme sensitivity of some intestinal crypt cells to X and gamma irradiation. *Nature*. 1977 Oct 6;269(5628):518–21.
8. Barker N, van Es JH, Kuipers J, Kujala P, van den Born M, Cozijnsen M, Haegebarth A, Korving J, Begthel H, Peters PJ, Clevers H. Identification of stem cells in small intestine and colon by marker gene Lgr5. *Nature*. Nature Publishing Group; 2007 Oct 14;449(7165):1003–7.

9. Yan KS, Chia LA, Li X, Ootani A, Su J, Lee JY, Su N, Luo Y, Heilshorn SC, Amieva MR, Sangiorgi E, Capecchi MR, Kuo CJ. The intestinal stem cell markers Bmi1 and Lgr5 identify two functionally distinct populations. *Proc Natl Acad Sci USA*. 2012 Jan 10;109(2):466–71.
10. Tian H, Biehs B, Warming S, Leong KG, Rangell L, Klein OD, de Sauvage FJ. A reserve stem cell population in small intestine renders Lgr5-positive cells dispensable. *Nature*. 2011 Oct 13;478(7368):255–9.
11. Takeda N, Jain R, LeBoeuf MR, Wang Q, Lu MM, Epstein JA. Interconversion between intestinal stem cell populations in distinct niches. *Science*. 2011 Dec 9;334(6061):1420–4.
12. Wong VWY, Stange DE, Page ME, Buczacki S, Wabik A, Itami S, van de Wetering M, Poulsom R, Wright NA, Trotter MWB, Watt FM, Winton DJ, Clevers H, Jensen KB. Lrig1 controls intestinal stem-cell homeostasis by negative regulation of ErbB signalling. *Nat Cell Biol*. 2012 Apr;14(4):401–8.
13. Muñoz J, Stange DE, Schepers AG, van de Wetering M, Koo B-K, Itzkovitz S, Volckmann R, Kung KS, Koster J, Radulescu S, Myant K, Versteeg R, Sansom OJ, van Es JH, Barker N, van Oudenaarden A, Mohammed S, Heck AJR, Clevers H. The Lgr5 intestinal stem cell signature: robust expression of proposed quiescent “+4” cell markers. *EMBO J*. 2012 Jul 18;31(14):3079–91.
14. Buczacki SJA, Zecchini HI, Nicholson AM, Russell R, Vermeulen L, Kemp R, Winton DJ. Intestinal label-retaining cells are secretory precursors expressing Lgr5. *Nature*. 2013 Mar 7;495(7439):65–9.
15. van Es JH, Haegebarth A, Kujala P, Itzkovitz S, Koo B-K, Boj SF, Korving J, van den Born M, van Oudenaarden A, Robine S, Clevers H. A critical role for the Wnt effector Tcf4 in adult intestinal homeostatic self-renewal. *Mol Cell Biol*. 2012 May;32(10):1918–27.

16. Ireland H, Kemp R, Houghton C, Howard L, Clarke AR, Sansom OJ, Winton DJ. Inducible Cre-mediated control of gene expression in the murine gastrointestinal tract: effect of loss of beta-catenin. *Gastroenterology*. 2004 May;126(5):1236–46.
17. Korinek V, Barker N, Moerer P, van Donselaar E, Huls G, Peters PJ, Clevers H. Depletion of epithelial stem-cell compartments in the small intestine of mice lacking Tcf-4. *Nat Genet*. 1998 Aug;19(4):379–83.
18. Marchbank T, Goodlad RA, Lee CY, Playford RJ. Luminal epidermal growth factor is trophic to the small intestine of parenterally fed rats. *Clin Sci*. 1995 Aug;89(2):117–20.
19. Suzuki A, Sekiya S, Gunshima E, Fujii S, Taniguchi H. EGF signaling activates proliferation and blocks apoptosis of mouse and human intestinal stem/progenitor cells in long-term monolayer cell culture. *Lab Invest*. 2010 Oct;90(10):1425–36.
20. Haramis A-PG, Begthel H, van den Born M, van Es J, Jonkheer S, Offerhaus GJA, Clevers H. De novo crypt formation and juvenile polyposis on BMP inhibition in mouse intestine. *Science*. 2004 Mar 12;303(5664):1684–6.
21. Thorne CA, Chen IW, Sanman LE, Cobb MH, Wu LF, Altschuler SJ. Enteroid Monolayers Reveal an Autonomous WNT and BMP Circuit Controlling Intestinal Epithelial Growth and Organization. *Dev Cell*. 2018 Mar 12;44(5):624–4.
22. Batts LE, Polk DB, Dubois RN, Kulessa H. Bmp signaling is required for intestinal growth and morphogenesis. *Dev Dyn*. 2006 Jun;235(6):1563–70.
23. Sato T, van Es JH, Snippert HJ, Stange DE, Vries RG, van den Born M, Barker N, Shroyer NF, van de Wetering M, Clevers H. Paneth cells constitute the niche for Lgr5 stem cells in intestinal crypts. *Nature*. 2011 Jan 20;469(7330):415–8.
24. Farin HF, Jordens I, Mosa MH, Basak O, Korving J, Tauriello DVF, de Punder K, Angers S, Peters PJ, Maurice MM, Clevers H. Visualization of a short-range Wnt gradient in the intestinal stem-cell niche. *Nature*. 2016 Feb 10.

25. Kim T-H, Escudero S, Shivdasani RA. Intact function of Lgr5 receptor-expressing intestinal stem cells in the absence of Paneth cells. *2012 Mar 6;109(10):3932–7.*
26. Shoshkes-Carmel M, Wang YJ, Wangenstein KJ, Tóth B, Kondo A, Massassa EE, Itzkovitz S, Kaestner KH. Subepithelial telocytes are an important source of Wnts that supports intestinal crypts. *Nature.* 2018 May 2.
27. Lei NY, Jabaji Z, Wang J, Joshi VS, Brinkley GJ, Khalil H, Wang F, Jaroszewicz A, Pellegrini M, Li L, Lewis M, Stelzner M, Dunn JCY, Martín MG. Intestinal subepithelial myofibroblasts support the growth of intestinal epithelial stem cells. *PLoS ONE.* 2014;9(1):e84651.
28. Sasaki N, Sachs N, Wiebrands K, Ellenbroek SIJ, Fumagalli A, Lyubimova A, Begthel H, van den Born M, van Es JH, Karthaus WR, Li VSW, López-Iglesias C, Peters PJ, van Rheenen J, van Oudenaarden A, Clevers H. Reg4+ deep crypt secretory cells function as epithelial niche for Lgr5+ stem cells in colon. *Proc Natl Acad Sci USA.* 2016 Sep 13;113(37):E5399–407.
29. Sato T, Clevers H. Growing Self-Organizing Mini-Guts from a Single Intestinal Stem Cell: Mechanism and Applications. *Science.* 2013 Jun 6;340(6137):1190–4.
30. Yin X, Farin HF, van Es JH, Clevers H, Langer R, Karp JM. Niche-independent high-purity cultures of Lgr5+ intestinal stem cells and their progeny. *Nat Meth.* 2013 Dec 1;11(1):106–12.
31. Sato T, Stange DE, Ferrante M, Vries R, Van Es JH. Long-term expansion of epithelial organoids from human colon, adenoma, adenocarcinoma, and Barrett's epithelium. *Gastroenterology.* 2011.
32. Jung P, Sato T, Merlos-Suárez A, Barriga FM, Iglesias M, Rossell D, Auer H, Gallardo M, Blasco MA, Sancho E, Clevers H, Batlle E. Isolation and in vitro expansion of human colonic stem cells. *Nat Med.* 2011 Oct;17(10):1225–7.

33. Sugimoto S, Sato T. Establishment of 3D Intestinal Organoid Cultures from Intestinal Stem Cells. *Methods Mol Biol.* 2017;1612:97–105.
34. Jung P, Sommer C, Barriga FM, Buczacki SJ, Hernando-Momblona X, Sevillano M, Duran-Frigola M, Aloy P, Selbach M, Winton DJ, Batlle E. Stem Cell Reports. *Stem Cell Reports.* The Authors; 2015 Dec 8;5(6):979–87.
35. Middendorp S, Schneeberger K, Wiegerinck CL, Mokry M, Akkerman RDL, van Wijngaarden S, Clevers H, Nieuwenhuis EES. Adult stem cells in the small intestine are intrinsically programmed with their location-specific function. *Stem Cells.* 2014 May;32(5):1083–91.
36. López-Otín C, Blasco MA, Partridge L, Serrano M, Kroemer G. The Hallmarks of Aging. *Cell.* 2013 Jun;153(6):1194–217.
37. Oh J, Lee YD, Wagers AJ. Stem cell aging: mechanisms, regulators and therapeutic opportunities. Nature Publishing Group. *Nature Publishing Group*; 2014 Aug 1;20(8):870–80.
38. Liu L, Rando TA. Manifestations and mechanisms of stem cell aging. *The Journal of Cell Biology.* 2011 Apr 18;193(2):257–66.
39. Sipos F, Leiszter K, Tulassay Z. Effect of ageing on colonic mucosal regeneration. *World J Gastroenterol.* 2011 Jul 7;17(25):2981–6.
40. Man AL, Bertelli E, Rentini S, Regoli M, Briars G, Marini M, Watson AJM, Nicoletti C. Age-associated modifications of intestinal permeability and innate immunity in human small intestine. *Clin Sci.* 2015 Oct 1;129(7):515–27.
41. Schepers AG, Vries R, van den Born M, van de Wetering M, Clevers H. Lgr5 intestinal stem cells have high telomerase activity and randomly segregate their chromosomes. *EMBO J.* 2011 Mar 16;30(6):1104–9.
42. Kozar S, Morrissey E, Nicholson AM, van der Heijden M, Zecchini HI, Kemp R, Tavaré S, Vermeulen L, Winton DJ. Short Article. *Stem Cell.* Elsevier Inc; 2013 Nov 7;13(5):626–33.

43. Vermeulen L, Snippert HJ. Stem cell dynamics in homeostasis and cancer of the intestine. *Nat Rev Cancer*. 2014 Jul;14(7):468–80.
44. Martin K, Potten CS, Roberts SA, Kirkwood TB. Altered stem cell regeneration in irradiated intestinal crypts of senescent mice. *Journal of Cell Science*. 1998 Aug;111 (Pt 16):2297–303.
45. Nalapareddy K, Nattamai KJ, Kumar RS, Karns R, Wikenheiser-Brokamp KA, Sampson LL, Mahe MM, Sundaram N, Yacyshyn M-B, Yacyshyn B, Helmrath MA, Zheng Y, Geiger H. Canonical Wnt Signaling Ameliorates Aging of Intestinal Stem Cells. *Cell Rep*. ElsevierCompany; 2017 Mar 14;18(11):2608–21.
46. Igarashi M, Guarente L. mTORC1 and SIRT1 Cooperate to Foster Expansion of Gut Adult Stem Cells during Calorie Restriction. *Cell*. Elsevier Inc; 2016 Jul 14;166(2):436–50.
47. Yilmaz ÖH, Katajisto P, Lamming DW, Gültekin Y, Bauer-Rowe KE, Sengupta S, Birsoy K, Dursun A, Yilmaz VO, Selig M, Nielsen GP, Mino-Kenudson M, Zukerberg LR, Bhan AK, Deshpande V, Sabatini DM. mTORC1 in the Paneth cell niche couples intestinal stem-cell function to calorie intake. *Nature*. 2012 May 20.
48. Merlos-Suárez A, Barriga FM, Jung P, Iglesias M, Céspedes MV, Rossell D, Sevillano M, Hernando-Momblona X, da Silva-Diz V, Muñoz P, Clevers H, Sancho E, Manges R, Batlle E. The intestinal stem cell signature identifies colorectal cancer stem cells and predicts disease relapse. *Cell Stem Cell*. 2011 May 6;8(5):511–24.
49. Barker N, Ridgway RA, van Es JH, van de Wetering M, Begthel H, van den Born M, Danenberg E, Clarke AR, Sansom OJ, Clevers H. Crypt stem cells as the cells-of-origin of intestinal cancer. *Nature*. 2008 Dec 17;457(7229):608–11.

50. Mihaylova MM, Cheng C-W, Cao AQ, Tripathi S, Mana MD, Bauer-Rowe KE, Abu-Remaileh M, Clavain L, Erdemir A, Lewis CA, Freinkman E, Dickey AS, La Spada AR, Huang Y, Bell GW, Deshpande V, Carmeliet P, Katajisto P, Sabatini DM, Yilmaz ÖH. Fasting Activates Fatty Acid Oxidation to Enhance Intestinal Stem Cell Function during Homeostasis and Aging. *Cell Stem Cell*. 2018 May 3;22(5):769–778.e4.
51. Barker N. Adult intestinal stem cells: critical drivers of epithelial homeostasis and regeneration. *Nat Rev Mol Cell Biol*. 2013 Dec 11;15(1):19–33.

Chapter 2: Regional differences in gut stem cell behavior *in vitro*

Sophia Kuo Lewis, Dana Leanne Jones

A version of this chapter is in preparation for publication

Acknowledgements

We would like to thank the UCLA Translational Pathology Core Laboratory for assistance with histology, and the UCLA Jonsson Comprehensive Cancer Center Flow Cytometry core for help with cell sorting for single cell assays. We also would like to acknowledge OneLegacy, the organ donors and their families for giving the gift of knowledge by their generous donations. This work was supported by: the UCLA Broad Stem Cell Research Center Predoctoral Training Grant and the Rose Hills Foundation (SL); the UCLA Broad Stem Cell Research Center Innovation Award and the Rose Hills Foundation (DLJ); the CURE: Digestive Diseases Research Center at UCLA Pilot and Feasibility Study Award (center grant P30 DK 41301) (DLJ); and the UCLA CTSI/BSCRC/DGSOM Regenerative Medicine Theme Award (DLJ).

Abstract

Although Lgr5+ actively cycling stem cells have been identified at the base of small intestine and colon crypts, the majority of analyses of stem cell behavior have been conducted in mouse small intestine, and less is known about human colon stem cells, especially in human. Unlike small intestine, the colon is prone to adenocarcinoma, a malignancy proposed to derive from stem cells; however, given the limited data on colon stem cell biology, little is known about regional differences in stem cell behavior or susceptibility to disease. Here, we utilize stem cell-enriched three-dimensional intestinal organoids, known as spheroids, to investigate behavioral differences between small intestine and colon stem cells. We demonstrate that *in vitro* colon stem cells are slow cycling and have decreased stem cell function compared to small intestine, resulting in cultures that are difficult to expand. We find that colon spheroids have a tendency to differentiate, which can be prevented by antagonizing BMP signaling – a pathway that, when active, inhibits stemness and promotes differentiation. We show that BMP inhibition increases colon stem cell function and proliferation, indicating that additional refinement to human organoid culture conditions may be warranted. Interestingly, BMP inhibition did not enhance colon stem cell proliferation rate to the level of small intestine stem cells, suggesting that there may be regional differences in stem cell behavior and that colon stem cells may be slower cycling than original hypothesized.

Introduction

The inner epithelial lining of the mammalian gut acts as both an absorptive layer, functioning to digest and absorb nutrients and water, and as a barrier, preventing toxins and microorganisms from entering the body. To maintain proper digestive function in the face of constant damage from luminal contents, the intestinal epithelium undergoes rapid regeneration, a process maintained by tissue-specific stem cells that reside in protective niches, the invaginating crypts [1,2].

Within the small intestine and colon, intestinal stem cells (ISCs) and colonic stem cells (CoSCs) are both marked by the Wnt target gene *Lgr5*[3]. *Lgr5*⁺ stem cells rapidly proliferate throughout life and are multipotent – capable of regenerating all the terminally differentiated lineages that make up the surface epithelium of both organs [3]. Opposing gradients of stem cell-promoting signals, like Wnt, and differentiation signals, such as BMP, act to maintain a homeostatic balance between proliferation and differentiation [4,5]. Alterations between turnover and regeneration could lead to impaired epithelial repair after injury or a tendency toward overproliferation, intestinal dysplasia, and tumor formation.

In humans, colorectal adenocarcinoma (CRC) is prevalent in older populations and is a leading cause of cancer-associated death. The pathogenesis of CRC is thought to be a multi-step process known as the “adenoma-carcinoma” sequence, in which an initial mutation, often leading to aberrant Wnt activation, is followed by a further oncogenic mutations, increasing genetic instability, and overproliferation of the epithelium [6-8]. Mouse studies have demonstrated that *Lgr5*⁺ stem cells are likely the cell of origin for CRC, as a Wnt-activating mutation in stem cells give rise to more tumors than the equivalent mutation in differentiated epithelial cells [9]. Interestingly, these experiments demonstrated high mutation-induced tumor burden in the mouse small intestine. By contrast, human small intestinal adenocarcinomas are very rare and are estimated to be 50 fold less common than CRC [6]. Given the close proximity of the small intestine and colon and the presence of actively proliferating *Lgr5*⁺ stem cells in

both tissues, the resistance to adenocarcinoma in the small bowel is striking. Several features that differ between small intestine and colon have been proposed to contribute to the diverging incidence of tumors, including immune cell composition, microbiome composition and bacteria load, pH of luminal contents, and altered transit time [10], [11]. Yet, there remains limited direct evidence to support these hypotheses.

As Lgr5+ stem cells serve as the cell of origin for CRC, it is also feasible that molecular differences between Lgr5+ ISC and CoSC contribute to the variable susceptibility of the small intestine and colon to cancer. While the pathogenesis of small bowel adenocarcinoma is less well understood than CRC, there are known differences in the mutational changes in the two organs during malignant transformation [12]. Additionally, a seminal study by Tomasetti and Vogelstein demonstrated that, in general, life time risk for cancer across tissues is correlated with total number of stem cell divisions due to accumulation of replication-induced errors[13]. This study suggests that a higher proliferation rate of CoSCs compared to ISCs could underlie the increased incidence of adenocarcinoma in the colon versus small intestine, but there has been limited direct comparison of stem cell self-renewal kinetics in the two organs to support this hypothesis, particularly in human.

Due to potential interspecies differences in gut stem cell function and regional tumor susceptibility, experimental models that highlight human biology are necessary. Three-dimensional organoid cultures have proven to be effective model systems for studying a number of stem/progenitor cells, ranging from breast epithelium to the mammalian brain. In particular, human gut organoids are easily derived *in vitro*, maintained by self-renewing stem cells, and are capable of multi-lineage differentiation [14-16], making these ideal models for investigating small intestine and colon stem cell molecular and functional differences, including proliferation rates. Importantly, most scientific inquiry into stem cell behavior, including in organoids, has been conducted in murine small intestine. Little is known about human CoSC behavior, or how CoSCs differ from ISCs.

In this study, we uncover regional differences in ISC and CoSC proliferation rates using stem cell-enriched spheroids. We find that CoSCs divide less frequently than ISCs *in vitro*. We show that supplemental BMP inhibition increases CoSC proliferation, enhances stem cell function and inhibits differentiation; however, even in the presence of BMP inhibition, CoSCs remain slower cycling than ISCs.

Materials and Methods

Human bowel tissue

De-identified and discarded surgical specimens were retrieved from the UCLA Translational Pathology Core Laboratory (TPCL). Following clinical surgical pathology evaluation, normal adjacent tissue was obtained. Experimentation using TPCL-derived human tissues was approved by the UCLA institutional review board, which waived the informed consent requirement for specimens acquired from the TPCL (IRB#11-002504). Paired jejunum and colon from anonymous post-mortem donors was facilitated by OneLegacy Foundation, Los Angeles, CA.

Intestinal mucosa and crypt isolation

Tissues were washed in phosphate buffered saline (PBS), and mucosa was isolated by removal of outer muscle layers using surgical scissors. Mucosae were cut into 1 cm pieces and washed with PBS until the supernatant was clear. Small intestine and colonic crypts were isolated using modified existing methods [15,17]. Specimens were incubated at 4°C in 8mM EDTA and 1mM Dithiothreitol for 30 minutes to 1 hour, with gentle agitation. Supernatant was removed and replaced with fresh PBS. Specimens were vortexed to release crypts. Crypts were collected into 15ml Falcon tubes and the process was repeated to collect 4-6 fractions. Fractions were centrifuged at 100xg to pellet crypts. SI crypts were subsequently filtered with 100um mesh to remove villus domains and epithelial debris. Colon crypts were not filtered. Isolated crypts were resuspended in basic medium containing ADMEM/F12, 1X Glutamax, 10mM HEPES buffer, and 1X Penicillin/Streptomycin (all ThermoFisher) for spheroid cultures.

In vitro organoid cultures

To generate cystic 3D spheroids, isolated crypts were seeded at 150 crypts/25ul of Growth Factor Reduced Matrigel (BD Biosciences, 356231) in a 48 well plate. Matrigel was allowed to solidify for 15 minutes at 37°C. Cells were overlaid with 250ul of slightly modified “stem cell” media [17,18], consisting of 50% Wnt3A Conditioned Medium (see below), 50% ADMEM/F12, 1X Penicillin/Streptomycin, 1X Glutamax, 10mM HEPES, 1mM N-acetyl-L-cysteine (Sigma A9165), 1x N2 supplement (Life Technologies 17502), 1x B27 minus Vitamin A (Life Technologies 12587), 50ng/ml EGF (Peprotech 316-09), 1ug/ml human R-spondin (R&D 4645-RS), 100ng/ml murine Noggin (Peprotech 250-38), 10mM Nicotinamide (Sigma N0636), 10nM Gastrin (Sigma G9145), 10uM SB202190 (Sigma S7067), and 100nM PGE2 (Sigma P5640). Medium was changed every 2-3 days. Spheroids were passaged every 5-7 days by dissociation for 3 minutes in TrypLE Express (Life Technologies 12604021) at 37°C followed by reseeding in Matrigel. For two days after splitting, 10uM Rock inhibitor Y27632 (Sigma Y0503) was added to the medium. To achieve differentiation of stem cell-enriched cultures, Nicotinamide, SB202190 and PGE2 were withdrawn; Wnt3A conditioned medium was reduced to 10%; and 10uM DAPT gamma secretase inhibitor (Sigma, D5942) was added for 4 days of differentiation [15]. For BMP inhibition analysis, the BMP inhibitor LDN193189 (Sigma SML0559) was used at 200nM final concentration. For TGF- β inhibition analysis, the ALK5 inhibitor A-8301 (Tocris 2939) was used at 500nM final concentration.

Wnt3A conditioned medium

L Wnt-3A cells (ATCC, CRL-2647) were cultured until 80-90% confluency in DMEM (ThermoFisher 11995065) + 10% Fetal Bovine Serum (ThermoFisher 10437-010) + 1X Pencillin/Streptomycin (ThermoFisher 15140122). Cells were then split to approximately 10% density and cultured for 4 days in t75 flasks. Supernatant was collected on day 4 and sterile

filtered. Fresh medium was replaced for 3 more days. Day 7 supernatant was sterile filtered, and combined with Day 4 medium [15]. Aliquoted stocks were stored at -20°C.

5-Ethynyl-2'-deoxyuridine Labeling

Spheroids were split to chamber slides (ThermoFisher 62407-355) in stem cell medium containing Y27632 (Sigma Y0503). Ethynyl-2'-deoxyuridine (EdU) labeling was done using the Click-iT EdU Alexa 594 Imaging Kit (Invitrogen C10339). For proliferation analysis in stem cell vs. differentiation conditions: two days after splitting, half of the wells were changed to Differentiation medium, as above, and half were maintained in stem cell medium. Cells were treated with 50 uM EdU for the last 16 hours before fixation. For proliferation of paired jejunum and colon: two days after splitting spheroids to chamber slides, cells were treated with 50uM EdU for 4 hours before fixation. Organoids were fixed in 4% paraformaldehyde [16]. Click-iT reaction was conducted according to manufacturer protocols. Samples were mounted in Vectashield with DAPI (Vector Laboratories H-1200) to mark nuclei.

Histological analysis and immunofluorescence staining

Intestinal mucosa samples were fixed in 10% neutral buffered formalin overnight, embedded in paraffin, and sectioned at 5-um. Organoids were fixed in 5% neutral buffered formalin for 30 minutes, embedded in HistoGel specimen processing gel (ThermoFisher HG-4000-012) prior to embedding in paraffin, and sectioned at 5-um. Intestinal alkaline phosphatase was detected using NBT/BCIP according to published methods [19]. For immunostaining on paraffin sections, slides were dewaxed in xylene, rehydrated, and heat mediated antigen retrieval was conducted with citrate buffer (pH 6). For Goblet cells, sections were immunostained with Mucin-2 primary antibody (sc-15334; 1:50 dilution). For whole mount staining of mitotic events, organoids were split to chamber slides (ThermoFisher 62407-355) and subsequently fixed and stained according to published methods [20], with primary antibody against phospho-histone H3

(Millipore 06-570; 1:200 dilution). Secondary staining was conducted with Alexa 568 goat anti-rabbit IgG (ThermoFisher Scientific A-11011; 1:1000 dilution). Samples were mounted in Vectashield with DAPI (Vector Laboratories H-1200) to mark nuclei.

Reverse Transcription and quantitative PCR

To isolate total RNA, samples were lysed in Trizol reagent (Invitrogen 15596026), followed by chloroform extraction and isopropanol precipitation. RNA was DNase treated and reverse transcribed to complementary DNA using the iScript Reverse Transcription Supermix (Bio-Rad 15596026). Quantitative RT-PCR was conducted using SSO Advanced Universal SYBR Green Supermix (Bio-Rad) and gene specific primers (see below). Data were obtained on the CFX96 Real Time System (Bio-Rad) using recommended device settings. Samples were analyzed in triplicate. The human ribosomal gene RPL13A was used as reference for quantification of gene expression. Fold-change of mRNA expression between undifferentiated and differentiated organoids was calculated using the $2^{-\Delta\Delta CT}$ method. Oligonucleotide primers used were as follows: *RPL13A*, 5'-GCCCTACGACAAGAAAAAGCG-3' (forward) / 5'-TACTTCCAGCCAACC TCGTGA-3' (reverse); *Lgr5*, 5'-ACCAGACTATGCCTTTGGAAAC-3' (forward)/ 5'-TTCCCAGGGAGTGGATTCTAT-3' (reverse); *Sucrase Isomaltase*, 5'-TTTTGGCATCCAGATTCGAC-3' (forward)/ 5'-ATCCAGGCAGCCAAGAATC-3' (reverse); and *Carbonic anhydrase-1*, 5'-TGGTTTGGCAGTTATTGGTG -3' (forward)/ 5'-GCCAGGGTAGGTCCAGAAAT -3' (reverse).

Recovery of three-dimensional organoids and FACS sorting

Duodenal and colonic spheroids were expanded in Matrigel with stem cell-supporting medium, as above. Spheroids were washed with PBS and subsequently collected in Cell Recovery Solution (Corning, USA, 354253) in 15 ml Falcon tube on ice for 45 minutes. Spheroids were collected by centrifugation at 100xg 4°C for 2 minutes. After a wash in PBS, spheroids were re-

suspended in dissociation buffer containing TrypLE Express (Life Technologies 12604021), 10uM Y27632 (Sigma Y0503) and 100ug/ml DNase I (Sigma D4513), and incubated at 37°C for up to 1 hour. To achieve single cell preparation, samples were gently re-suspended with a P1000 pipette every 5 minutes. Cells were passed through a 40um mesh (BD Falcon) and re-suspended in sorting media, containing: ADMEM/F12, 1X Penicillin/Streptomycin, 1X Glutamax, 10mM HEPES, 1mM N-acetyl-L-cysteine, 1x N2 supplement, 1x B27 minus Vitamin A, 1% Fetal Bovine Serum, 2.5uM PGE2, 10um Y27632 and 100ug/ml DNaseI (Sigma D4513). To discriminate against dead cells, DAPI (ThermoFisher Scientific D1306) was added to media prior to sorting on FACS Aria 2.0 (BD Biosciences). Cell aggregates were eliminated using forward scatter. Dead cells were removed by discarding the DAPI+ subpopulation, and viable singlets were collected in collection media (sorting media supplemented with 10% Fetal Bovine Serum).

For single cell assays, cells were resuspended at 200 cells/ul of Matrigel (BD Biosciences 356231), and 1000 cells were plated in each well of a prewarmed 96 well plate. After Matrigel solidified for 15 minutes at 37°C, single cells were overlaid with stem cell medium, as above, containing 10uM Y27632. The BMP inhibitor LDN193189 was added at 200nM where described. Media was changed every 2-3 day, and Y27632 was maintained in culture for 7 days. After 7 days, colony forming efficiency was measured microscopically; the number of seeded cells giving rise to spheroids with cystic lumen was quantified. Spheroid size at day 7 was also measured microscopically.

Immunoblotting

Spheroids were cultured +/- BMP inhibitor LDN for 4 days. Spheroids were harvested in Cell Recovery Solution for 45 minutes on ice, pelleted and rinsed in 1x PBS before lysis. Samples were resolved on 10% acrylamide gels. Immunoblots were probed with rabbit anti-pSmad 1/5 (Cell Signaling #9516, 1:1000 dilution) or mouse anti-gamma tubulin (Sigma T6557, 1:10,000

dilution), and detected with donkey anti-rabbit or donkey anti-mouse-HRP (Jackson ImmunoResearch 711-036-152 and 715-036-151, 1:10,000 dilutions) secondary antibodies, followed by chemiluminescent detection with Clarity ECL (Bio-Rad). Immunoblots were imaged on the Chemidoc Imaging System (Bio-Rad).

Results

Organoid culture conditions permit growth of stem and differentiated epithelial cells from human small intestine and colon

Using isolated human intestinal and colonic crypts from pathologically normal duodenum and colon surgical specimens, a library of primary, three-dimensional cell cultures was established. This culture method permits establishment and expansion of the intestinal epithelium as stem cell-enriched undifferentiated “spheroids”, as well as induction of differentiated “enteroids” or “colonoids” through modification of stem cell-promoting growth factors in the medium for small intestine and colon samples, respectively.

Spheroids are cystic, while enteroids and colonoids adopt dense, folded morphologies (Figure 2-1A; Figure S2-1A). Stem cell-enriched spheroids undergo regular cell division marked by EdU incorporation, whereas proliferative potential is significantly reduced during differentiation, with loss of EdU incorporation by day 4 in differentiation medium (Figure 2-1B; Figure S2-1B). Quantitative PCR analysis confirmed that expression of the classic CBC marker *Lgr5* is enriched in spheroids and is lost upon differentiation (Figure 2-1C).

Moreover, spheroids maintain multi-lineage differentiation potential, a characteristic of stemness. Specifically, quantitative PCR analysis revealed that small intestinal spheroids, which lack expression of the sucrase isomaltase, upregulate this enterocyte gene during differentiation (Figure 2-1D). Similarly, enterocyte-derived alkaline phosphatase and Goblet cell-derived Mucin-2 were detected in sections of differentiated enteroids but not in undifferentiated spheroids (Figure 2-1E-F). Comparable results demonstrating differentiation potential were obtained using spheroids derived from primary colon specimens. In particular, we see that colon spheroids are capable of differentiation into colonoids, which express mature epithelial markers such as carbonic anhydrase-1 (CA1) [21] (Figure S2-1C). Taken together, these results indicate that human small intestine and colon spheroids exhibit hallmarks of gut stem cells, including frequent proliferation, expression of stem cell-associated genes, and differentiation capacity.

Human CoSCs are slow cycling under basal conditions *in vitro*

Little is known about behavioral differences between human ISCs and CoSCs. To determine whether ISCs and CoSCs have similar growth potential *in vitro*, we first generated spheroids from isolated duodenal and colon crypts under basal, stem cell promoting culture conditions (Figure 2-1). There was no significant difference between initial spheroid forming efficiency for duodenum and colon crypts (see Appendix A). Notably, at day 3 after initial plating, colon spheroids had significantly larger area than duodenal spheroids, consistent with the typical longer crypt length in the colon [22] (Figure 2-2A). However, during subsequent expansion, the average colon spheroid size declined while the average duodenal spheroid size increased. Thus, at later passages, colon spheroid size was significantly smaller than duodenal spheroids (Figure 2-2B).

To determine if this discrepancy in colony expansion was due to a difference in proliferative capacities of cultured ISCs and CoSCs, the number of dividing cells per spheroid was counted using phospho-histone H3 as a marker of mitosis. Under stem cell promoting culture conditions, the number of CoSCs undergoing mitosis in colonic spheroids was significantly lower than the number of mitotic ISCs within duodenal spheroids (average mitotic cells: 2.0 and 10.3 in colon and duodenum, respectively; n=3 colon, n=3 duodenum) (Figure 2-2C). While these duodenal and colonic samples were derived from surgical resections from different individuals, we have conducted preliminary proliferation analysis of paired jejunum and colon spheroids from the same donor. The percentage of cells incorporating EdU after four hours was significantly lower in colon spheroids than in jejunum spheroids from the same individual (see Appendix B). These data suggest that *in vitro*-expanded CoSCs exhibit slower cycling behavior compared to ISCs.

In addition to active cycling capacity, the ability to give rise to single cell-derived organoids is a hallmark of Lgr5+ gut stem cells [14,15]. Therefore, we next compared the single cell colony forming efficiency of *in vitro* expanded human CoSCs and ISCs using a cohort of

three samples from each region. Single CoSCs derived from colon spheroids exhibited significantly decreased colony forming efficiency compared to single ISCs derived from duodenal spheroids (Figure 2-2D). Moreover, the spheroids that did form from CoSCs tended to be smaller than spheroids from single ISCs, though this difference was not significant (Figure 2-2D).

These data are consistent with a recent report that human CoSCs in organoids are slow cycling, and they maintain this slow proliferation behavior when engrafted into a mouse colon [23]. Our data provides further evidence that colon spheroids may have decreased stem cell function under *in vitro* culture conditions. Furthermore, we see that in contrast to CoSCs, human ISCs in organoids derived from the small intestine are rapidly cycling. Together, this suggests that there are regional differences in gut stem cell behavior under basal conditions *in vitro*.

Supplemental BMP inhibition increases colon spheroid formation and CoSC proliferation *in vitro*

It is possible that the slow cycling behavior of human CoSCs *in vitro* is representative of slow proliferation rates *in vivo*. However, it is also possible that basal culture conditions recapitulate the small intestinal stem cell niche more accurately than the colon stem cell niche. Our results indicate that a smaller proportion of colon spheroid-derived cells maintained the ability to give rise to single cell colonies compared to small intestine, suggesting decreased CoSC function *in vitro*. The decreased proliferation and single cell viability of CoSCs *in vitro* could be attributed to culture conditions that are not optimal for CoSC maintenance.

For example, we noticed a greater tendency for a subset of colon spheroids to spontaneously differentiate, indicated by loss of cystic structure and adoption of a dense morphology consistent with differentiation (Figure 2-3A). This suggests that despite stem cell-enriching basal media, there may be still additional signals permitting or directing differentiation

in colon cultures. Therefore, we sought to identify signaling factors that could enhance CoSC growth *in vitro* and inhibit differentiation.

BMP signaling is thought to inhibit stemness and promote differentiation in intestinal epithelium, whereas BMP inhibition leads to *de novo* crypt formation and increased proliferation [4,24-28]. Intra-villus mesenchymal cells were initially proposed to be the primary source of BMP signals [28]; however, recent evidence suggests that differentiated epithelial cells may be an additional source of intrinsic BMP signaling[4,25]. Therefore, we examined the expression of BMPs in colon cultures. We found that BMP2 was undetectable by quantitative PCR in both spheroids and colonoids (data not shown). BMP4 mRNA was barely detected in spheroids, but was induced during colonoid differentiation (Figure 2-3B), consistent with differentiated colon epithelial cells as a source of BMP signaling. Although BMP4 mRNA levels were low in CoSC-enriched spheroids, phosphorylated BMP-associated Smads 1/5 (P-Smad) were detected by Western blot, indicating active BMP signaling (Figure 2-3C). These data suggest that a small subset of differentiated cells within CoSC-enriched spheroids may produce sufficient BMP4, even at low levels, to trigger active BMP signaling. We also found active BMP signaling, as marked by P-Smad, in colonoids after differentiation (Figure 2-3C).

We next sought to determine if BMP signaling plays a role in regulating CoSC proliferation and differentiation in spheroids. While basal spheroid culture conditions contain the BMP antagonist Noggin, we tested the effect of additional BMP inhibition on colon spheroid formation and CoSC behavior using the BMP type 1 receptor inhibitor LDN193189 (LDN) [4,24]. Treatment of colon spheroids with LDN led to loss of P-Smad signal, indicating inhibition of BMP activity (Figure 2-3C). In the presence of LDN, there was a trend toward increased spheroid forming efficiency at initial plating of isolated colonic crypts, though this difference was not significant (Figure 2-3D).

BMPs are members of the transforming growth factor- β (TGF- β) superfamily, and while BMP receptors signal through Smads1/5/8, other TGF- β ligands signal preferentially through Smads

2 and 3[29]. Several studies have utilized a TGF- β type I receptor ALK5 kinase inhibitor in human gut organoid cultures (see Introduction Table 2), which blocks phosphorylation of Smad2. However, we found that, in contrast to BMP inhibition with LDN which blocks phosphorylation of Smad 1/5/8 (Figure 2-3C), TGF- β inhibition by A8301 did not impact initial spheroid forming efficiency (Figure 2-3D).

BMP inhibition with LDN additionally increased proliferation of established colon spheroids, as indicated by increased phospho-histone H3-positive cells per spheroid (Figure 2-3E). Treatment of duodenal spheroids with LDN similarly increased ISC proliferation (Figure S2-2). However, the magnitude of the increase was less than that for colon spheroids treated with LDN (fold change in mitotic cells for colon and duodenum was 2.5 and 1.3, respectively). Notably, while BMP inhibition with LDN led to increased proliferation for both colon and duodenum, colon spheroid proliferation rate remained less than that of small intestine. These results suggest that BMP signaling regulates stem cell proliferation *in vitro*, and BMP inhibition improves the formation and expansion of colonic spheroids. However, even in the presence of BMP inhibitor, cultured CoSCs are still slow cycling, relative to small intestine ISCs.

BMP inhibition in colon spheroids enhances stemness and prevents differentiation

As previously noted, colon spheroids occasionally differentiate and adopt dense structures under stem cell-promoting conditions; however with short-term LDN supplementation, colon cultures uniformly maintained cystic spheroid morphology (Figure 2-3F). Similar to stem cell growth factor withdrawal, starvation due to lack of growth factor replenishment results in differentiation and morphological transformation of cystic spheroids to dense colonoids (see Appendix C). Our preliminary data suggests that supplementation of colon spheroids with the BMP inhibitor LDN, prior to starvation, prevents differentiation and enables maintenance of stem cell-associated cystic morphology even when growth factors have been exhausted (Appendix C).

Additionally, BMP inhibition with LDN enhanced the colony forming efficiency of *in vitro* CoSCs, as assayed by single cell spheroid formation (Figure 2-3G). Taken together, this implies that supplemental BMP inhibition concomitantly prevents differentiation and promotes stem cell function for CoSCs *ex vivo*.

Discussion

The intestinal epithelium has long been known to regularly self-renew, with mitotic cells within invaginating crypts giving rise to short-lived post-mitotic cells lining the surface epithelium[2,30]. Since the identification of Lgr5 as a unique marker of these mitotic crypt based columnar cells (CBCs), our understanding of intestinal stem cell biology has grown dramatically[3]. Early observations that proliferative cells within crypts must be balanced by periodic shedding of surface epithelial cells have now been validated through the use of Lgr5-labeled transgenic mice and lineage tracing experiments[3,30,31]. It is now evident that Lgr5+ cells are actively cycling, multi-potent stem cells that give rise to all epithelial lineages within both small intestine and colon[3].

Many tissue-specific stem cells cannot be expanded or cultured *in vitro* indefinitely because they will ultimately senesce or undergo transformation[31]. Mammalian gut stem cells, however, appear to divide daily and persist throughout the lifespan of the organism, thus defying the “Hayflick limit” – the limited capacity for cells to divide before telomere shortening reaches a critical threshold and senescence occurs[32]. Consistent with the observation that gut stem cells maintain cycling capacity throughout life, Lgr5+ cells from mice were found to have higher telomerase activity than differentiated progeny[33], a potential mechanism to prevent telomere erosion over time.

Moreover, it is now apparent that intestinal and colonic stem cells from both mouse and human can be culture *in vitro* longterm through the use of three-dimensional organoids supplemented with growth factors that recapitulate the stem cell niche *in vivo* [5,14,17]. In mice, small intestinal organoids maintain epithelial architecture, with distinct proliferative crypt and differentiated cell domains[14]. These *in vitro* organoids are thought to preserve self-renewal kinetics found *in vivo*: stem cells in crypt domains give rise to differentiated progeny that are ultimately shed into the lumen after a few days[14]. In contrast to murine small intestine, murine colon organoids and human small intestine and colon organoids all require supplemental Wnt

and are, thus, commonly grown as stem cell-enriched cultures known as spheroids [15,17]. To date, however, it is unclear whether these cultures recapitulate the self-renewal kinetics seen *in vivo*. Moreover, the vast majority of analyses of gut stem cell behavior have been conducted in the mouse small intestine, and the behavior of CoSCs, especially human CoSCs, remains largely uncharacterized.

Tomasetti et al. mathematically estimated a greater number of stem cell divisions in human colon, suggesting that the higher incidence of CRC could be largely explained by increased cell division of CoSCs compared to small intestine stem cells[13]. However, previous evidence demonstrated a higher bromodeoxyuridine labeling index in human ileum *in vivo* compared to colon, indicating, by contrast, an inverse relationship between division rate and cancer susceptibility [22,34]. Although these labeling experiments were conducted before the characterization of specific gut stem cell markers, recent experiments have validated that human Lgr5+ CoSCs may truly be slow cycling, at least in organoids *in vitro* and when engrafted into a mouse colon, where human CoSCs divided less frequently than adjacent mouse CoSCs [23]. However, no direct comparison to small intestine was conducted. Given these conflicting observations, further investigation into proliferation rates and susceptibility to tumorigenesis is warranted in human small intestine and colon.

Here, we employed three-dimensional organoid models to grow ISCs and CoSCs *in vitro* as spheroids, which provide a unique tool for investigating regional differences in stem cell kinetics. We have shown that human CoSCs are slow cycling compared to ISCs *in vitro*, with fewer mitotic events per spheroid and decreased expansion capacity. We additionally report that cultured CoSCs have decreased stem cell function, as measured by the ability of single cells to give rise to new spheroids after sorting. We speculate that this decreased stem cell function may be due to incomplete recapitulation of the CoSC niche *in vitro*. To this end, we observed occasional spontaneous differentiation of colon spheroids to differentiated colonoids, something not observed in ISC cultures.

BMP signaling has been shown to play a role in regulating crypt proliferation and differentiation. Specifically, a recent report showed that BMP signaling inhibits Lgr5+ stem cell function through Smad-mediated repression of core stemness genes, thereby helping to maintain a proper balance of proliferation and differentiation[26]. Here, we find that BMP4 is expressed in differentiated colonoids *in vitro*, providing further evidence that there is an epithelial-intrinsic source of BMP signaling in addition to the signals derived from subepithelial mesenchyme [4,25,28]. Although we note minimal BMP4 expression in CoSC-enriched spheroids, phospho-Smad 1/5 was detected, indicating active BMP signaling in these cultures even in the presence of low levels of BMP4. We find that supplementation of colon spheroids with the BMP inhibitor LDN eliminates BMP signaling, improves spheroid formation, increases CoSC proliferation, enhances stem cell function, and prevents spontaneous differentiation. Although human intestinal organoid cultures contain basal BMP inhibition via Noggin, these data suggest that there may be increased requirement for BMP antagonism, at least for CoSC maintenance in culture. Whether BMP inhibition functions to increase stemness through direct regulation of stem cell gene expression warrants future investigation. Additionally, further examination of BMP signaling in cultured ISCs is necessary to determine if there are regional differences in BMP expression and activity *in vitro* or *in vivo*.

Interestingly, even in the presence of BMP inhibition, CoSC proliferation rate remained lower than ISCs. Therefore, our data provides further evidence, that contrary to the mathematical predictions presented by Tomasetti et al, CoSCs may exhibit slower cycling than ISCs[13]. If this is true, then proliferation rate is likely not the major contributing factor to increased susceptibility to oncogenic transformation within the colon. Notably, the link between proliferation rate and cancer incidence is based on the idea that increased cell division is associated with higher risk of replication induced mutations. Interestingly, examination of adult stem cell mutation accumulation by Blokzijl et al. showed that despite the variable incidence of cancer, there was a consistent rate of novel mutation across liver, small intestine and colon.

While mutation accumulation rate was similar in these gastrointestinal tissues, the types of mutations differed. Small intestine and colon are rapidly proliferative and harbored many mutations associated with deamination of methylated cytosines, while liver stem cells, which divide less frequently, exhibited a distinct mutational signature[35]. This suggests that the mutational rate and spectrum of small intestine and colon may be similar, at least with respect to somatic point mutations, despite the different incidences of adenocarcinoma[35].

Many have speculated that differences in immune cells, bacterial composition, and regional differences in physiology could contribute to the different vulnerabilities of small intestine and colon to adenocarcinoma[11]. Examination of regional differences in structural variants, chromosomal instability, and tissue clonality may reveal factors relevant for differences in tissue susceptibility to cancer[35-37].

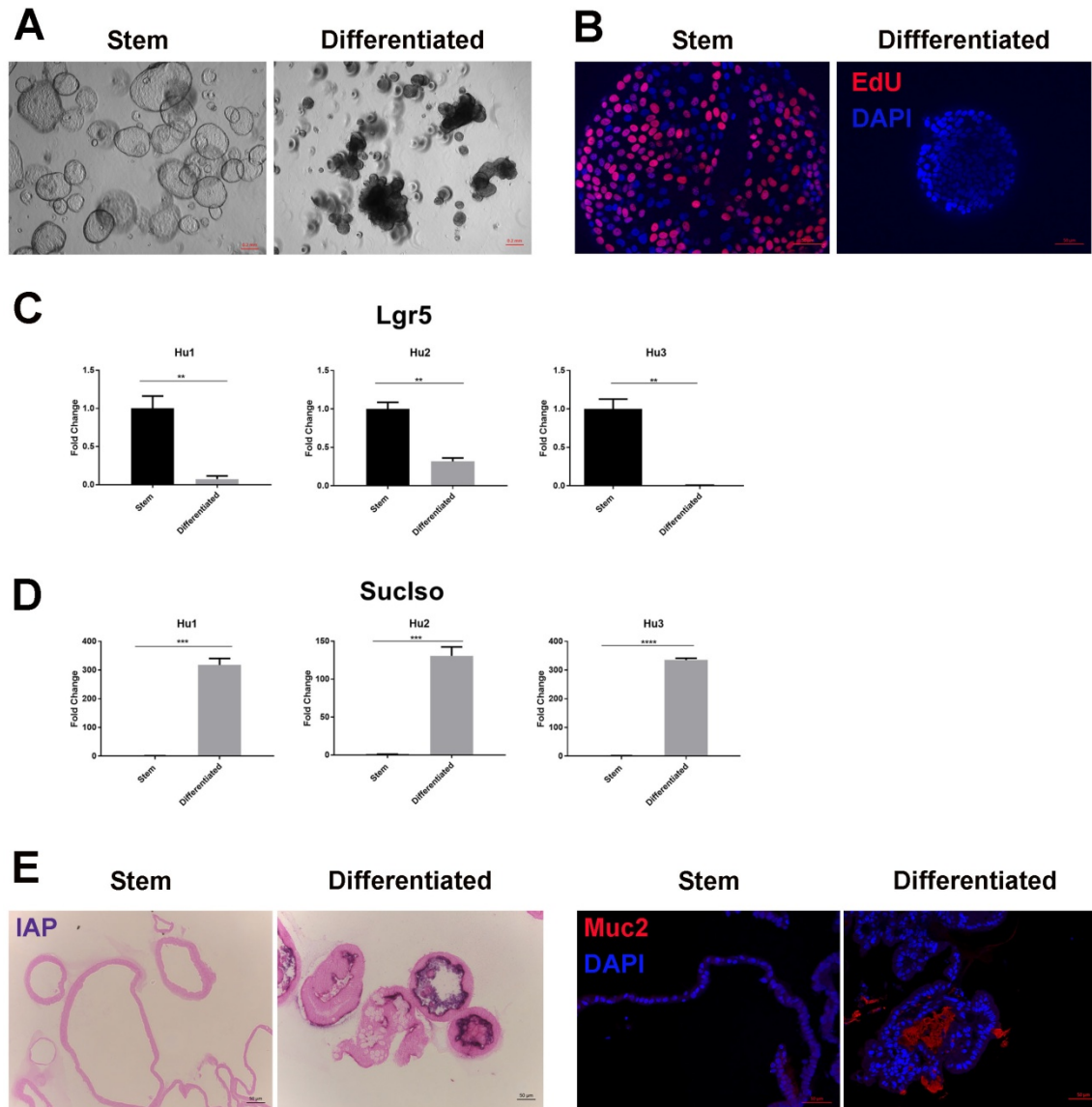


Figure 2-1: Stem and differentiated cell markers in human small intestine-derived spheroids and enteroids. (A) Brightfield images of undifferentiated spheroids (left) and differentiated enteroids (right); scale bar = 200um. (B) 16 hour 5-Ethynyl-20-deoxyuridine incorporation in whole mount undifferentiated spheroids and enteroids after 4 days of differentiation; scale bar = 50um. (C-D) Quantitative PCR analysis showing fold change in mRNA expression for stem cell marker Lgr5 (C) and enterocyte marker sucrase-isomaltase [Suclo] (D) in undifferentiated spheroids and differentiated enteroids derived from three unique

duodenal specimens. Results are mean +/- SEM. Samples were run in triplicate. (E-F) NBT/BCIP intestinal alkaline phosphatase [IAP] staining for enterocytes (E) and immunostaining for Goblet cell-secreted Mucin-2 [Muc2] (F) on 5-um paraffin sections of undifferentiated spheroids and differentiated enteroids; scale bar = 50um. Statistics: Students t-test; ** $p < 0.01$, *** $p < 0.001$, **** $p < 0.0001$.

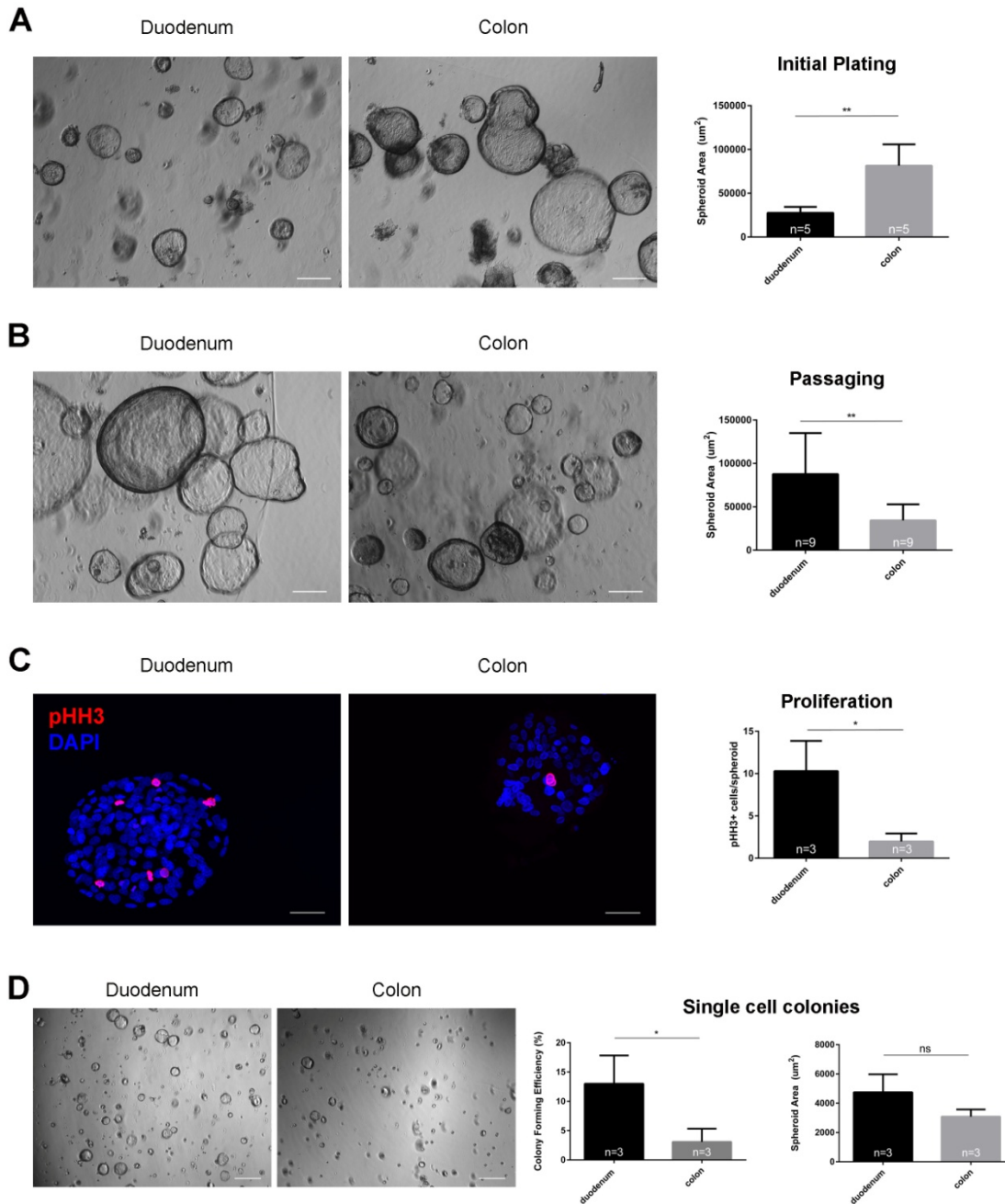


Figure 2-2: Human CoSCs are slow cycling compared to ISC under *in vitro* stem cell-promoting conditions. (A-B) *Left*: Representative brightfield images of initial spheroid formation from duodenal and colonic crypts at day 3 (A) and spheroids at later passages (passages 1-5) (B). *Right*: Spheroid area (um²), quantified as the area around the cystic lumen,

for duodenum and colon at day 3 (A) and at later passages (B). At least 20 spheroids per sample were quantified. (C) *Left*: Representative whole mount immunofluorescence stains for mitotic events, marked by phospho-histone H3 (pHH3), for duodenal and colon spheroids. *Right*: Quantification of number of pHH3-positive cells per spheroid. At least 10 spheroids per sample were analyzed. (D) Single cell colony formation for *in vitro* expanded ISCs and CoSCs. *Left*: Representative bright field images of single cell-derived colonies at day 7 after sorting. *Middle*: Colony forming efficiency was quantified as the percentage of plated singlets that gave rise to spheroids at day 7. *Right*: Colony size, measured as spheroid area (μm^2) at day 7; at least 15 spheroids per sample were measured. Results are mean \pm standard deviation. Statistics: Students t-test; * $p < 0.05$, ** $p < 0.01$, *** $p < 0.001$, **** $p < 0.0001$. (A,B,D) Scale bars = 200 μm ; (C) Scale bars = 50 μm .

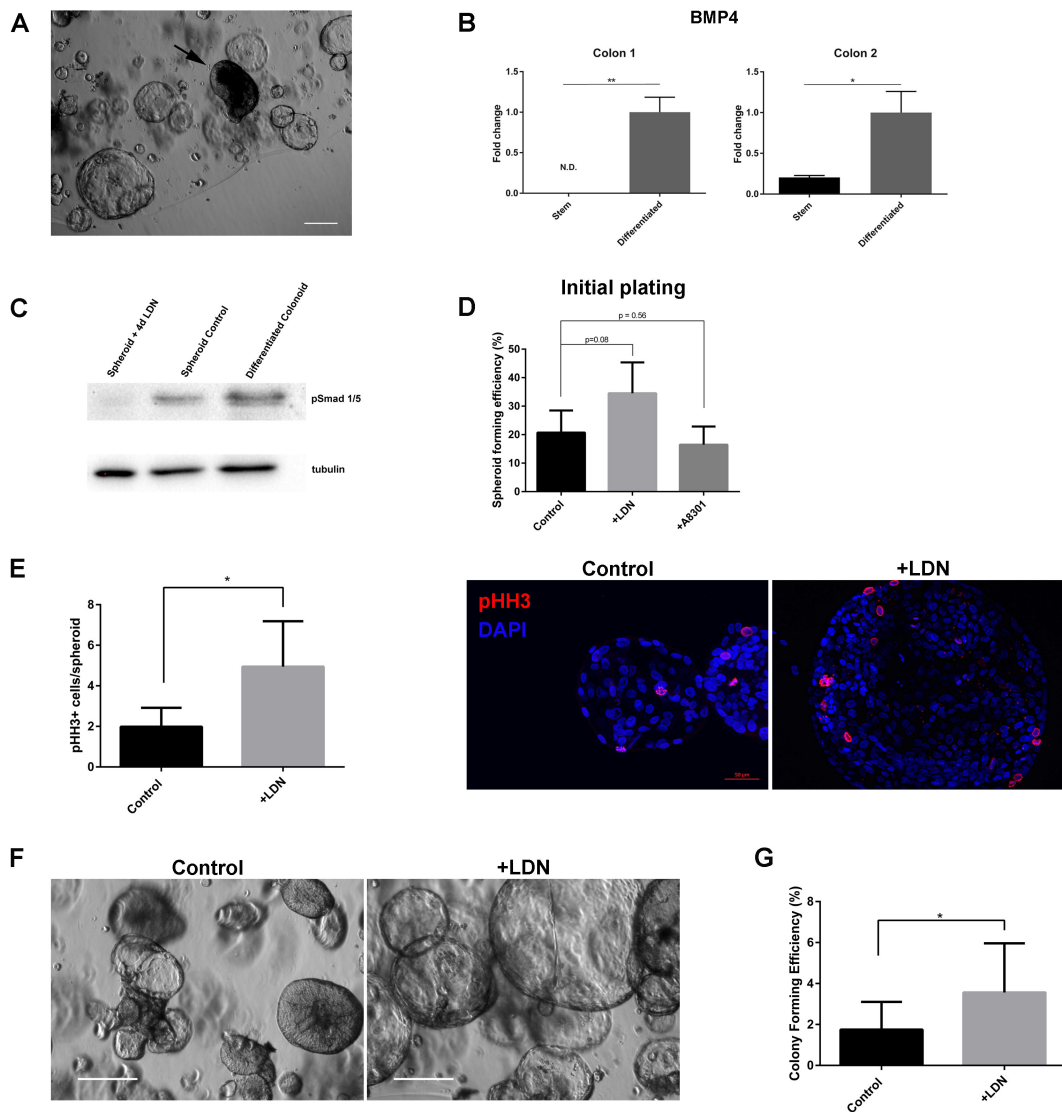


Figure 2-3: BMP inhibition increases proliferation and inhibits differentiation of CoSCs *in vitro*. (A) Representative brightfield image of colon spheroid culture. Arrow indicates differentiated structure. (B) Quantitative PCR analysis showing fold change in mRNA expression for BMP4 in undifferentiated spheroids and colonoids after 4 days of differentiation for two unique colon specimens. Results are mean +/- SD. Samples were run in triplicate. Statistics = Student's t-test. (C) Western blot for phospho-Smads 1/5 (pSmad), indicating active BMP signaling, in stem cell-enriched spheroids and differentiated colon cultures. Note loss of pSmad in spheroids treated with the BMP inhibitor LDN for 4 days. Gamma tubulin used as

loading control. (D) Spheroid forming efficiency at day 3 after plating crypts in stem cell media +/- inhibitors; n=4 colon samples, plated in triplicate. (E) *Left*: Number of mitotic events per spheroid, indicated by phospho-histone H3 (pHH3) positive cells, for control vs. LDN-treated spheroids (3 day). *Right*: Whole mount immunostaining for pHH3; n=3 different colon spheroid lines, at least 10 spheroids were measured per sample per condition. (F) Representative bright field image indicating spontaneous differentiation of spheroids under control conditions (left), compared to maintenance of cystic spheroids in the presence of LDN. (G) Colony forming efficiency of single dissociated CoSCs plated in control media or media supplemented with LDN for 6 days; n=3 different colon spheroid lines. Scale bars = 200um, unless otherwise noted. Statistics = paired t-test. * $p < 0.05$, ** $p < 0.01$.

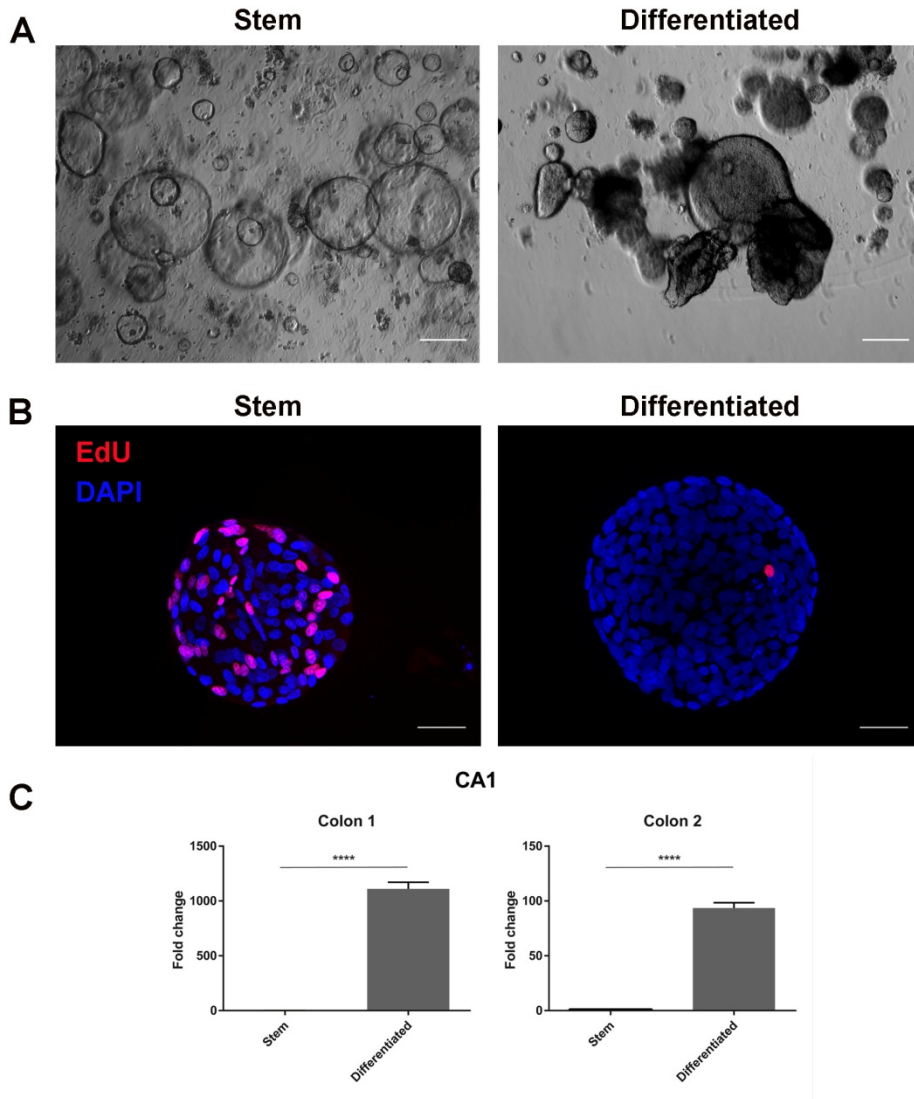


Figure S2-1: Human colon derived spheroids and differentiated colonoids. (A) Brightfield images of stem cell-enriched spheroids (left) and differentiated colonoids (right); scale bar = 200um. (B) 16 hour 5-Ethynyl-20-deoxyuridine incorporation in whole mount stem cell-enriched spheroids and colonoids after 4 days of differentiation; scale bar = 50um. (C) Quantitative PCR analysis for two colon samples. Fold change in mRNA expression of carbonic anhydrase 1 (CA1) is shown for stem cell enriched spheroids versus differentiated colonoids. Results are mean +/- SD. Samples were run in triplicate. Statistics: Students t-test; **** $p < 0.0001$.

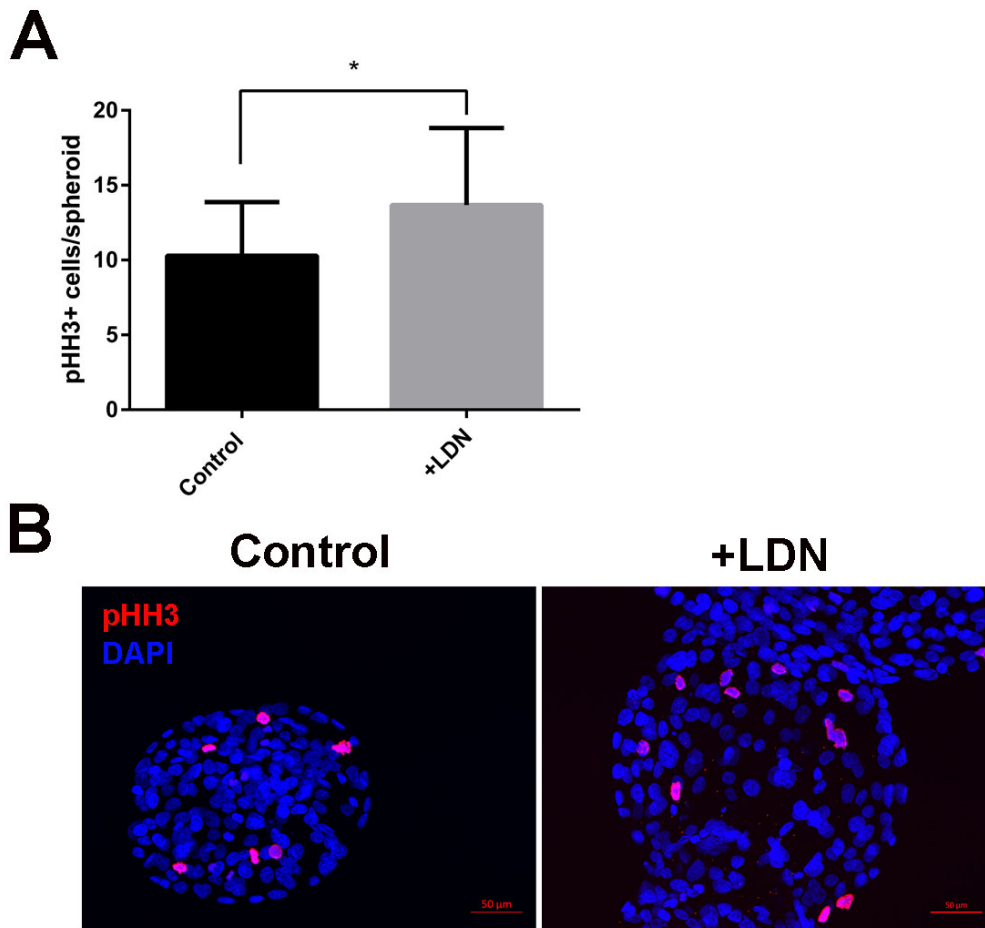


Figure S2-2: BMP inhibition increases proliferation of ISCs *in vitro*. (A) Number of mitotic events per spheroid, indicated by phospho-histone H3 (pHH3) positive cells, for control vs. LDN-treated spheroids from the small intestine (left). (B) Whole mount immunostaining for pHH3; n=3 different small intestine spheroid lines. Scale bars = 50μm. Statistics = paired t-test; * $p < 0.05$.

References

1. Barker N. Adult intestinal stem cells: critical drivers of epithelial homeostasis and regeneration. *Nat Rev Mol Cell Biol.* 2013 Dec 11;15(1):19–33.
2. Cheng H, Leblond CP. Origin, differentiation and renewal of the four main epithelial cell types in the mouse small intestine. III. Entero-endocrine cells. *Am J Anat.* 1974 Dec;141(4):503–19.
3. Barker N, van Es JH, Kuipers J, Kujala P, van den Born M, Cozijnsen M, Haegebarth A, Korving J, Begthel H, Peters PJ, Clevers H. Identification of stem cells in small intestine and colon by marker gene *Lgr5*. *Nature.* Nature Publishing Group; 2007 Oct 14;449(7165):1003–7.
4. Thorne CA, Chen IW, Sanman LE, Cobb MH, Wu LF, Altschuler SJ. Enteroid Monolayers Reveal an Autonomous WNT and BMP Circuit Controlling Intestinal Epithelial Growth and Organization. *Dev Cell.* 2018 Mar 12;44(5):624–4.
5. Sato T, Clevers H. Growing Self-Organizing Mini-Guts from a Single Intestinal Stem Cell: Mechanism and Applications. *Science.* 2013 Jun 6;340(6137):1190–4.
6. Raghav K, Overman MJ. Small bowel adenocarcinomas--existing evidence and evolving paradigms. *Nat Rev Clin Oncol.* 2013 Sep;10(9):534–44.
7. Delaunoit T, Neczyporenko F, Limburg PJ, Erlichman C. Pathogenesis and risk factors of small bowel adenocarcinoma: a colorectal cancer sibling? *Am J Gastroenterol.* 2005 Mar;100(3):703–10.
8. Cho KR, Vogelstein B. Suppressor gene alterations in the colorectal adenoma-carcinoma sequence. *J Cell Biochem Suppl.* 1992;16G:137–41.
9. Barker N, Ridgway RA, van Es JH, van de Wetering M, Begthel H, van den Born M, Danenberg E, Clarke AR, Sansom OJ, Clevers H. Crypt stem cells as the cells-of-origin of intestinal cancer. *Nature.* 2008 Dec 17;457(7229):608–11.

10. Mowat AM, Agace WW. Regional specialization within the intestinal immune system. *Nat Rev Immunol*. 2014 Oct;14(10):667–85.
11. Lamprecht S, Fich A. Small Intestinal Cancer: Why the Rarity? *Trends Cancer*. 2016 Aug;2(8):395–7.
12. Breuhahn K, Singh S, Schirmacher P, Bläker H. Large-scale N-terminal deletions but not point mutations stabilize beta-catenin in small bowel carcinomas, suggesting divergent molecular pathways of small and large intestinal carcinogenesis. *J Pathol*. 2008 Jul;215(3):300–7.
13. Tomasetti C, Vogelstein B. Cancer etiology. Variation in cancer risk among tissues can be explained by the number of stem cell divisions. *Science*. 2015 Jan 2;347(6217):78–81.
14. Sato T, Vries RG, Snippert HJ, van de Wetering M, Barker N, Stange DE, van Es JH, Abo A, Kujala P, Peters PJ, Clevers H. Single Lgr5 stem cells build crypt–villus structures in vitro without a mesenchymal niche. *Nature*. Nature Publishing Group; 2009 Mar 29;459(7244):262–5.
15. Jung P, Sato T, Merlos-Suárez A, Barriga FM, Iglesias M, Rossell D, Auer H, Gallardo M, Blasco MA, Sancho E, Clevers H, Batlle E. Isolation and in vitro expansion of human colonic stem cells. *Nat Med*. 2011 Oct;17(10):1225–7.
16. Foulke-Abel J, In J, Yin J, Zachos NC, Kovbasnjuk O, Estes MK, de Jonge H, Donowitz M. Human Enteroids as a Model of Upper Small Intestinal Ion Transport Physiology and Pathophysiology. *Gastroenterology*. 2016 Mar;150(3):638–8.
17. Sato T, Stange DE, Ferrante M, Vries R, Van Es JH. Long-term expansion of epithelial organoids from human colon, adenoma, adenocarcinoma, and Barrett's epithelium. *Gastroenterology*. 2011.
18. Jung P, Sommer C, Barriga FM, Buczacki SJ, Hernando-Momblona X, Sevillano M, Duran-Frigola M, Aloy P, Selbach M, Winton DJ, Batlle E. *Stem Cell Reports*. Stem Cell Reports. The Authors; 2015 Dec 8;5(6):979–87.

19. San Roman AK, Aronson BE, Krasinski SD, Shivdasani RA, Verzi MP. Transcription factors GATA4 and HNF4A control distinct aspects of intestinal homeostasis in conjunction with transcription factor CDX2. *J Biol Chem*. 2015 Jan 16;290(3):1850–60.
20. Lee GY, Kenny PA, Lee EH, Bissell MJ. Three-dimensional culture models of normal and malignant breast epithelial cells. *Nat Meth*. 2007 Apr;4(4):359–65.
21. Sasaki N, Sachs N, Wiebrands K, Ellenbroek SIJ, Fumagalli A, Lyubimova A, Begthel H, van den Born M, van Es JH, Karthaus WR, Li VSW, López-Iglesias C, Peters PJ, van Rheenen J, van Oudenaarden A, Clevers H. Reg4+ deep crypt secretory cells function as epithelial niche for Lgr5+ stem cells in colon. *Proc Natl Acad Sci USA*. 2016 Sep 13;113(37):E5399–407.
22. Potten CS, Kellett M, Rew DA, Roberts SA. Proliferation in human gastrointestinal epithelium using bromodeoxyuridine in vivo: data for different sites, proximity to a tumour, and polyposis coli. *Gut*. 1992 Apr;33(4):524–9.
23. Sugimoto S, Ohta Y, Fujii M, Matano M, Shimokawa M, Nanki K, Date S, Nishikori S, Nakazato Y, Nakamura T, Kanai T, Sato T. Reconstruction of the Human Colon Epithelium In Vivo. *Cell Stem Cell*. 2018 Feb 1;22(2):171–5.
24. Whissell G, Montagni E, Martinelli P, Hernando-Momblona X, Sevillano M, Jung P, Cortina C, Calon A, Abuli A, Castells A, Castellvi-Bel S, Nacht AS, Sancho E, Stephan-Otto Attolini C, Vicent GP, Real FX, Battle E. The transcription factor GATA6 enables self-renewal of colon adenoma stem cells by repressing BMP gene expression. *Nat Cell Biol*. 2014 Jul;16(7):695–707.
25. Batts LE, Polk DB, Dubois RN, Kulesa H. Bmp signaling is required for intestinal growth and morphogenesis. *Dev Dyn*. 2006 Jun;235(6):1563–70.
26. Qi Z, Li Y, Zhao B, Xu C, Liu Y, Li H, Zhang B, Wang X, Yang X, Xie W, Li B, Han J-DJ, Chen Y-G. BMP restricts stemness of intestinal Lgr5+ stem cells by directly suppressing their signature genes. *Nature Communications*. 2017 Jan 6;8:13824.

27. He XC, Zhang J, Tong W-G, Tawfik O, Ross J, Scoville DH, Tian Q, Zeng X, He X, Wiedemann LM, Mishina Y, Li L. BMP signaling inhibits intestinal stem cell self-renewal through suppression of Wnt-beta-catenin signaling. *Nat Genet.* 2004 Oct;36(10):1117–21.
28. Haramis A-PG, Begthel H, van den Born M, van Es J, Jonkheer S, Offerhaus GJA, Clevers H. De novo crypt formation and juvenile polyposis on BMP inhibition in mouse intestine. *Science.* 2004 Mar 12;303(5664):1684–6.
29. Moustakas A, Heldin C-H. The regulation of TGFbeta signal transduction. *Development.* 2009 Nov;136(22):3699–714.
30. Leblond CP, STEVENS CE. The constant renewal of the intestinal epithelium in the albino rat. *Anat Rec.* 1948 Mar;100(3):357–77.
31. Clevers H. The Intestinal Crypt, A Prototype Stem Cell Compartment. *Cell.* 2013 Jul;154(2):274–84.
32. Shay JW, Wright WE. Hayflick, his limit, and cellular ageing. Vol. 1, *Nature reviews. Molecular cell biology.* 2000. 5 p.
33. Schepers AG, Vries R, van den Born M, van de Wetering M, Clevers H. Lgr5 intestinal stem cells have high telomerase activity and randomly segregate their chromosomes. *EMBO J.* 2011 Mar 16;30(6):1104–9.
34. Potten CS, Kellett M, Roberts SA, Rew DA, Wilson GD. Measurement of in vivo proliferation in human colorectal mucosa using bromodeoxyuridine. *Gut.* 1992 Jan;33(1):71–8.
35. Blokzijl F, de Ligt J, Jager M, Sasselli V, Roerink S, Sasaki N, Huch M, Boymans S, Kuijk E, Prins P, Nijman IJ, Martincorena I, Mokry M, Wiegerinck CL, Middendorp S, Sato T, Schwank G, Nieuwenhuis EES, Verstegen MMA, van der Laan LJW, de Jonge J, Ijzermans JNM, Vries RG, van de Wetering M, Stratton MR, Clevers H, Cuppen E, van Boxtel R. Tissue-specific mutation accumulation in human adult stem cells during life. *Nature.* 2016 Oct 13;538(7624):260–4.

36. Kozar S, Morrissey E, Nicholson AM, van der Heijden M, Zecchini HI, Kemp R, Tavaré S, Vermeulen L, Winton DJ. Short Article. *Stem Cell*. Elsevier Inc; 2013 Nov 7;13(5):626–33.
37. Hsieh JCF, Van Den Berg D, Kang H, Hsieh C-L, Lieber MR. Large chromosome deletions, duplications, and gene conversion events accumulate with age in normal human colon crypts. *Aging Cell*. 2013 Apr;12(2):269–79.

Chapter 3: DNA methylation analysis reveals differences in aging between human small intestine and colon

Sophia Kuo Lewis, Daniel Nachun, Martin G. Martin, Steve Horvath, Giovanni Coppola, Leanne Jones

A version of this chapter has been submitted for publication

Abstract

The epithelia of the intestine and colon turn over rapidly and are maintained by adult stem cells in the base of crypts. While the small intestine and colon have distinct, well-characterized physiological functions, it remains unclear if there are fundamental regional differences in stem cell behavior or region-dependent degenerative changes during aging. Mesenchyme-free organoids provide useful tools for investigating segment-specific stem cell biology and age-related changes in stem cell function *in vitro*. However, it is important to confirm whether organoids maintain regional identity and hallmarks of age in the absence of an aging niche. Here we establish that human intestine and colon crypts display regional differences in methylation patterns, which are largely preserved in stem cell-enriched spheroid cultures. Using the human epigenetic clock as a biomarker of age, we determine that stem-like spheroids also display DNA methylation-based aging profiles similar to the crypts from which they were derived, with small intestine exhibiting striking epigenetic age reduction relative to colon. Our data demonstrate regional differences in susceptibility to aging that appear to be maintained *in vitro*.

Introduction

Maintenance of the gut epithelium throughout life relies on intestinal and colonic stem cells, known as ISCs and CoSCs, respectively. These tissue-specific stem cells reside in the invaginating crypts of both the small intestine (SI) and colon. Under homeostasis, stem cells marked by the Wnt target gene *Lgr5* rapidly divide to maintain the stem cell population or differentiate to generate specialized absorptive and secretory epithelial cells [1]. After injury, relatively quiescent, label-retaining stem cells are activated to divide and act as a clonogenic reserve [2].

Although the SI and colon have distinct, well-characterized digestive functions, it remains unclear if there are fundamental differences in SI and colonic stem cell behavior. The majority of existing data on stem cells is derived from the mouse SI; however, a major caveat to using mice to investigate intestinal physiology relevant to humans is species-specific differences in regional biology. For example, mouse models of colon cancer are prone to develop predominantly SI tumors, while in humans, colon cancer is significantly more prevalent than SI cancer [3]. Therefore, it is imperative that we utilize reliable *ex vivo* models to study human ISC behavior, as human *in vivo* analyses are generally impractical. The development of three-dimensional organoids, long-term self-organizing cultures of ISCs and their progeny, has provided a useful tool for studying intestinal physiology and stem cell function [4,5]. Furthermore, it is now feasible to reconstruct human gut epithelium *in vivo* through orthotopic xenografts of human organoids into the mouse gut [6], though species-specific differences in the stem cell niche may persist.

Aging of many organs is associated with impaired regenerative capacity due to altered activity of tissue-specific stem cells and their niches [7,8]. Key features of human gastrointestinal (GI) aging include altered motility, inflammation, barrier dysfunction, and increased risk of colon cancer [9-11]. *Lgr5*⁺ ISC/CoSCs have been implicated as the cell of origin for cancer [12]; yet, the precise role(s) the tissue stem cell plays in age-related pathology

requires further investigation. Furthermore, it is unclear whether there are regional differences in susceptibility to degenerative cellular changes during aging, especially in human. In the murine small intestine, aging has been linked to impaired crypt repair after high dose irradiation [13]. Additionally, decreased Wnt signaling with age impaired the ability of mouse ISCs to maintain tissue homeostasis and led to decreased organoid forming capacity *in vitro* [14]. By contrast, calorie restriction, a lifespan extending intervention, enhanced stem cell numbers and improved regenerative capacity [15,16]. These data suggest that ISC/CoSC behavior is likely impacted by the aging process, but the precise molecular changes that occur and how these vary from individual to individual are unknown. To address this, one possibility is to adapt the use of 3D organoid cultures to study SI and colon stem cell aging, but in order to do so, it is important to confirm whether these mesenchyme-free cultures maintain regional identity and hallmarks of biological age in the absence of an aging intestinal microenvironment.

There are many hallmarks of aging, including cellular senescence, telomere shortening, increases in DNA damage, gene expression changes, and epigenetic alterations [8]. At the epigenetic level, genome-wide DNA methylation changes are pervasive during aging and are consistent with increased methylation variability over time – a process known as “epigenetic-drift” [17-20]. It is also apparent that the methylation status of many CpG sites in the genome is tightly correlated with age, such that a subset of these sites can be used as an “epigenetic clock” to accurately predict the age of human tissues [21,22]. While epigenetic clocks demonstrate tight correlations between chronological age and predicted DNA methylation age across populations, it is also apparent that over- and under-prediction of age can be biologically and clinically meaningful. For example, patients with conditions associated with early onset of age-related clinical features, such as Down Syndrome or HIV, showed a premature age advancement according to the epigenetic clock [23,24]. Conversely, lifespan extending perturbations such as calorie restriction caused a decrease in the ticking rate of the epigenetic clock in mice, indicating that the clock may reflect a biologically relevant state of aging [25].

Here, we investigate differences in human ISCs and CoSCs and determine that culturing stem cells *in vitro* is a viable method for studying their behavior during aging. Specifically, we analyzed whether human SI and colon cells maintain region specificity, at the DNA methylation level, *in vitro*. Then using the epigenetic clock as a biomarker of aging, we determined whether human SI and colon have similar aging profiles. We find that region-dependent methylation patterns are largely preserved *in vitro* and that human SI and colon organoids have epigenetic ages similar to the primary crypt cells from which they were derived. Unexpectedly, we observe a marked decrease in epigenetic aging rate in human SI, when compared to colon, in both crypt epithelial cells and stem cell-enriched organoids, referred to as 'spheroids'. Strikingly, the change in the rate of aging in the small intestine appears in midlife. Taken together, our data reveal significant differences in the human small intestine and colon and provide the foundation for uncovering the mechanistic basis for region-specific gastrointestinal and age-onset disease.

Materials and Methods

Human bowel tissue

De-identified and discarded surgical specimens were retrieved from the UCLA Translational Pathology Core Laboratory (TPCL). Following clinical surgical pathology evaluation, normal adjacent tissue was obtained. Experimentation using TPCL-derived human tissues was approved by the UCLA institutional review board, which waived the informed consent requirement for specimens acquired from the TPCL (IRB#11-002504). The age of the human specimen was provided as a 5-year age range, according to TPCL practices. Procurement of paired jejunum and colon from anonymous post-mortem donors was facilitated by OneLegacy Foundation (Los Angeles, CA). Samples are summarized in Supplementary Table 3-1.

Intestinal mucosa and crypt isolation

Tissues were washed in phosphate buffered saline (PBS), and mucosa was isolated by removal of outer muscle layers using surgical scissors. Mucosae were cut into 1 cm pieces and washed with PBS until the supernatant was clear. Small intestine and colonic crypts were isolated using modified existing methods [5,26]. Specimens were incubated at 4°C in 8mM EDTA and 1mM Dithiothreitol for 30 minutes to 1 hour, with gentle agitation. Supernatant was removed and replaced with fresh PBS. Specimens were vortexed to release crypts. Crypts were collected into 15ml tubes and the process was repeated to collect 4-6 fractions. Fractions were centrifuged at 100xg to pellet crypts. SI crypts were subsequently filtered with 100um mesh to remove villus domains and epithelial debris. Isolated crypts were resuspended in basic medium containing ADMEM/F12, 1X Glutamax, 10mM HEPES buffer, and 1X Penicillin/Streptomycin (all ThermoFisher) for spheroid cultures, or resuspended in PBS for DNA lysis.

Genomic DNA extraction

Duodenal and colonic mucosal specimens were chopped into 5mm pieces and homogenized; crypts were isolated as above. Homogenized mucosa and isolated crypts were lysed and

genomic DNA was isolated using standard phenol-chloroform extraction with ethanol precipitation. DNA was stored at -20°C prior to downstream processing.

Bisulfite conversion and methylation arrays

Bisulfite conversion of 500ng DNA per sample was conducted using the EZ-96 DNA Methylation Gold Kit (Zymo Research). Samples were subsequently processed for Illumina HumanMethylation450 BeadChips and Infinium MethylationEPIC arrays according to manufacturer's instruction, and specimens were randomized across arrays. Methylation status was reported as the beta value (range 0-1, with 0 = unmethylated and 1 = fully methylated). For differential methylation analysis and principle component analysis the M-value, or log₂-beta value, was utilized[27].

Differential methylation analysis

Array pre-processing was run with the RnBeads package [28]. Probes outside CpG contexts, on sex chromosomes or in SNPs or with missing values were removed. The greedycut algorithm in RnBeads was used to remove probes with low detection score p-values, and probes with a standard deviation below 0.005 were also removed. Only probes shared between the HumanMethylation450K and HumanMethylationEPIC chips were retained. Background correction was performed with the out of band method implemented by ENMix [29] and arrays were normalized using beta mixture quantile dilation (BMIQ) [30]. Beta values were averaged across promoters (1.5kb before TSS to 0.5kb after TSS), gene bodies, or CpG islands and converted to M-values. M-values were corrected for batch effect using the parametric empirical Bayes method from ComBat [31]. Differential methylation was assessed using linear modeling with the limma package [32], with age and sex included as covariates, and a cutoff of FDR < 0.01 was used to determine significance.

DNA methylation age analysis using the epigenetic clock

After standard quality control, all samples were submitted to the methylation biological clock [22], and the predicted biological age was compared to the chronological age for each sample. Age correlation was calculated using the Pearson correlation coefficient between chronological age and predicted DNAm age. DNAm age acceleration/deceleration was calculated as the absolute difference between chronological age and DNAm age. Aging rates were calculated as the ratio between predicted molecular age and chronological age [21]. The comparison of aging rates between small bowel and colonic mucosa or crypts was done by analysis of variance where appropriate.

In vitro organoid cultures

To generate cystic 3D spheroids, isolated crypts were seeded at 150 crypts/25ul of Growth Factor Reduced Matrigel (BD Biosciences 356231) in a 48 well plate. Matrigel was allowed to solidify for 15 minutes at 37°C. Cells were overlaid with 250ul of slightly modified “stem cell” media [26,33], consisting of 50% Wnt3A Conditioned Medium (see below), 50% ADMEM/F12, 1X Penicillin/Streptomycin, 1X Glutamax, 10mM HEPES, 1mM N-acetyl-L-cysteine (Sigma A9165), 1x N2 supplement (Life Technologies 17502), 1x B27 minus VitA (Life Technologies 12587), 50ng/ml EGF (Peprotech 316-09), 1ug/ml human R-spondin (R&D 4645-RS), 100ng/ml murine Noggin (Peprotech 250-38), 10mM Nicotinamide (Sigma N0636), 10nM Gastrin (Sigma G9145), 10uM SB202190 (Sigma S7067), and 100nM PGE2 (Sigma P5640). Medium was changed every 2-3 days. Spheroids were passaged every 5-7 days by dissociation for 3 minutes in TrypLE Express (Life Technologies) at 37°C followed by reseeded in Matrigel. For two days after splitting, 10uM Rock inhibitor Y27632 (Sigma) was added to the medium. To achieve differentiation of stem-like cultures, Nicotinamide, SB202190 and PGE2 were withdrawn; Wnt3A conditioned medium was reduced to 10%; and 10uM DAPT gamma secretase inhibitor (Sigma, D5942) was added for 4 days of differentiation [5].

Wnt3A conditioned medium

L Wnt-3A cells (ATCC, CRL-2647) were cultured until 80-90% confluency in DMEM + 10% FBS + 1X Pencillin/Streptomycin. Cells were then split to approximately 10% density and cultured for 4 days in t75 flasks. Day 4 supernatant was sterile filtered. Fresh medium was replaced for 3 more days. Day 7 supernatant was sterile filtered, and combined with Day 4 medium [5]. Aliquoted stocks were stored at -20°C.

RNA extraction and gene expression microarray analysis

Samples were homogenized and lysed in Trizol (Invitrogen) and RNA was isolated using RNA Clean & Concentrator kit (Zymo Research). RNA integrity was analyzed on the Agilent 2200 TapeStation, and RIN > 7.0 was used as threshold for HT12 microarray analysis.

Results

Regional differences in methylation profiles for human small intestine and colon

To begin a comparison between stem cells in the proximal and distal regions of the human intestine, we began by assaying DNA methylation patterns of the SI (duodenum and jejunum segments) and colon. SI specimens were obtained from individuals aged 0-85 years, while colonic specimens were collected from patients aged 30-80 years (Supplemental Table 3-1). Genomic DNA was isolated from 14 SI and 12 colonic mucosa segments, consisting of epithelium, lamina propria and muscularis mucosae, in addition to the stem cell-containing crypts of 18 SI and 18 colonic samples (Figure 3-1A); all samples used were pathologically normal. Subsequently, genome-wide methylation was assayed using commercially available methylation arrays (see Materials and Methods).

Principle component analysis (PCA) of promoter methylation data from these samples showed clustering by both tissue type (small intestine vs. colon) and cell type (mucosa vs. crypts) (Figure 3-1B, 3-1C). This suggests distinct methylation patterns between small intestine and colon and between different cell types within the same tissue, as was recently reported for ileum and colon [34]. Similar tissue and cell type clustering was observed when analyzing methylated sites within CpG islands or gene bodies; samples did not cluster by batch, indicating batch effect is a not a major source of variation (Figure S3-1). We excluded pediatric samples (0-5 years of age) for PCA, as these samples were outliers.

To identify region-specific methylation patterns, we conducted differential methylation analysis. Interestingly, there were a greater number of differentially methylated CpG positions (DMPs) between SI and colon epithelial crypts, when compared to the DMPs between SI and colon whole mucosa. This trend was observed when analyzing methylation within promoters (Figure 3-1E) or within CpG islands and gene bodies (Figure S3-1). This suggests that these two organs have the greatest epigenetic variability at the level of the epithelial cells, as opposed to surrounding, non-epithelial, mucosa cells, which supports the idea that is it distinct epithelial

cell programs that enables SI and colon to perform highly specialized and region-specific digestive functions.

Segment-specific methylation patterns are maintained *in vitro*

Prior data suggests that organoids derived from mouse and human small intestine maintain transcript-level expression of segment-specific markers *in vitro* [35]; however, it is unclear if location-specific identity is maintained more broadly, including protein-level expression and epigenetic patterns. Moreover, whether human colonic samples cultured as organoids maintain regional identity has not yet been determined.

To determine whether small intestine and colon spheroids maintain segmental identity *in vitro*, we first analyzed expression of the region-specific transcription factor GATA4, which has been shown to be expressed in crypts and villi of murine duodenum and jejunum but is absent from the epithelium of ileum and colon [36]. We confirmed expression of GATA4 in epithelial cells within the human proximal small intestine at the mRNA level by *in situ* hybridization; GATA4 was undetected in colon epithelial cells, as expected (see Appendix D). We next tested if this segment-specific transcription factor is expressed in stem cells and maintained in a region-specific expression pattern at the protein level *in vitro*. We detected GATA4 protein in the nuclei of ISCs within small intestinal spheroids, but not within CoSCs (Appendix D), supporting the conclusion that regional-identity is maintained in cultured stem cells.

To determine if segment-specific epigenetic patterns are also maintained *in vitro*, we generated stem cell enriched spheroids from duodenum and colon for methylation analysis [5,37] (Figure 3-1A). PCA of methylation patterns at promoters revealed that duodenum and colon spheroids clustered away from one another and closely to crypts from the same region, revealing that methylation patterns are not altered dramatically in culture and that spheroids maintain some level of regional identity at the epigenetic level (Figure 3-1C). Again, similar PCA clustering was observed when analyzing methylation at CpG islands or gene bodies (Figure S3-

1). We also see that the DNA methylation levels of regional DMPs are correlated between crypts and organoids from SI and colon (Figure 3-1D, Figure S3-2). Taken together, these data help support recent reports that human intestinal organoids maintain regional methylation patterns *in vitro* [34].

Interestingly, colon spheroids clustered more tightly with colon crypts than SI spheroids with SI crypts (Figure 3-1C). Occasionally, spontaneous differentiation of colon spheroids is observed, which is not noted in SI spheroids (refer to Chapter 2). Crypts are heterogeneous, containing stem and transit-amplifying cells, as well as cells initiating terminal differentiation programs. By contrast, spheroids are, theoretically, homogeneous stem cell-enriched cultures. Therefore, spheroids that are not uniformly stem-like, such as in colon samples, could cluster more closely with their respective crypts, thus explaining the difference between SI and colon PCA clustering. Consistent with these observations, we noted greater number of differentially methylated sites between SI crypts and spheroids than between colon crypts and spheroids (Figure 3-1F; Figure S3-2).

Next we wanted to determine whether DNA methylation patterns are altered upon differentiation. Therefore, we subjected duodenal spheroids to differentiation conditions for four days and analyzed the methylation pattern of cells contained in these organoids, when compared to the spheroids from which they were derived (Figure 3-1A). Methylation patterns were fairly stable during differentiation [34], and duodenal differentiated organoids clustered closely with stem cell-like spheroids (Figure 3-1C). Moreover, we found minimal DMPs between SI spheroids and differentiated organoids (data not shown). Altogether, our data support the notion that methylation signatures are stable during differentiation, and epigenetic patterns that help regulate gene expression during differentiation may already be established in adult stem cells [38].

DNA methylation age is reduced in crypts from the small intestine

DNA methylation patterns change dynamically with age [17,18]. Having established that regional methylation patterns are maintained *in vitro*, we wanted to investigate differences in aging profiles between the proximal and distal regions of the gastrointestinal tract. Several algorithms, referred to as ‘epigenetic clocks,’ use DNA methylation changes to predict age for multiple species. In particular, the Horvath epigenetic clock is accurate across all reported cell and tissue types, except sperm [22], and as such, can be used as a biomarker of aging. We used the methylation status of 353 age-associated CpGs that comprise the Horvath clock to calculate the DNA methylation (DNAm) age of human SI (n=14) and colon (n=12) mucosa, as well as isolated SI (n=18) and colon (n=18) crypts (Figure 3-2A).

Across all samples, there was a linear relationship between predicted DNAm age and chronological age, as expected, with a correlation coefficient of 0.84 ($p < 0.0001$). We next examined the linear relationship between predicted and chronological age for each organ and tissue type separately. In SI, the correlation coefficient was higher for mucosa ($r = 0.95$, $p < 0.0001$) than for crypts ($r = 0.86$, $p < 0.0001$). In colon, the correlation coefficient was similar for mucosa and crypts ($r = 0.96$, $p < 0.0001$ and $r = 0.95$, $p < 0.0001$, respectively).

We then compared the DNAm ages of SI and colon mucosa to the corresponding crypts from these organs by calculating the absolute difference between DNAm age and chronological age, a difference known as DNA age acceleration or deceleration (Figure 3-2B). Remarkably, crypts isolated from the SI displayed a significant age deceleration compared to surrounding mucosa (mean error -18.5 vs. -3.6 years, respectively). Additionally, SI crypts had a significant age deceleration, when compared to that seen for colon crypts (mean error -18.5 vs. -5.8 years, respectively). These data indicate that epithelial cells within SI crypts undergo a considerably slower epigenetic ‘ticking rate’ than either cells within colonic crypts or other cells contained within the SI mucosa.

There was also a decreased epigenetic age in colon crypts compared to whole colonic mucosa (mean error -5.8 vs. +3.1 years, respectively); however the magnitude of this difference was smaller than that detected for SI. Similar results were obtained when limiting analysis to paired mucosa and crypts from the same tissue (Figure S3-3A), and when examining the epigenetic aging rate – the ratio of predicted DNAm age to the individual’s chronological age (Figure S3-3B).

Small intestine DNAm aging rate slows in midlife

Strikingly, the ticking rate of the epigenetic clock in SI is in sync with the chronological clock up until middle age (approximately 40 years), when it begins to slow, most markedly in the crypt compartment of the epithelium. Specifically, we found that the degree of DNAm age deceleration in SI samples, especially crypts, increased with greater chronological age (Figure 3-2C). There is a negative correlation between age prediction error and chronological age for SI crypts ($r = -0.90$, $p < 0.0001$). A similar trend was seen in SI mucosa though to a lesser extent than in crypts ($r = -0.76$, $p\text{-value} = 0.001$). By contrast, in colon crypts, the ticking rate of the epigenetic clock is in sync with the chronological clock, even in older age.

Gender is known to impact DNAm aging profiles, and the epigenetic aging rate for women tends to be lower than men, at least for blood cells [21]. Given that we uncovered a change in the rate of aging for small intestine at middle age (~40 years), it was important to consider how males and females were distributed between our young (<40 year) and older (>40 year) populations. Overall, for small intestine and colon crypt samples, our samples included almost equal proportions of male and female samples. Notably, this distribution did not change dramatically after 40 years of age (Figure S3-4), indicating that gender is likely not a major contributing factor to the slowed ticking rate of the epigenetic clock at middle age for small intestine crypts.

Cell composition analysis of small intestine and colon crypt preparations

The multi-tissue epigenetic clock used in this study measures cell-intrinsic changes in methylation during aging [22]. As our data revealed DNAm age differences between crypts and surrounding mucosal cells, it is possible that different cell populations within the gut lining have different intrinsic aging rates. Therefore, we sought to determine whether the differences we detected were due to differences in cell composition and represent contamination of crypt isolations with non-epithelial, mucosal cells during preparation. To address this, differential gene expression of markers of various mucosal lineages were examined using microarrays from SI and colon crypt samples (Fig S3-5). No differences in blood cell markers, genes expressed in the enteric nervous system, or genes associated with smooth muscle or subepithelial myofibroblasts were detected. Additionally, there was no significant difference in the expression of epithelial and stem cell markers common to both SI and colon, such as EPCAM, KRT20, E-Cadherin, or Lgr5. Significant differences in the expression of region-specific genes was observed, further validating our isolation methods. These data suggest that the divergence in DNAm aging rates between SI and colon crypts is not likely attributable to non-epithelial cell contamination in crypt isolations.

DNA methylation age deceleration for small intestine is observed in paired intestinal samples

To address the confounding factor of different underlying medical histories in SI versus colon surgical samples and to account for inter-individual variation, we collected four paired SI (jejunum) and transverse colon segments from organ donors immediately post-mortem. The predicted DNAm age of jejunum crypts was younger than the DNAm age of paired colon crypts for all three adult donors, consistent with our findings that crypts isolated from the SI display decreased epigenetic aging rates when compared to colon crypts (Figure 3-3). Notably, the 17-year-old donor showed congruence between DNAm and chronological age for both jejunum and

colon, supporting our data that the epigenetic clock in crypts from the SI is in sync with the chronological clock in the young, but diverges in older individuals.

DNA methylation age deceleration of human small intestine is maintained in cultured spheroids and is not lost during differentiation

Preliminary analysis of duodenal crypts from human patients 50-60, 60-70, and 70-90 years of age demonstrated no clear age-associated change in organoid forming capacity, a proxy for stem cell function (Appendix E). It is possible that *in vitro* culture conditions alter or reset aging profiles, thereby minimizing detection of age-associated function changes. To determine if human stem cells cultured *in vitro* maintain epigenetic aging profiles similar to cells found in primary, uncultured epithelial crypts, we analyzed cystic spheroids from human duodenum and colon crypts. These spheroids are enriched for cells harboring ISC characteristics – they divide rapidly and are capable of multilineage differentiation [5]. Specifically, upon withdrawal of Wnt3A and other growth factors, spheroids change morphology to dense folded organoids, stop dividing, and begin to express markers of absorptive and secretory lineages. During differentiation, most spheroids downregulate Lgr5 and begin to express markers of mature cells (see Chapter 2 for validation).

We compared the DNAm aging rate of duodenal and colonic crypts to their corresponding spheroid cultures (Figure 3-4A). Consistent with our previous data, spheroids and crypts derived from the duodenum both displayed a slower DNAm age rate, though there was a slight decrease in spheroid DNAm aging rate compared to the crypts from which they were derived (aging rate 0.57 and 0.68, respectively, $p=0.016$). In contrast, in colon, we found that spheroids have an epigenetic aging rate close to 1, similar to the crypts from which they were derived (aging rate 0.91 and 0.87, respectively, $p=0.25$). These data confirm the differences we observed between the SI and colon, demonstrating potential differences in stem cell aging, as reflected by DNAm, even in closely related tissues.

Furthermore, when stem cell-enriched spheroids from duodenum were allowed to differentiate for 4 days *in vitro*, the decreased epigenetic aging rate was maintained (Figure 3-4B), indicating that youthful progenitor cells may be responsible for maintaining a lower epigenetic age of SI epithelium as a whole. Our data establish that *in vitro* organoid culture methods do not dramatically reset or alter the 'age' of cells isolated from human gut epithelium, supporting the use of organoid cultures to investigate mechanisms that regulate aging of cells within human intestinal crypts. Furthermore, given that only subtle differences were observed between highly proliferative stem cell-containing spheroids and organoids containing non-proliferating cells, these data support the notion that epigenetic clocks do not simply reflect differences in cell division rates [22].

Discussion

In this study, we examined whether human SI and colon organoids can be used as reliable tools to investigate both regional stem cell biology and stem cell-intrinsic aging *in vitro*. Our data suggest that *in vitro* culture of human intestinal cells maintains regional identity and age, as assessed using DNA methylation patterns. A recent study demonstrated distinct methylation patterns for colon and the terminal ileum, the most distal segment of the SI, that were largely maintained in cultured organoids [34]. However, our examination focused on proximal regions of the SI, namely the duodenum and jejunum. Using these datasets, it should be possible to derive a region specific methylation map that extends along the length of the human intestine.

It is well known that lifestyle and environmental factors can influence aging, and there is increasing interest in understanding the relationship between inter-individual variability in aging rates and susceptibility to age-associated pathologies, including cancer and neurodegenerative disease. DNA methylation-based age predictions now provide us with a tool to quantify aging rates across individuals and between tissue types [21,22]. Across tissues, the Horvath multi-tissue epigenetic clock shows tight linear correlations between DNAm age and chronological age. However, some tissues, such as cerebellum, demonstrate a decreased DNAm aging rate, while other organs, such as breast, demonstrate an increased DNAm aging rate, indicating that not all tissues within the same individual age similarly [39,40].

In this study, we find that the DNAm age of human SI crypt cells is markedly lower than the chronological age of the patient from which they were isolated (on average -18.5 years). Remarkably, the epigenetic clock accurately measured the age of SI tissue until middle age, after which time age deceleration was observed. A subtle yet significant difference was also observed for crypts derived from the colon, yet these differences were within the normal range observed for other tissues[22,39,40]. The magnitude of the DNAm age reduction we observed for the SI is considerably larger than that found for other tissues, providing a striking example of

an organ for which DNAm age diverges from chronological age in an age-dependent fashion. It has remained unclear whether all cells within an organ age uniformly or whether different lineages display variable aging profiles. Here, we identify that in intestine and colon, epithelial cells within crypts have lower DNAm aging rates compared to surrounding mucosal cells, which include smooth muscle and mesenchymal cells in addition to epithelium. Our data suggests fundamental differences in SI versus colonic aging profiles, at least within epithelial cells of the crypts, and indicates that different cells within a single tissue do not age uniformly. This emphasizes the need to analyze various lineages within tissues for aging studies, particularly when investigating age-onset disease.

Data from our lab and others revealed that DNA methylation patterns are not considerably altered by a variety of culture methods, which indicate that the epigenetic clock is a valid method to assess the viability of intestinal organoids as a model to study ISC aging [34]. Indeed, our data suggest that *in vitro* stem-like spheroids largely display global methylation patterns and DNAm aging rates similar to the crypts from which they were derived (Figure 3-1C, Figure 4). Therefore, we conclude that organoids, despite lacking additional components of the aging niche, are valid models for studying stem cell-intrinsic aging. Moreover, we find that cultured colon stem-like cells have DNAm aging profiles that more reflective of chronological age, when compared to the SI (Figure 3-4).

Much of what we know about stem cell behavior comes from studies in the SI, particularly in mice, and little is known about how human colon stem/progenitor cells compare to those from the SI, especially during aging. Recent findings highlight age-related changes in the mammalian intestine and have begun to address the role stem cells may play in functional decline. Nalapareddy et al. reported that ISCs from mouse, and potentially humans, do exhibit decreased regenerative capacity [14]; however, whether similar changes were found in the colon was not addressed. Given our findings, further investigation into age-related changes in regenerative capacity of colonic stem cells is warranted. Based on our results, we predict that

age-related functional changes in colon stem cells will be more dramatic than any detected in the SI.

Of the age-related pathologies of the GI tract, colorectal adenocarcinoma is perhaps the most well-characterized and is thought to arise from accumulation of mutations in colon stem cells over time, leading to aberrant activation of proliferative signals and tumor formation [12,41]. Colon adenocarcinomas are increasingly prevalent with age; by contrast, SI adenocarcinoma remains rare throughout life [42]. It is hypothesized that differences in exposure to toxins and microbiome composition could underlie different rates of cancer in SI versus colon, yet which factors directly contribute to the risk of malignancy requires further investigation [42]. One hypothesis to explain differences in cancer incidence between the two tissues in humans is that higher stem cell division rate, and thus increased replication errors, leads to increased risk of malignancy in high turnover tissues such as the colon [43]. While mathematical estimates predict human colonic progenitor cells proliferate more rapidly than SI cells, recent evidence from our lab and others suggests that human colon stem cells may actually be cycling slower than predicted [6,43] (see Chapter 2). Furthermore, adult stem cells in the human SI and colon accumulate somatic point mutations with age at a similar rate [44], suggesting that other factors must contribute to variable incidence of malignancy. In this study, we uncover differential rates of aging in the SI and colon, as measured by a multi-tissue epigenetic clock – a finding that may help partially explain the disparity in age-associated disease risk between these two organs. Future studies are focused on unraveling mechanisms that slow the rate of epigenetic aging in the SI, which may help to identify therapeutic targets to counter aging of colonic stem cells that may be used to treat age-onset gastrointestinal disease.

Author Contributions

LJ and SL designed the study and analysis. SL carried out procurement and isolation of all human bowel specimens and conducted all in vitro organoid experimentation. DN performed differential methylation analysis. SL and DN analyzed epigenetic clock data with help from SH. MM provided technical support and resources. LJ and SL wrote the manuscript with assistance from GC and DN.

Acknowledgements

We would like to thank Jiafang Wang for technical assistance. We would like to thank the UCLA Neuroscience Genomics Core for assistance with Illumina Methylation assays, and the UCLA Translational Pathology Core Laboratory for facilitating procurement of human specimens and for histology support. This work was funded by the Broad Stem Cell Research Center Predoctoral Training Grant (SL); CURE Digestive Disease Research Center Pilot and Feasibility Study Award (LJ); Broad Stem Cell Research Center Innovation Award (LJ); and the David Geffen School of Medicine Regenerative Medicine Theme Award (LJ).

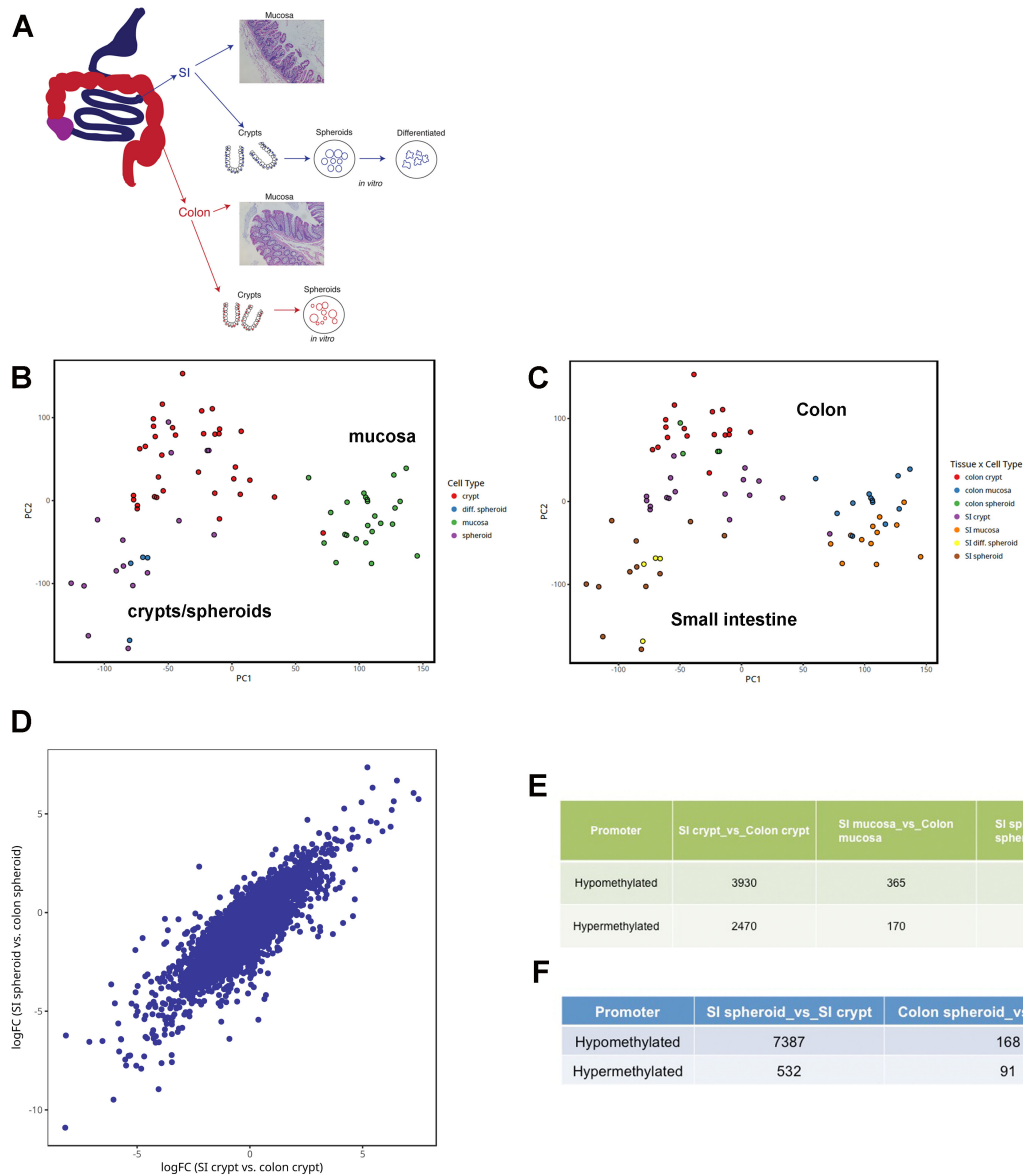


Figure 3-1: Differential methylation analysis of human intestinal and colonic mucosa, crypts and organoids. (A) Schematic of samples used. Representative H&E-stained sections of mucosae shown (scale bar, 100um). Mucosa, isolated crypts, and *in vitro* organoids were used for methylation arrays for both human SI and colon. (B-C) Principle component analysis of methylation at promoters. (B) PCA showing clustering by cell type (mucosa, crypts, organoids).

(C) PCA for cell and tissue type, showing clustering by tissue (small intestine vs. colon) and cell type (mucosa, crypts, organoids). (D) Plot showing regional differences in methylation between crypts (x-axis) and spheroids (y-axis). Log-fold-change (logFC) of methylation values at CpG sites within promoters is plotted. (E-F) Number of differentially methylated sites (DMRs) within promoter regions. (E) DMRs between crypts, mucosa and spheroids from SI vs colon. (F) DMRs between cell types (crypts and spheroids) within the same tissue. Number of hypo/hypermethylated sites listed. Methylation beta values were averaged across promoters and converted to M-values. Cutoff of FDR < 0.01 was used to determine significance.

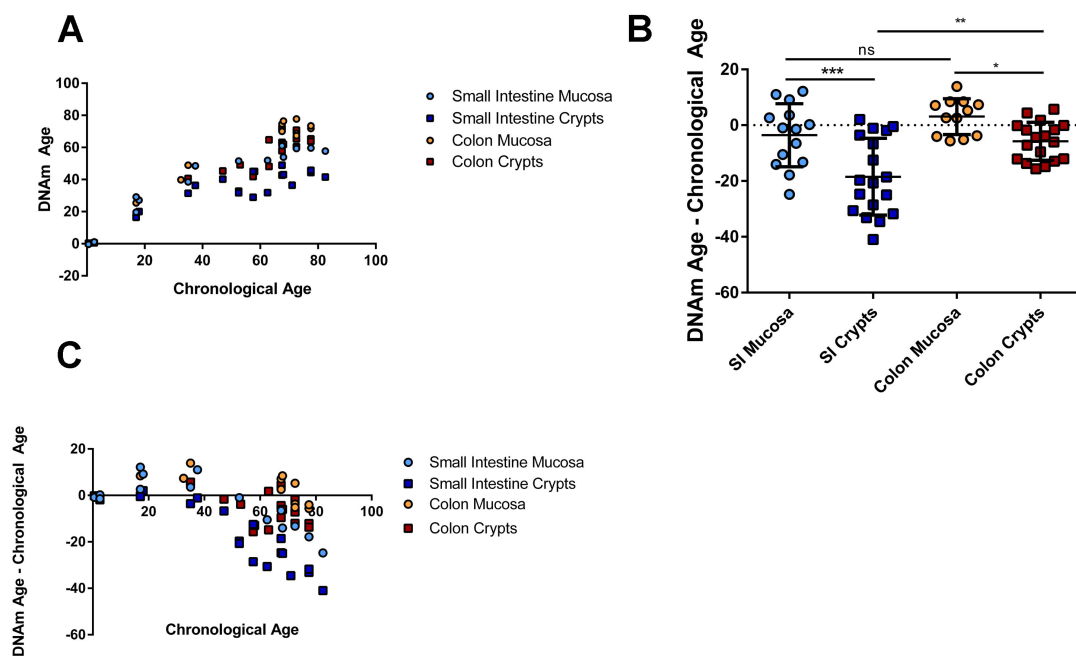


Figure 3-2: Epigenetic clock analysis of human small intestine and colon reveals decreased ticking rate in crypt cells. (A) Scatter plot of DNAm age based on the epigenetic clock (y-axis), versus chronological age (x-axis) for human small intestine and colon mucosa and crypts. Pearson correlation coefficient = 0.84, p-value < 0.0001. (B) Relationship between cell type (x-axis) and the difference between DNAm age and chronological age (y-axis) for duodenum and colon. Statistics: One-way ANOVA with Holm-Sidak's multiple comparison test. Data presented as mean +/- standard deviation. (C) Relationship between chronological age (x-axis) and the absolute difference between DNAm age and chronological age (y-axis). *p<0.05, **p<0.01, ***p<0.001.

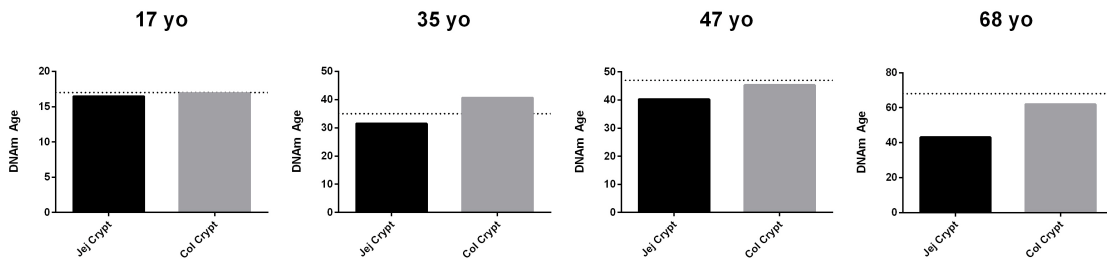


Figure 3-3: Epigenetic clock analysis of paired jejunum and colon crypts isolated from four individuals. DNAm based age prediction (y-axis) for paired jejunum and transverse colon crypts from 4 individuals. Dotted line indicates individual's chronological age.

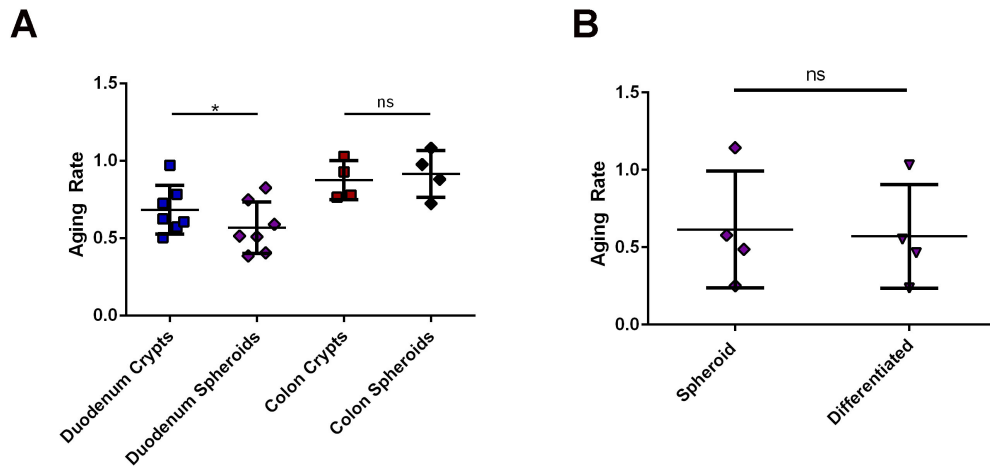


Figure 3-4: Epigenetic clock analysis of in vitro human intestinal stem-like and differentiated cultures. (A) The difference between DNAm age and chronological age, a measure of age acceleration/deceleration (y-axis), for duodenum and colon crypts vs. spheroids. (B) The difference between DNAm age and chronological age (y-axis) for paired duodenum stem-like spheroids vs. differentiated cells after 4 days of *in vitro* differentiation. Data presented as mean +/- SD. Statistics: non-parametric, paired Wilcoxon signed-rank test.

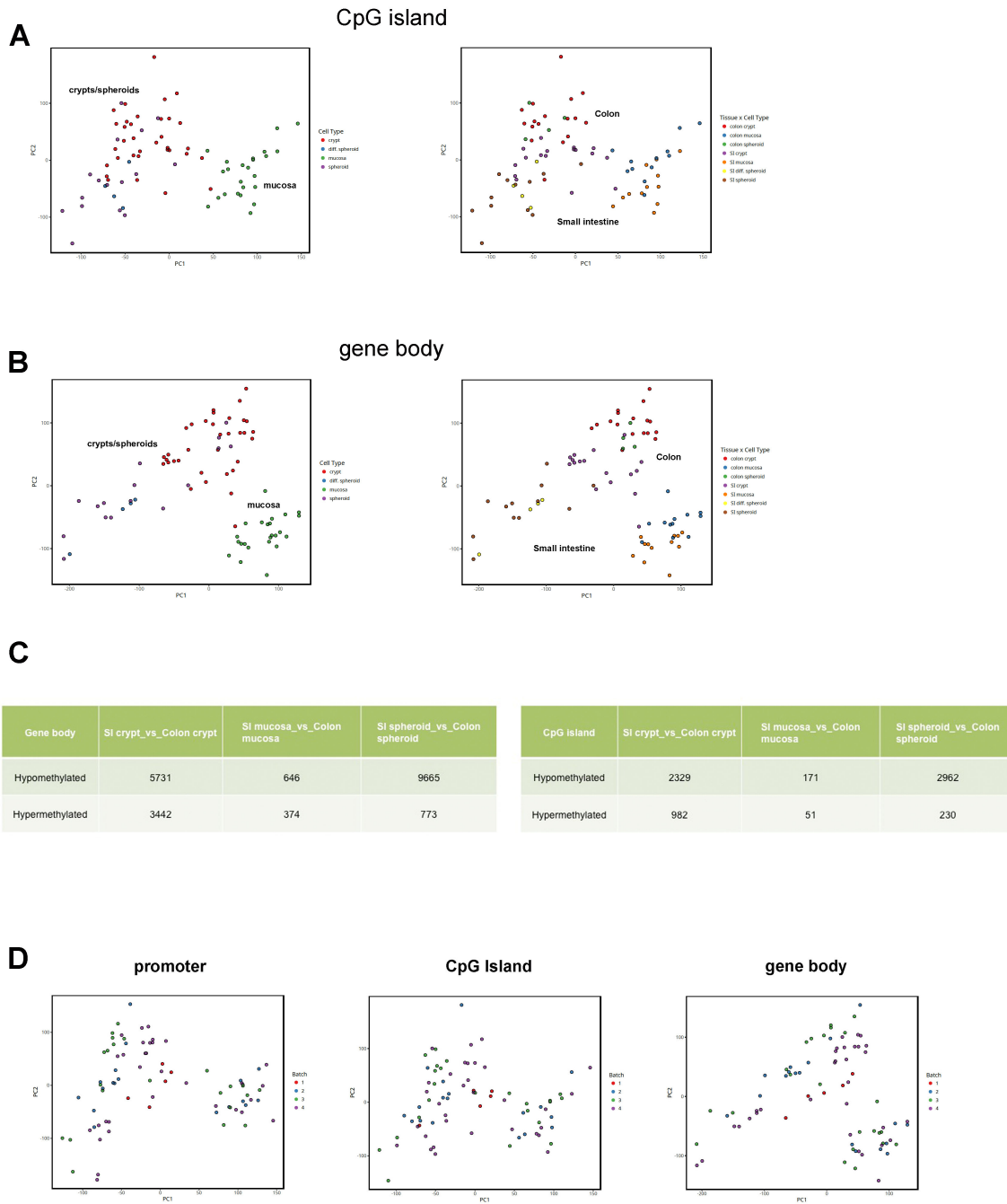
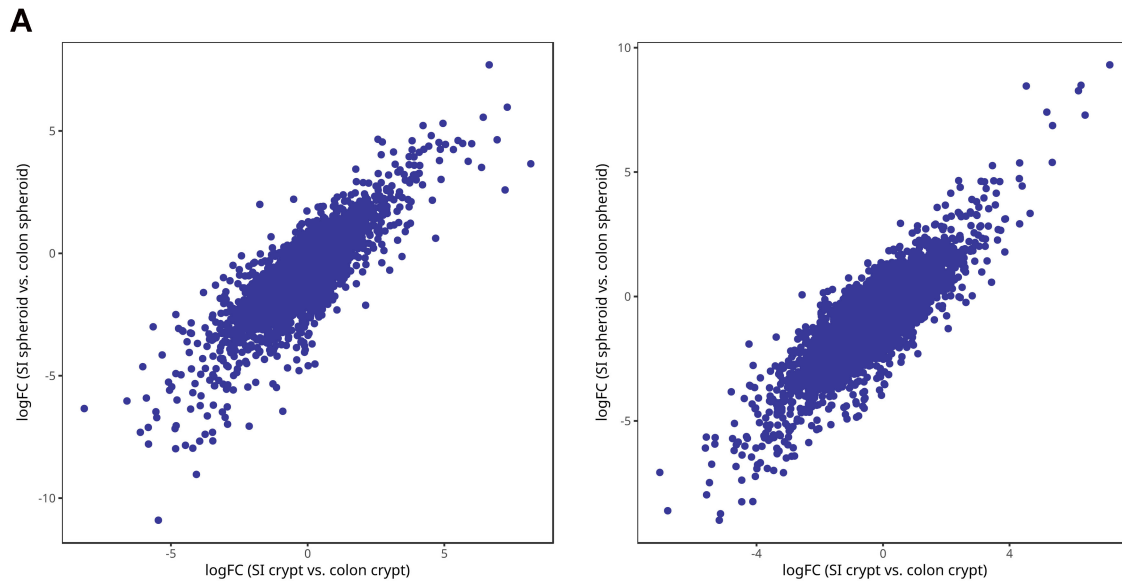


Figure S3-1: Batch effect and differential methylation analysis at CpG islands and gene bodies. (A-B) Principle component analysis of methylation M-values for (A) gene bodies and (B) CpG islands. Note clustering by tissue (small intestine vs. colon) and cell type (mucosa, crypts, spheroids, differentiated enteroids). (C) Differential methylation analysis for gene body

and CpG islands between crypts, mucosa and spheroids from different regions. Number of hypo/hypermethylated sites listed. (D) PCA analysis for methylation at promoters, gene bodies and CpG island, color coded by batches. Note that samples do not cluster by batch.

Methylation beta values were averaged across promoters and converted to M-values. Cutoff of $FDR < 0.01$ was used to determine significance.



B

Gene body	SI spheroid_vs_SI crypt	Colon spheroid_vs_Colon crypt	CpG Island	SI spheroid_vs_SI crypt	Colon spheroid_vs_Colon crypt
Hypomethylated	10922	378	Hypomethylated	3935	21
Hypermethylated	673	204	Hypermethylated	381	24

Figure S3-2: Differential methylation analysis at gene bodies and CpG islands for human intestinal and colonic crypts and organoids. (A) Plot showing regional differences in methylation between crypts (x-axis) and spheroids (y-axis). Log-fold-change (logFC) of methylation values at CpG sites within gene bodies (left) or CpG islands (right) are plotted. (B) DMRs between cell types (crypts and spheroids) within the same tissue for gene bodies (left) and CpG islands (right). Number of hypo/hypermethylated sites listed.

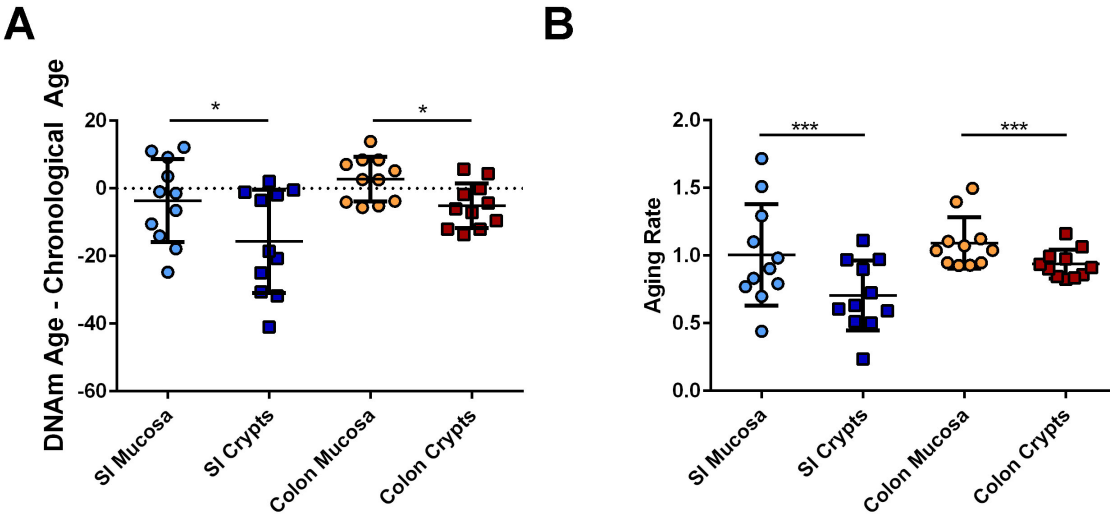


Figure S3-3: Epigenetic clock analysis of paired small intestine and colon mucosa and crypts. (A) Difference between DNAm age prediction and chronological age (y-axis) for paired SI mucosa and crypts, as well as paired colon mucosa and crypts. Dotted line at $y=0$ indicates where DNAm age and chronological age align. Statistics = paired t-test. (B) Aging rate (y-axis) for paired SI mucosa and crypts, as well as paired colon mucosa and crypts. Dotted line at $y=1$ indicates where DNAm age and chronological age align. Aging rate = DNAm age/chronological age. Statistics = paired t-test.

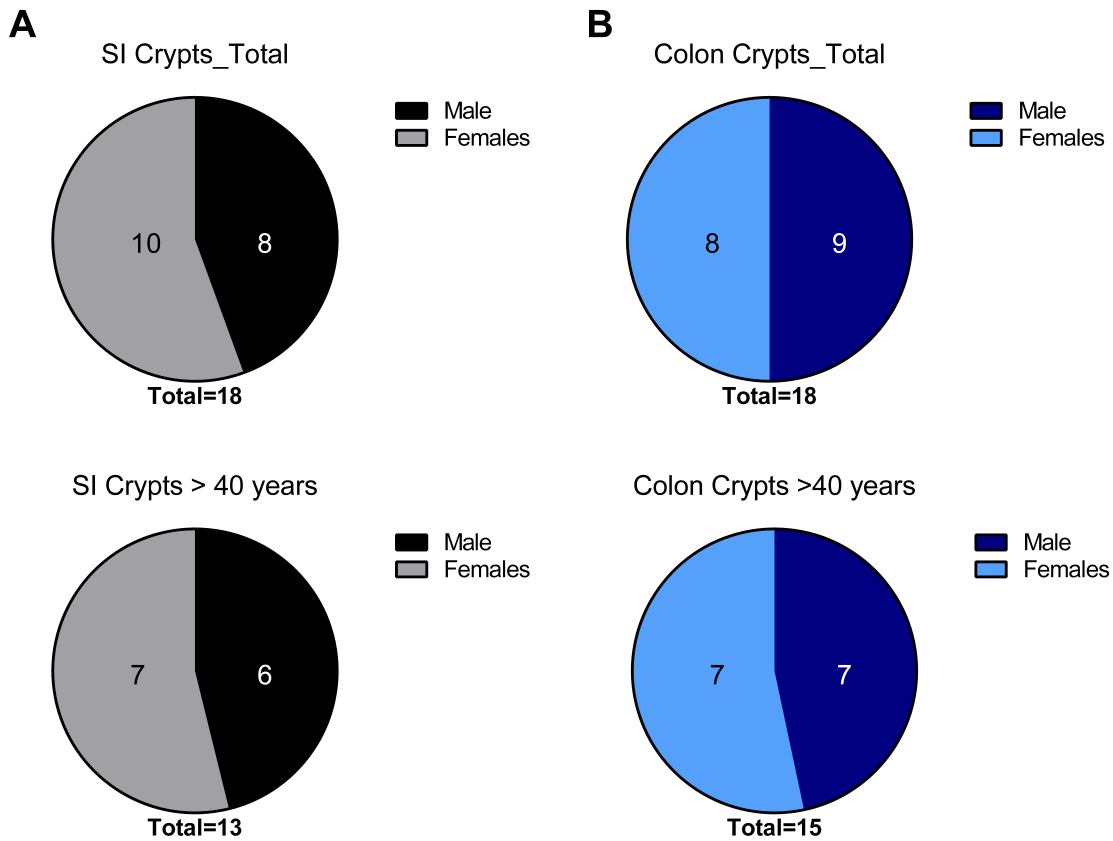
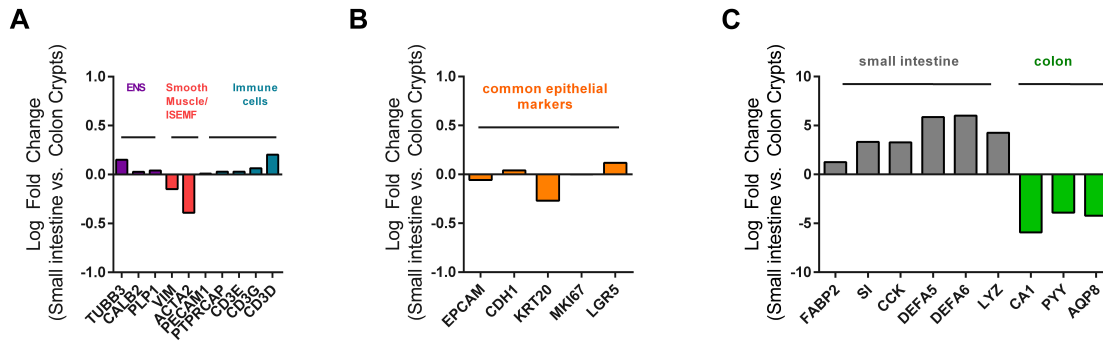


Figure S3-4: Gender distribution among samples used for DNAm analysis. (A-B) Pie charts demonstrating proportion of males vs. females represented in SI crypt (A) and colon crypt (B) samples. Total samples analyzed (top) and those restricted to >40 years (bottom).



D

Gene Symbol	log fold change (SI vs Colon)	p.value	Significant	Category (reference)
TUBB3	0.151	0.129	ns	Enteric Nervous System
Calb2	0.0281	0.614	ns	Enteric Nervous System
PLP1	0.0404	0.49	ns	Enteric glia
Vim	-0.149	0.297	ns	ISEMF
Acta2	-0.391	0.0882	ns	ISEMF
Pecam1	0.0099	0.891	ns	Immune Cells
PTPRCAP	0.0285	0.773	ns	Immune Cells
CD3E	0.0292	0.659	ns	Immune Cells
CD3G	0.0644	0.635	ns	Immune Cells
CD3D	0.202	0.694	ns	Immune Cells
Epcam	-0.0569	0.61	ns	Epithelial
CDH1	0.041	0.782	ns	Epithelial
KRT20	-0.269	0.623	ns	Epithelial
MKI67	-0.0000406	1	ns	Stem/Progenitor Cell
Lgr5	0.117	0.0912	ns	Stem/Progenitor Cell
SI	3.33	2.08E-11	sig	Small intestine
CCK	3.27	1.46E-08	sig	Small intestine
DEFA5	5.86	5.1E-13	sig	Small intestine
DEFA6	6.01	9E-18	sig	Small intestine
LYZ	4.26	1E-10	sig	Small intestine
CA1	-5.92	1.16E-14	sig	Colon
PYY	-3.9	4.44E-14	sig	Colon
AQP8	-4.22	1.22E-07	sig	Colon

Figure S3-5: Gene expression analysis of small intestine and colon crypt preparations.

Average gene expression measured on HT12 microarrays for 16 small intestine crypt preps and 6 colon crypt isolations. (A) Expression of non-epithelial markers. (B) Expression of common

epithelial and common progenitor cell markers. (C) Expression of small intestine and colon-specific genes. Y-axis indicates log fold change (SI vs. colon) for target genes. (D) Table of p -values for log fold change in gene expression. ENS = enteric nervous system. ISEMF = intestinal subepithelial myofibroblasts.

Supplemental Table 3-1: Summary of Samples used

Sample #	Tissue Type	Cell Types isolated	Reason for surgery	Gender	Age Range
1	Duodenum	Crypts	Post-mortem organ donation	Male	71
2	Duodenum	Crypts, Spheroid	Unspecified pancreatic disease	Male	55-60
3	Duodenum	Crypts, Spheroid	Unspecified pancreatic disease	Male	75-80
4	Small intestine	Mucosa	Fetal abortion	Male	15 weeks
5	Duodenum	Crypts, spheroid	Unspecified pancreatic disease	Male	50-55
6	Duodenum	Crypts, spheroid	Unspecified pancreatic disease	Female	65-70
7	Jejunum	Mucosa, crypts	Developmental abnormality	Female	0-5
8	Duodenum	Mucosa, Crypts	Unspecified pancreatic disease	Female	75-80
9	Duodenum	Mucosa, Crypts, Spheroid, Spheroid - Differentiated	Unspecified pancreatic disease	Female	50-55
10	Duodenum	Mucosa, Crypts	Unspecified pancreatic disease	Female	60-65
11	Duodenum	Mucosa	Unspecified pancreatic disease	Male	70-75
12	Duodenum	Mucosa, Crypts	Unspecified pancreatic disease	Female	65-70
13	Duodenum	Spheroid, Spheroid - Differentiated	Unspecified pancreatic disease	Male	60-65
14	Duodenum	Crypts, Spheroid, Spheroid - Differentiated	Biliary stricture and high grade dysplasia of pancreas	Male	55-60
15	Duodenum	Mucosa, Spheroid	Inflammatory Bowel Disease	Female	17
16	Duodenum	Mucosa, Crypts, Spheroid	Pancreatic tumor	Female	35-40
17	Duodenum	Mucosa, Crypts	Pancreatic tumor	Female	80-85
18	Duodenum	Mucosa, Crypts, Spheroid, Spheroid - Differentiated	Pancreatic tumor	Female	16-20
19	Colon	Crypts	Unspecified colonic disease	Male	55-60
20	Colon	Mucosa, Crypts	Unspecified colonic disease	Female	70-75
21	Colon	Mucosa	Unspecified colonic disease	Male	30-35
22	Colon	Mucosa, Crypts	Unspecified colonic disease	Female	75-80

23	Colon	Mucosa, Crypts	Colorectal Cancer	Female	65-70
24	Colon	Mucosa, Crypts	Diverticulitis	Female	65-70
25	Colon	Mucosa, Crypts	Diverticulitis	Female	65-70
26	Colon	Mucosa, Crypts	Colorectal Cancer	Female	75-80
27	Colon	Mucosa, Crypts	Colorectal Cancer	Female	70-75
28	Colon	Mucosa, Crypts	Colorectal Cancer	Male	70-75
29	Colon	Crypts	Developmental Abnormality	Female	0.5
30	Colon	Crypts, Spheroid	Colorectal Cancer	Male	61-65
31	Colon	Crypts, Spheroid	Colorectal Cancer	Male	51-55
32	Colon	Crypts, Spheroid	Colorectal Cancer	Male	56-60
33	Colon	Crypts, Spheroid	Colorectal Cancer	Male	61-65
34	Jejunum, Colon	Jejunum Mucosa, Jejunum crypts, colon mucosa, colon crypts	Post-mortem organ donation	Female	68
35	Jejunum, Colon	Jejunum Mucosa, Jejunum crypts, colon mucosa, colon crypts	Post-mortem organ donation	Male	17
36	Jejunum, Colon	Jejunum Mucosa, Jejunum crypts, colon mucosa, colon crypts	Post-mortem organ donation	Male	35
37	Jejunum, Colon	Jejunum crypts, colon crypts	Post-mortem organ donation	Male	47

References

1. Barker N, van Es JH, Kuipers J, Kujala P, van den Born M, Cozijnsen M, Haegebarth A, Korving J, Begthel H, Peters PJ, Clevers H. Identification of stem cells in small intestine and colon by marker gene Lgr5. *Nature*. Nature Publishing Group; 2007 Oct 14;449(7165):1003–7.
2. Buczacki SJA, Zecchini HI, Nicholson AM, Russell R, Vermeulen L, Kemp R, Winton DJ. Intestinal label-retaining cells are secretory precursors expressing Lgr5. *Nature*. 2013 Mar 7;495(7439):65–9.
3. Tetteh PW, Kretschmar K, Begthel H, van den Born M, Korving J, Morsink F, Farin H, van Es JH, Offerhaus GJA, Clevers H. Generation of an inducible colon-specific Cre enzyme mouse line for colon cancer research. *Proc Natl Acad Sci USA*. 2016 Oct 18;113(42):11859–64.
4. Sato T, Clevers H. Growing Self-Organizing Mini-Guts from a Single Intestinal Stem Cell: Mechanism and Applications. *Science*. 2013 Jun 6;340(6137):1190–4.
5. Jung P, Sato T, Merlos-Suárez A, Barriga FM, Iglesias M, Rossell D, Auer H, Gallardo M, Blasco MA, Sancho E, Clevers H, Battle E. Isolation and in vitro expansion of human colonic stem cells. *Nat Med*. 2011 Oct;17(10):1225–7.
6. Sugimoto S, Ohta Y, Fujii M, Matano M, Shimokawa M, Nanki K, Date S, Nishikori S, Nakazato Y, Nakamura T, Kanai T, Sato T. Reconstruction of the Human Colon Epithelium In Vivo. *Cell Stem Cell*. 2018 Feb 1;22(2):171–5.
7. Oh J, Lee YD, Wagers AJ. Stem cell aging: mechanisms, regulators and therapeutic opportunities. Nature Publishing Group. Nature Publishing Group; 2014 Aug 1;20(8):870–80.
8. López-Otín C, Blasco MA, Partridge L, Serrano M, Kroemer G. The Hallmarks of Aging. *Cell*. 2013 Jun;153(6):1194–217.

9. Man AL, Bertelli E, Rentini S, Regoli M, Briars G, Marini M, Watson AJM, Nicoletti C. Age-associated modifications of intestinal permeability and innate immunity in human small intestine. *Clin Sci*. 2015 Oct 1;129(7):515–27.
10. Ren W-Y, Wu K-F, Li X, Luo M, Liu H-C, Zhang S-C, Hu Y. Age-related changes in small intestinal mucosa epithelium architecture and epithelial tight junction in rat models. *Aging Clin Exp Res*. 2014 Apr;26(2):183–91.
11. Bhutto A, Morley JE. The clinical significance of gastrointestinal changes with aging. *Curr Opin Clin Nutr Metab Care*. 2008 Sep;11(5):651–60.
12. Barker N, Ridgway RA, van Es JH, van de Wetering M, Begthel H, van den Born M, Danenberg E, Clarke AR, Sansom OJ, Clevers H. Crypt stem cells as the cells-of-origin of intestinal cancer. *Nature*. 2008 Dec 17;457(7229):608–11.
13. Martin K, Potten CS, Roberts SA, Kirkwood TB. Altered stem cell regeneration in irradiated intestinal crypts of senescent mice. *Journal of Cell Science*. 1998 Aug;111 (Pt 16):2297–303.
14. Nalapareddy K, Nattamai KJ, Kumar RS, Karns R, Wikenheiser-Brokamp KA, Sampson LL, Mahe MM, Sundaram N, Yacyshyn M-B, Yacyshyn B, Helmrath MA, Zheng Y, Geiger H. Canonical Wnt Signaling Ameliorates Aging of Intestinal Stem Cells. *Cell Rep*. ElsevierCompany; 2017 Mar 14;18(11):2608–21.
15. Igarashi M, Guarente L. mTORC1 and SIRT1 Cooperate to Foster Expansion of Gut Adult Stem Cells during Calorie Restriction. *Cell*. Elsevier Inc; 2016 Jul 14;166(2):436–50.
16. Yilmaz ÖH, Katajisto P, Lamming DW, Gültekin Y, Bauer-Rowe KE, Sengupta S, Birsoy K, Dursun A, Yilmaz VO, Selig M, Nielsen GP, Mino-Kenudson M, Zukerberg LR, Bhan AK, Deshpande V, Sabatini DM. mTORC1 in the Paneth cell niche couples intestinal stem-cell function to calorie intake. *Nature*. 2012 May 20.

17. Fraga MF, Ballestar E, Paz MF, Ropero S, Setien F, Ballestar ML, Heine-Suñer D, Cigudosa JC, Urioste M, Benitez J, Boix-Chornet M, Sanchez-Aguilera A, Ling C, Carlsson E, Poulsen P, Vaag A, Stephan Z, Spector TD, Wu Y-Z, Plass C, Esteller M. Epigenetic differences arise during the lifetime of monozygotic twins. *Proc Natl Acad Sci USA*. 2005 Jul 26;102(30):10604–9.
18. Heyn H, Li N, Ferreira HJ, Moran S, Pisano DG, Gomez A, Diez J, Sanchez-Mut JV, Setien F, Carmona FJ, Puca AA, Sayols S, Pujana MA, Serra-Musach J, Iglesias-Platas I, Formiga F, Fernandez AF, Fraga MF, Heath SC, Valencia A, Gut IG, Wang J, Esteller M. Distinct DNA methylomes of newborns and centenarians. *Proc Natl Acad Sci USA*. 2012 Jun 26;109(26):10522–7.
19. Maegawa S, Hinkal G, Kim HS, Shen L, Zhang L, Zhang J, Zhang N, Liang S, Donehower LA, Issa J-PJ. Widespread and tissue specific age-related DNA methylation changes in mice. *Genome Res*. 2010 Mar;20(3):332–40.
20. Jones MJ, Goodman SJ, Kobor MS. DNA methylation and healthy human aging. *Aging Cell*. 2015 Dec;14(6):924–32.
21. Hannum G, Guinney J, Zhao L, Zhang L, Hughes G, Sada S, Klotzle B, Bibikova M, Fan J-B, Gao Y, Deconde R, Chen M, Rajapakse I, Friend S, Ideker T, Zhang K. Genome-wide Methylation Profiles Reveal Quantitative Views of Human Aging Rates. *Molecular Cell*. 2013 Jan;49(2):359–67.
22. Horvath S. DNA methylation age of human tissues and cell types. *Genome Biol*. 2013;14(10):R115.
23. Gross AM, Jaeger PA, Kreisberg JF, Licon K, Jepsen KL, Khosroheidari M, Morse BM, Swindells S, Shen H, Ng CT, Flagg K, Chen D, Zhang K, Fox HS, Ideker T. Methylome-wide Analysis of Chronic HIV Infection Reveals Five-Year Increase in Biological Age and Epigenetic Targeting of HLA. *Molecular Cell*. Elsevier Inc; 2016 Apr 21;62(2):157–68.

24. Horvath S, Garagnani P, Bacalini MG, Pirazzini C, Salvioli S, Gentilini D, Di Blasio AM, Giuliani C, Tung S, Vinters HV, Franceschi C. Accelerated epigenetic aging in Down syndrome. *Aging Cell*. 2015 Jun;14(3):491–5.
25. Wang T, Tsui B, Kreisberg JF, Robertson NA, Gross AM, Yu MK, Carter H, Brown-Borg HM, Adams PD, Ideker T. Epigenetic aging signatures in mice livers are slowed by dwarfism, calorie restriction and rapamycin treatment. *Genome Biology*; 2017 Mar 17;:1–11.
26. Sato T, Stange DE, Ferrante M, Vries R, Van Es JH. Long-term expansion of epithelial organoids from human colon, adenoma, adenocarcinoma, and Barrett's epithelium. *Gastroenterology*. 2011.
27. Du P, Zhang X, Huang C-C, Jafari N, Kibbe WA, Hou L, Lin SM. Comparison of Beta-value and M-value methods for quantifying methylation levels by microarray analysis. *BMC Bioinformatics*. 2010 Nov 30;11:587.
28. Assenov Y, Müller F, Lutsik P, Walter J, Lengauer T, Bock C. Comprehensive analysis of DNA methylation data with RnBeads. *Nat Meth*. 2014 Nov;11(11):1138–40.
29. Xu Z, Niu L, Li L, Taylor JA. ENmix: a novel background correction method for Illumina HumanMethylation450 BeadChip. *Nucleic Acids Res*. 2016 Feb 18;44(3):e20.
30. Teschendorff AE, Marabita F, Lechner M, Bartlett T, Tegner J, Gomez-Cabrero D, Beck S. A beta-mixture quantile normalization method for correcting probe design bias in Illumina Infinium 450 k DNA methylation data. *Bioinformatics*. 2013 Jan 15;29(2):189–96.
31. Johnson WE, Li C, Rabinovic A. Adjusting batch effects in microarray expression data using empirical Bayes methods. *Biostatistics*. 2007 Jan;8(1):118–27.
32. Ritchie ME, Phipson B, Wu D, Hu Y, Law CW, Shi W, Smyth GK. limma powers differential expression analyses for RNA-sequencing and microarray studies. *Nucleic Acids Res*. 2015 Apr 20;43(7):e47.

33. Jung P, Sommer C, Barriga FM, Buczacki SJ, Hernando-Momblona X, Sevillano M, Duran-Frigola M, Aloy P, Selbach M, Winton DJ, Batlle E. Stem Cell Reports. Stem Cell Reports. The Authors; 2015 Dec 8;5(6):979–87.
34. Kraiczy J, Nayak KM, Howell KJ, Ross A, Forbester J, Salvestrini C, Mustata R, Perkins S, Andersson-Rolf A, Leenen E, Liebert A, Vallier L, Rosenstiel PC, Stegle O, Dougan G, Heuschkel R, Koo B-K, Zilbauer M. DNA methylation defines regional identity of human intestinal epithelial organoids and undergoes dynamic changes during development. Gut. 2017 Nov 15.
35. Middendorp S, Schneeberger K, Wiegerinck CL, Mokry M, Akkerman RDL, van Wijngaarden S, Clevers H, Nieuwenhuis EES. Adult stem cells in the small intestine are intrinsically programmed with their location-specific function. Stem Cells. 2014 May;32(5):1083–91.
36. Bosse T, Piaseckyj CM, Burghard E, Fialkovich JJ, Rajagopal S, Pu WT, Krasinski SD. Gata4 Is Essential for the Maintenance of Jejunal-Ileal Identities in the Adult Mouse Small Intestine. Mol Cell Biol. 2006 Nov 14;26(23):9060–70.
37. Foulke-Abel J, In J, Yin J, Zachos NC, Kovbasnjuk O, Estes MK, de Jonge H, Donowitz M. Human Enteroids as a Model of Upper Small Intestinal Ion Transport Physiology and Pathophysiology. Gastroenterology. 2016 Mar;150(3):638–8.
38. Kaaij LTJ, van de Wetering M, Fang F, Decato B, Molaro A, van de Werken HJG, van Es JH, Schuijers J, de Wit E, de Laat W, Hannon GJ, Clevers HC, Smith AD, Ketting RF. DNA methylation dynamics during intestinal stem cell differentiation reveals enhancers driving gene expression in the villus. Genome Biol. 2013 May 28;14(5):R50.
39. Horvath S, Mah V, Lu AT, Woo JS, Choi O-W, Jasinska AJ, Riancho JA, Tung S, Coles NS, Braun J, Vinters HV, Coles LS. The cerebellum ages slowly according to the epigenetic clock. Aging (Albany NY). 2015 May;7(5):294–306.

40. Sehl ME, Henry JE, Storniolo AM, Ganz PA, Horvath S. DNA methylation age is elevated in breast tissue of healthy women. *Breast Cancer Res Treat.* 2017 Jul;164(1):209–19.
41. Vermeulen L, Snippert HJ. Stem cell dynamics in homeostasis and cancer of the intestine. *Nat Rev Cancer.* 2014 Jul;14(7):468–80.
42. Delaunoy T, Neczyporenko F, Limburg PJ, Erlichman C. Pathogenesis and risk factors of small bowel adenocarcinoma: a colorectal cancer sibling? *Am J Gastroenterol.* 2005 Mar;100(3):703–10.
43. Tomasetti C, Vogelstein B. Cancer etiology. Variation in cancer risk among tissues can be explained by the number of stem cell divisions. *Science.* 2015 Jan 2;347(6217):78–81.
44. Blokzijl F, de Ligt J, Jager M, Sasselli V, Roerink S, Sasaki N, Huch M, Boymans S, Kuijk E, Prins P, Nijman IJ, Martincorena I, Mokry M, Wiegerinck CL, Middendorp S, Sato T, Schwank G, Nieuwenhuis EES, Verstegen MMA, van der Laan LJW, de Jonge J, Ijzermans JNM, Vries RG, van de Wetering M, Stratton MR, Clevers H, Cuppen E, van Boxtel R. Tissue-specific mutation accumulation in human adult stem cells during life. *Nature.* 2016 Oct 13;538(7624):260–4.

Chapter 4: Conclusions and Future Directions

The mammalian gut epithelium is the most rapidly self-renewing tissue and is maintained by regularly proliferating tissue-specific stem cells marked by the Wnt target gene *Lgr5*. These *Lgr5*⁺ stem cells reside in invaginating crypts in both the small intestine and colon. Yet, despite their close physical proximity, the small intestine and colon exhibit distinct physiological functions, supported by different anatomical structures. Specifically, the small intestine is composed of repetitive crypt-villus units, structures that increase surface area for nutrient absorption, whereas the colon is composed of crypts and flat surface epithelium. Although the structural differences and distinct physiological functions of the small intestine and colon are well characterized, it is still unclear to what extent the behavior of stem cells in these two organs is similar.

Differences in stem cell biology between small intestine and colon could have implications for our understanding of cancer and aging. In particular, gut stem cells have been proposed to be the cell of origin for colon cancer, yet whether regional differences in stem cell biology could explain why colon cancers are far more common than small bowel cancers is incompletely understood. It is possible that there are segmental differences in stem cell proliferation dynamics, leading to different rates of replication-induced errors. Given that a major risk factor for colon cancer is increased age, it is also possible that there are regional differences in age-associated cellular changes, such as accumulation of DNA damage and genomic instability, epigenetic changes, and metabolic alterations[1,2]. When these degenerative changes occur in adult stem cells or their niches, they can lead to stem cell dysfunction and ultimately tissue level aging and age-dependent disease. This led us to examine molecular differences between stem cells of the small intestine and colon in human. In particular, we investigated whether human ISCs and CoSCs exhibit different self-renewal

kinetics *in vitro* (Chapter 2) and whether stem cell-containing crypts within the two organs exhibit different hallmarks of aging, in particular DNA methylation-based changes (Chapter 3).

In Chapter 2, we examined the proliferation of ISCs and CoSCs within *in vitro* stem cell-enriched spheroids. We found that CoSC tend to be more difficult to expand due to a slower cycling rate than ISCs. This decreased proliferative capacity was also associated with a greater tendency to spontaneously differentiate and decreased stem cell function, indicating that stem cell identity was not uniformly maintained in colon cultures, unlike small intestine. This led us to question whether signals permitting differentiation and preventing stemness, such as BMP, were active in colon spheroids[3-6]. We found that BMP signaling was active in CoSCs *in vitro*, likely due to expression of BMP4 from a subset of cells undergoing spontaneous differentiation. We found that supplemental BMP inhibition reversed these phenotypes. In particular, the addition of a small molecule BMP inhibitor increased CoSC proliferation, stem cell function and prevented differentiation; however CoSC proliferation still remained lower than baseline ISC proliferation.

It remains possible that the slower cycling behavior of CoSCs observed here and recently reported by Sugimoto et al. is an artifact of incomplete recapitulation of colon niche factors. Sugimoto et al. noted that human CoSCs divided less frequently than mouse CoSCs; however, these cells were analyzed in the context of the mouse colon crypt niche, which could differ from human. It is possible that even in the presence of supplemental BMP inhibition, *in vitro* culture conditions used here for human colon are still not optimal. In mice, distinct media conditions are commonly utilized for small intestine and colon, with supplemental Wnt required exclusively in colon organoids – a requirement attributed to the colon's lack of Wnt-secreting Paneth cells[7,8]. Additionally, while Wnt signaling is generally thought to be a pro-proliferative and stemness promoting factor, recent evidence suggests that sustained Wnt signaling can conversely inhibit proliferation, at least in two dimensional enteroid cultures[3]. Therefore, it would be interesting to investigate if there are different thresholds for Wnt signaling that support

human ISC and CoSC stem cell maintenance, thus necessitating region-specific growth conditions as has been done in mouse. One might hypothesize that combined modulation of Wnt and BMP signaling could optimize human CoSC growth *in vitro*.

While our proliferation data is *in vitro*, raising the question of suboptimal culture conditions for colon, Sugimoto et al. also reported endogenous proliferation analysis in human tissue sections. Via *in situ* hybridization for Lgr5, they demonstrated that a small proportion of human CoSCs co-stained for the proliferation marker Ki67, whereas the majority of mouse CoSCs were Ki67-positive[9]. This suggests that the slow cycling behavior we noted *in vitro* may actually hold true for human CoSCs *in vivo*. It would be interesting to conduct similar Lgr5/Ki67 co-expression analysis in paired human small intestine and colon sections for direct comparison of proliferation rates on endogenous tissues.

Chapter 3 expands on the molecular differences noted between colon and small intestine in Chapter 2 by examining whether aging hallmarks may differentially impact stem/progenitor cells within the two regions. In particular, we utilized the epigenetic clock, a measure of age based on age-related DNA methylation changes, to predict the ages of small intestine and colon crypts or surrounding mucosa. We found that, in general, crypt cells maintained a younger DNAm age than surrounding mucosa cells, especially in small intestine. Indeed, small intestine crypts exhibited on average an 18.5-year age deceleration, which was significantly lower than that observed in colon. This suggests that small intestine crypt cells may resist cellular changes associated with aging.

Strikingly, we noted the ticking rate of the epigenetic clock for small intestine crypts was in sync with chronological clock up until ~40 years of age, when the aging rate began to decline. What underlies this shift in small intestine DNAm aging in middle age is unclear. There is increasing evidence that the gut microbiome impacts organ and organismal health and aging, and that there may be age-related shifts in microbiome composition[10,11]. Additionally, recent data from Kaiko et al. suggest that microbial metabolites such as butyrate can impact

mammalian gut stem cell behavior upon exposure[12]. Given that the small intestine has significantly lower microbial load and different commensal bacterial species than the colon[13], it is possible that differences in exposure to microbial components within the crypts of small intestine and colon, or between the small intestine epithelium of younger and older individuals, could play a role in altered rates of cellular aging. Yet the precise role of the microbiome or microbial byproducts in gut aging requires future investigation.

Here we focused on the epigenetic clock, because it is a highly quantitative measure of cellular age and has been shown to be biologically relevant. In particular, the epigenetic clock has been assessed in the context of several disease states[14-17] and has been shown to respond to well-characterized environmental interventions such as calorie restriction, known to extend lifespan in mice [18,19]. Nevertheless, whether other hallmarks of aging, such as telomere attrition, accumulation of DNA damage or mitochondrial changes, differentially impact small intestine and colon progenitor cells warrants further investigation. We preliminarily examined the DNA damage response in ISCs and CoSCs *in vitro* and found that under homeostatic conditions neither cell type exhibits detectable DNA damage foci (data not shown). Additionally, shortly after damage with X-irradiation, both ISCs and CoSCs exhibit accumulation of 53BP1-associated DNA damage foci, which similarly repair over time (see Appendix F); however, a more detailed investigation of the kinetics of DNA damage and repair between ISCs and CoSCs is needed.

Intestinal organoids provide an invaluable tool for investigating stem cell biology and stem cell aging. Several groups have recently adapted the use of 3D organoid cultures to study small intestine stem cell aging in mouse[20,21], but to do so in human, it was important to first confirm whether these mesenchyme-free cultures maintain hallmarks of biological age in the absence of an aging intestinal microenvironment. In Chapter 3, we provide evidence that DNAm age, based on epigenetic clock analysis, is maintained in crypt-derived spheroids *in vitro*. In particular, we found that the DNAm age deceleration detected in small intestine spheroids, but

not in colon spheroids, is similar to the crypts from which they were established. This suggests that the “youthful” DNAm signature of small intestine crypts may be due to a protective mechanism against cellular aging that is established within the ISC. Additionally, these data provide evidence, for the first time, that molecular age of cultured gut stem cells closely reflects the age of endogenous cells. Our evidence suggests that organoid models can reliably be used to study the effects of aging on human ISCs and CoSCs. This opens the door to more in depth analysis of the differences in cellular aging between small intestine and colon. Further studies into the molecular differences between the two organs could help explain differences in susceptibility to age-onset disease, particularly cancer.

References

1. Oh J, Lee YD, Wagers AJ. Stem cell aging: mechanisms, regulators and therapeutic opportunities. *Nature Publishing Group*; 2014 Aug 1;20(8):870–80.
2. López-Otín C, Blasco MA, Partridge L, Serrano M, Kroemer G. The Hallmarks of Aging. *Cell*. 2013 Jun;153(6):1194–217.
3. Thorne CA, Chen IW, Sanman LE, Cobb MH, Wu LF, Altschuler SJ. Enteroid Monolayers Reveal an Autonomous WNT and BMP Circuit Controlling Intestinal Epithelial Growth and Organization. *Dev Cell*. 2018 Mar 12;44(5):624–4.
4. Haramis A-PG, Begthel H, van den Born M, van Es J, Jonkheer S, Offerhaus GJA, Clevers H. De novo crypt formation and juvenile polyposis on BMP inhibition in mouse intestine. *Science*. 2004 Mar 12;303(5664):1684–6.
5. Batts LE, Polk DB, Dubois RN, Kulesa H. Bmp signaling is required for intestinal growth and morphogenesis. *Dev Dyn*. 2006 Jun;235(6):1563–70.
6. Qi Z, Li Y, Zhao B, Xu C, Liu Y, Li H, Zhang B, Wang X, Yang X, Xie W, Li B, Han J-DJ, Chen Y-G. BMP restricts stemness of intestinal Lgr5⁺ stem cells by directly suppressing their signature genes. *Nature Communications*. 2017 Jan 6;8:13824.
7. Sato T, Stange DE, Ferrante M, Vries R, Van Es JH. Long-term expansion of epithelial organoids from human colon, adenoma, adenocarcinoma, and Barrett's epithelium. *Gastroenterology*. 2011.
8. Sato T, van Es JH, Snippert HJ, Stange DE, Vries RG, van den Born M, Barker N, Shroyer NF, van de Wetering M, Clevers H. Paneth cells constitute the niche for Lgr5 stem cells in intestinal crypts. *Nature*. 2011 Jan 20;469(7330):415–8.
9. Sugimoto S, Ohta Y, Fujii M, Matano M, Shimokawa M, Nanki K, Date S, Nishikori S, Nakazato Y, Nakamura T, Kanai T, Sato T. Reconstruction of the Human Colon Epithelium In Vivo. *Cell Stem Cell*. 2018 Feb 1;22(2):171–5.

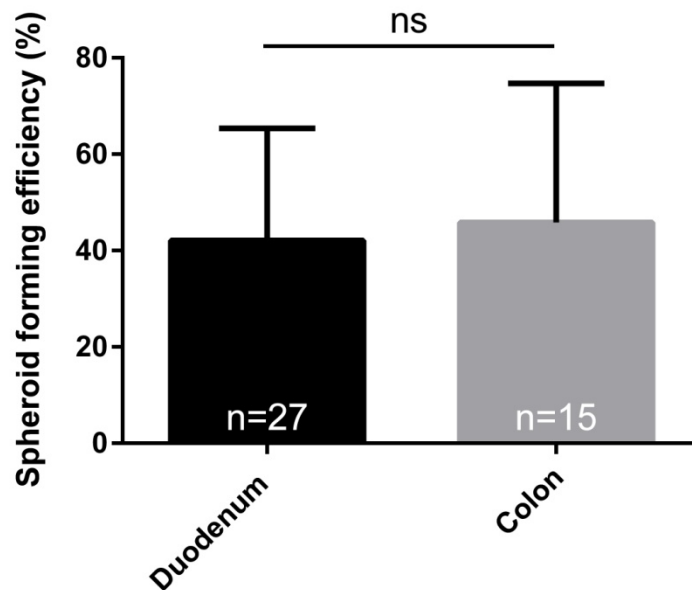
10. Clark RI, Salazar A, Yamada R, Fitz-Gibbon S, Morselli M, Alcaraz J, Rana A, Rera M, Pellegrini M, Ja WW, Walker DW. Distinct Shifts in Microbiota Composition during *Drosophila* Aging Impair Intestinal Function and Drive Mortality. *Cell Rep.* 2015 Sep 8;12(10):1656–67.
11. Clark RI, Walker DW. Role of gut microbiota in aging-related health decline: insights from invertebrate models. *Cell Mol Life Sci.* 2018 Jan;75(1):93–101.
12. Kaiko GE, Ryu SH, Koues OI, Collins PL, Solnica-Krezel L, Pearce EJ, Pearce EL, Oltz EM, Stappenbeck TS. The Colonic Crypt Protects Stem Cells from Microbiota-Derived Metabolites. *Cell.* 2016 Jun 16;165(7):1708–20.
13. Mowat AM, Agace WW. Regional specialization within the intestinal immune system. *Nat Rev Immunol.* 2014 Oct;14(10):667–85.
14. Horvath S, Mah V, Lu AT, Woo JS, Choi O-W, Jasinska AJ, Riancho JA, Tung S, Coles NS, Braun J, Vinters HV, Coles LS. The cerebellum ages slowly according to the epigenetic clock. *Aging (Albany NY).* 2015 May;7(5):294–306.
15. Horvath S, Langfelder P, Kwak S, Aaronson J, Rosinski J, Vogt TF, Eszes M, Faull RLM, Curtis MA, Waldvogel HJ, Choi O-W, Tung S, Vinters HV, Coppola G, Yang XW. Huntington's disease accelerates epigenetic aging of human brain and disrupts DNA methylation levels. *Aging (Albany NY).* 2016 Jul 27.
16. Gross AM, Jaeger PA, Kreisberg JF, Licon K, Jepsen KL, Khosroheidari M, Morse BM, Swindells S, Shen H, Ng CT, Flagg K, Chen D, Zhang K, Fox HS, Ideker T. Methylome-wide Analysis of Chronic HIV Infection Reveals Five-Year Increase in Biological Age and Epigenetic Targeting of HLA. *Molecular Cell.* Elsevier Inc; 2016 Apr 21;62(2):157–68.
17. Horvath S, Garagnani P, Bacalini MG, Pirazzini C, Salvioli S, Gentilini D, Di Blasio AM, Giuliani C, Tung S, Vinters HV, Franceschi C. Accelerated epigenetic aging in Down syndrome. *Aging Cell.* 2015 Jun;14(3):491–5.

18. Wang T, Tsui B, Kreisberg JF, Robertson NA, Gross AM, Yu MK, Carter H, Brown-Borg HM, Adams PD, Ideker T. Epigenetic aging signatures in mice livers are slowed by dwarfism, calorie restriction and rapamycin treatment. *Genome Biology*; 2017 Mar 17;:1–11.
19. Cole JJ, Robertson NA, Rather MI, Thomson JP, McBryan T, Sproul D, Wang T, Brock C, Clark W, Ideker T, Meehan RR, Miller RA, Brown-Borg HM, Adams PD. Diverse interventions that extend mouse lifespan suppress shared age-associated epigenetic changes at critical gene regulatory regions. *Genome Biology*; 2017 Mar 26;:1–16.
20. Nalapareddy K, Nattamai KJ, Kumar RS, Karns R, Wikenheiser-Brokamp KA, Sampson LL, Mahe MM, Sundaram N, Yacyshyn M-B, Yacyshyn B, Helmrich MA, Zheng Y, Geiger H. Canonical Wnt Signaling Ameliorates Aging of Intestinal Stem Cells. *Cell Rep. Elsevier Company*; 2017 Mar 14;18(11):2608–21.
21. Mihaylova MM, Cheng C-W, Cao AQ, Tripathi S, Mana MD, Bauer-Rowe KE, Abu-Remaileh M, Clavain L, Erdemir A, Lewis CA, Freinkman E, Dickey AS, La Spada AR, Huang Y, Bell GW, Deshpande V, Carmeliet P, Katajisto P, Sabatini DM, Yilmaz ÖH. Fasting Activates Fatty Acid Oxidation to Enhance Intestinal Stem Cell Function during Homeostasis and Aging. *Cell Stem Cell*. 2018 May 3;22(5):769–778.e4.

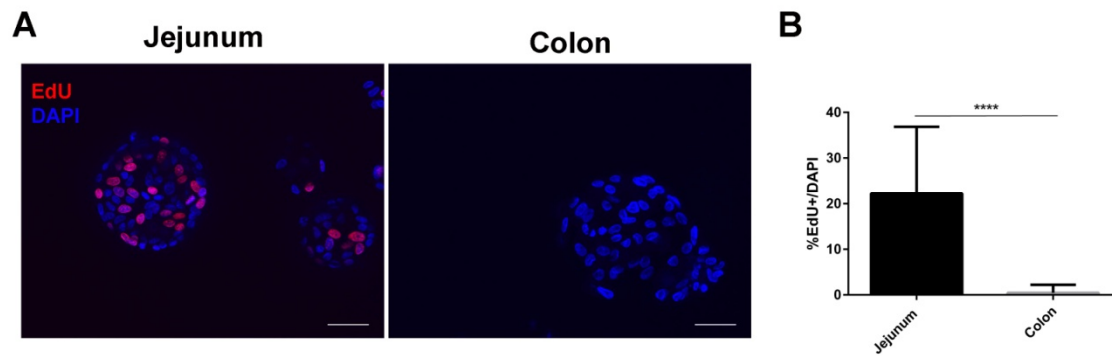
Appendix

Appendix A: Spheroid forming efficiency for human small intestine and colon samples.

The percentage of isolated crypts that gave rise to stem cell-enriched spheroids three days after initial plating was quantified. There is no significant difference ($p=0.64$) between average spheroid forming efficiency for human small intestine and colon samples; however, there is marked inter-individual variability. Crypt samples were plated in triplicate and spheroid forming efficiency was assayed on day 3. Data is shown as mean \pm standard deviation. Statistics: unpaired t-test.

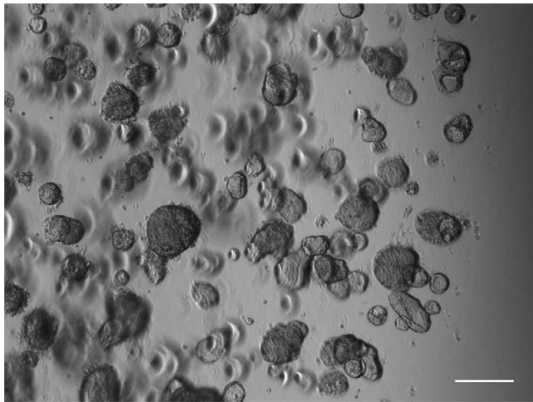


Appendix B: Proliferation rate of paired jejunum and transverse colon from the same donor. A) Four-hour EdU incorporation demonstrates decreased proliferation of CoSCs compared to ISC in spheroids derived from transverse colon and jejunum from same donor. Scale bar = 50um. B) The percentage of total nuclei that are EdU+ is quantified. At least 15 spheroids per region were analyzed. Results are shown as mean +/- standard deviation. Statistics: unpaired t-test; ****p < 0.0001.

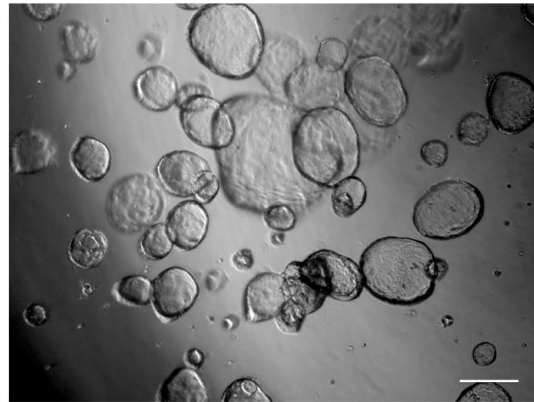


Appendix C: BMP inhibition prevents differentiation during starvation. Spheroids were maintained in control media or media supplemented with LDN for 7 days prior to 13 day starvation, during which media was not exchanged. Control spheroids show marked differentiation, indicated by dense morphology, while spheroids treated with LDN maintain cystic spheroid structure. Scale bar = 200um.

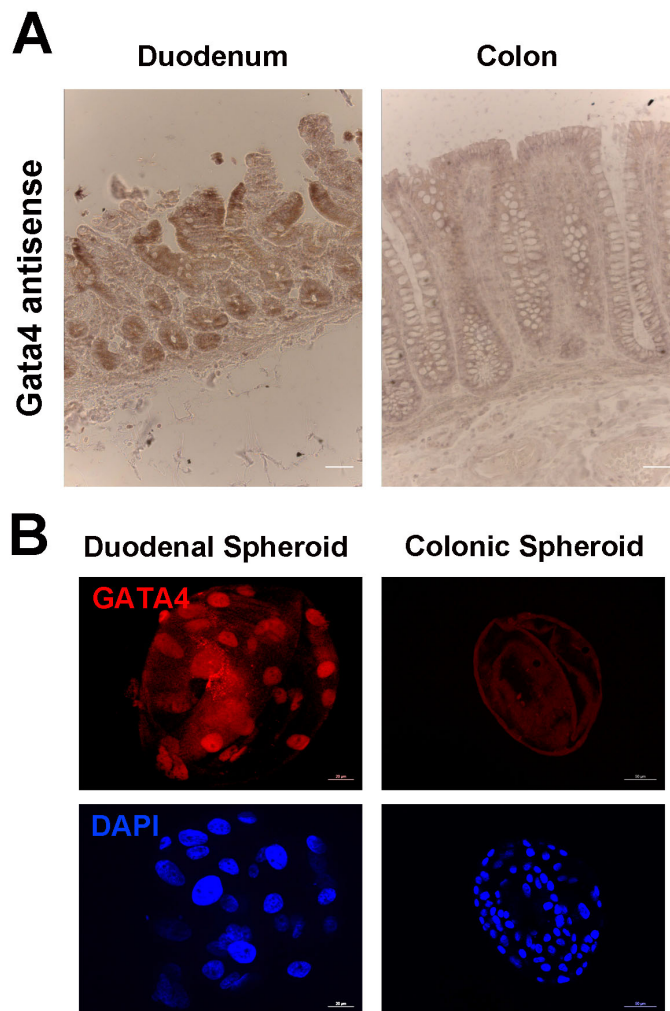
Control



+LDN

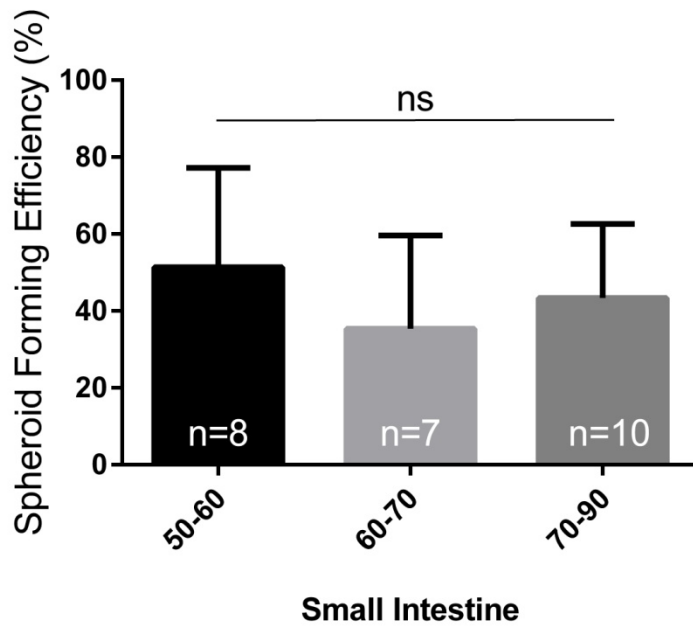


Appendix D: Regional expression of Gata4 is maintained in spheroids derived from human duodenum and colon. (A) In situ hybridization using anti-sense Gata4 probe in human duodenum (left) and colon (right). Gata4 transcript is detected within the epithelium of duodenum but not colon. (B) Whole mount immunofluorescence staining showing Gata4 transcription factor localized in the nuclei of duodenal spheroid cells, not colon spheroids. Scale bar (duodenum) = 20um. Scale bar (colon) = 50um.



Appendix E: Spheroid forming efficiency of adult human small intestine crypts by age.

The percentage of isolated duodenum crypts that gave rise to stem cell-enriched spheroids three days after initial plating was quantified and stratified by age (50-60, 60-70, 70-90 years). There is no significant difference between average spheroid forming efficiency across these age ranges; however, there is marked inter-individual variability. Data is shown as mean +/- standard deviation. Statistics: One-way ANOVA.



Appendix F: Response to irradiation-induced DNA damage for human small intestine and colon spheroids.

One hour after X-ray induced irradiation, both small intestine and colon spheroids exhibit accumulation of DNA damage foci and proliferation arrest. Five hours after irradiation, both small intestine and colon spheroids resume proliferation and have partially repaired DNA damage, as marked by decrease in DNA damage foci, but proliferation is not back to baseline at this time. (Left) Number of 53BP1 foci per nucleus was quantified in spheroids irradiated at 4Gy, 1 and 5 hours later. At least 40 nuclei per sample, and two samples per region were analyzed. (Right) Number of phospho-histone H3+ (pHH3) cells per spheroid was quantified to mark mitosis in unirradiated and irradiated spheroids (4Gy; 1 and 5 hours post-irradiation). Twenty spheroids per sample, and two samples per region were analyzed. Results are mean +/- standard error. Statistics: Two-way ANOVA with Tukey's multiple comparison test; ** $p < 0.01$, **** $p < 0.0001$.

